



**Ernest Orlando Lawrence**  
**Berkeley National Laboratory**  
1 Cyclotron Road, 70R0108B  
Berkeley CA 94720-8168  
(510) 495-2679; fax: (510) 486-4260

September 10, 2012

Mr. Tien Q. Duong  
EE-2G/Forrestal Building  
Office of Vehicle Technologies  
U.S. Department of Energy  
1000 Independence Avenue, S.W.  
Washington D.C. 20585

Dear Tien,

Here is the third quarter FY 2012 report for the Batteries for Advanced Transportation Technologies (BATT) Program. This report and prior Program reports can be downloaded from <http://batt.lbl.gov/reports/quarterly-reports/>.

Sincerely,

Venkat Srinivasan  
Acting Head  
BATT Program

edited by: V. Battaglia  
M. Foure  
S. Lauer

cc: J. Barnes DOE/OVT  
P. Davis DOE/OVT  
D. Howell DOE/OVT  
J. Muhlestein DOE-BSO

## *FEATURED HIGHLIGHTS*

### *Cell Analysis–*

- ✦ **Chen's Group uses single crystals to highlight the effect of  $Mn^{3+}$  on the rate performance of ordered and disordered  $LiNi_{1/2}Mn_{3/2}O_4$ .**

### *Anodes–*

- ✦ **Kumta's Group develops an interfacial material between carbon fibers and Si that facilitates its cycleability at 2500 mAh/g.**

### *Cathodes–*

- ✦ **Thackeray's Group uses a  $Li_2MnO_3$  precursor in the synthesis of Mn-rich layered-layered material with less voltage fade when cycled.**
- ✦ **Cabana's Group demonstrates that Ni-spinel cycling at 50°C can be improved with the addition of MgO.**

### *Diagnostics–*

- ✦ **Kostecki's Group finds that the addition of LiF or replacement of LiTFSI for  $LiPF_6$  results in an improved SEI on Sn.**

### *Modeling–*

- ✦ **Persson's Group, using GGA and GGA+U, predict the most thermodynamically stable morphology of  $LiMnO_4$ .**

## BATT TASK 1

### CELL ANALYSIS

**TASK 1.1 - PI, INSTITUTION:** Vincent Battaglia, Lawrence Berkeley National Laboratory

**TASK TITLE – PROJECT:** Cell Analysis - Electrode Fabrication and Failure Analysis

**BASELINE SYSTEMS:** Conoco Philips CPG-8 Graphite/1 M LiPF<sub>6</sub>+EC:DEC (1:2)/Toda High-energy layered (NMC)

**BARRIERS:** High energy systems: low energy; moderate cycle life; moderate calendar life

**OBJECTIVES:** There are six overarching objectives associated with this task. 1) To bring fundamental understanding to the electrode fabrication process. 2) To make “good” electrodes and “good” cells. Good electrodes means electrodes that help identify chemical and physical limitations of a material, be it an active or inactive component. Good cells mean that the material is being evaluated in an environment consistent with what is found in a large size, industrially produced cell. 3) Determine the source or sources of electrode and cell failure and provide samples from used cells for diagnostics. 4) Provide a means for testing electrochemical models. 5) Provide a resource for others in the BATT program for making their own cells.

**GENERAL APPROACH:** These objectives are accomplished through methodically changing different aspects of the electrode fabrication process and examining the results of the changes *via* electrochemical, physical, and chemical characterization techniques. They are also carried out through close collaboration with other BATT PIs, publishing and speaking about all of our findings, and the willingness to share our resources and produce electrodes and cells as requested.

**STATUS OCT. 1, 2011:** Powders of LiNi<sub>1/2</sub>Mn<sub>3/2</sub>O<sub>4</sub> from NEI were distributed to interested PIs as well as an electrolyte of 1 M LiPF<sub>6</sub> in EC:DEC 1:2 from Daikin, America. After a large initial capacity loss in a full cell, the NEI high-voltage spinel material shows good cyclability. VC has a higher reduction potential than EC but with slower kinetics. Slow formation processes of cells with and without VC do not show significant differences in the rate of the side reactions.

**EXPECTED STATUS SEP. 30, 2012:** Differences in performance of a baseline electrolyte *versus* a “high-voltage” electrolyte against LiNi<sub>1/2</sub>Mn<sub>3/2</sub>O<sub>4</sub> will be elucidated. The effects of mixing time on electrode uniformity and performance will have been studied. The dissolution of spinel materials will be measured at 55°C.

**RELEVANT USABC GOALS:** PHEV-40: 207 Wh/l; 5000 deep-discharge cycles; 15 years.

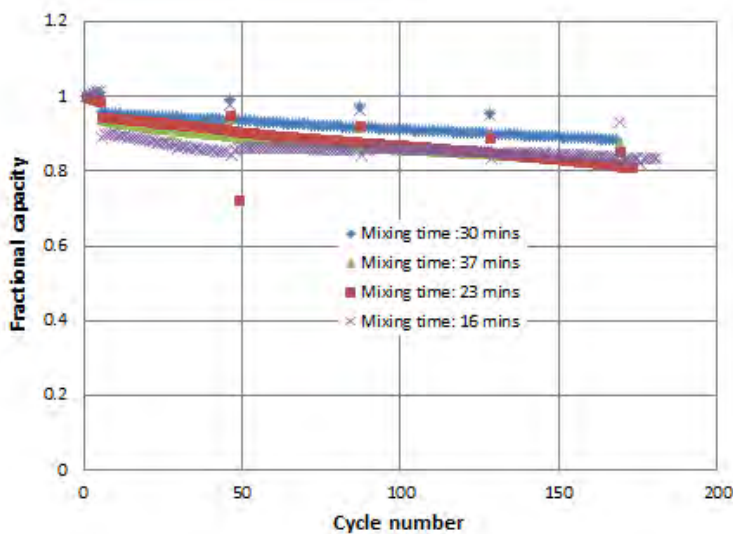
#### MILESTONES:

- (a) Measure the difference in performance of our baseline electrolyte when compared to a high voltage electrolyte from industry. (Dec. 11) **Complete**
- (b) Evaluate the effects of mixing time on cell performance. (Apr. 12) **Complete**
- (c) Compare the rate of side reaction and capacity fade of Gr./NCM\* with and without VC. (Apr. 12) **Complete**
- (d) Measure the rate of dissolution of a spinel material containing Mn. (Sep. 12) **On schedule**

## PROGRESS TOWARD MILESTONES

- a) Measure the difference in performance of our baseline electrolyte when compared to a high voltage electrolyte from industry. Dec. 2011 **Complete** (Reported in Q1 2012).
- b) Evaluate the effects of mixing time on cell performance; Apr. 2012 **Complete**

Positive electrode laminates were prepared with 92.8% NCM, 3.2% acetylene black, and 4% PVDF binder. Mixing times of 16, 23, 30, and 37 mins were used in the preparation of the slurries for casting. All electrodes, upon completion of the casting and initial drying step, were calendared to the same porosity. Coin cells were prepared and cycling tests initiated to understand the difference in performance of the electrodes. The first 10 cycles were performed at C/10; the rest of the cycles were performed at C/2. For the cell that only experienced 16 mins of mixing, there was a large drop in capacity from C/10 to C/2, otherwise the electrodes behaved similarly. In previous research, changes as a result of the method of preparation required over 400 cycles to reveal themselves; therefore, these cells will be allowed to continue to cycle. In the meantime, it was also determined that all four of these mixing times are at least 30% less than what anyone else in the group is accustomed to. It was also



revealed that some group members see a sharp decline in the viscosity from extended mixing, which is believed to be a result of a breakdown in the binder. As a result of the present results and group discussions, it is possible that the present mixing times in the figure are not representative of typical mixing times and may be too close together to show a difference. A new set of electrodes will be fabricated with mixing of one hour and longer and put on test. The possibility of changes to the binder molecular weight as a result of mixing has initiated a complimentary study of binder molecular weight (MW) on electrode performance and cycleability.

revealed that some group members see a sharp decline in the viscosity from extended mixing, which is believed to be a result of a breakdown in the binder. As a result of the present results and group discussions, it is possible that the present mixing times in the figure are not representative of typical mixing times and may be too close together to show a difference. A new set of electrodes will be fabricated with mixing of one hour and longer and put on test. The possibility of changes to the binder molecular weight as a result of mixing has initiated a complimentary study of binder molecular weight (MW) on electrode performance and cycleability.

- c) Compare the rate of side reaction and capacity fade of Gr./NCM with and without VC. April 2012 **Complete** (Reported in 2<sup>nd</sup> Quarterly)
- d) Measure the rate of dissolution of a spinel material containing Mn; Sep. 2012 **On schedule**

**TASK 1.2 - PI, INSTITUTION:** Thomas Richardson, Lawrence Berkeley National Laboratory

**TASK TITLE - PROJECT:** Cell Analysis - Cell and Component Diagnostics

**BASELINE SYSTEMS:** Conoco Philips CPG-8 Graphite/1 M LiPF<sub>6</sub>+EC:DEC (1:2)/Toda High-energy layered (NMC)

**BARRIERS:** Available energy (Goal: 11.6 kWh); Cycle life (Goal: 5,000cycles/58 MWh).

**OBJECTIVES:** Investigate the relationship of structure, morphology and performance of cathode and anode materials. Explore kinetic barriers, and utilize the knowledge gained to design and develop cells with improved energy density, rate performance and stability.

**GENERAL APPROACH:** Employ XRD, visible and electron microscopy, vibrational spectroscopies, and electro-analytical techniques to determine their applicability to BATT goals. Characterize known and modified electrode materials and establish correlations between performance and factors such as crystal structures, morphologies, and surface chemistry. Provide guidelines for materials synthesis and electrode fabrication processes.

**STATUS OCT. 1, 2011:** To have developed new techniques for visualizing the distributions of both materials and charge in lithium battery electrodes. These have been applied to LFP cathodes.

**EXPECTED STATUS SEP. 30, 2012:** Additional methods will have been demonstrated for diagnosis and evaluation of cell components. Charge distribution diagnostics will have been applied to electrodes harvested from commercial cells.

**RELEVANT USABC GOALS:** 40-mile PHEV: Energy/Weight 96 Wh/kg; CD Cycle Life 5000 cycles; Calendar Life @ 40°C 15 years.

**MILESTONES:**

- (a) Complete charge distribution assessments of harvested cathodes. (Mar. 12) **Delayed to Aug. 12 due to XRD equipment breakdown**
- (b) Develop new optical microscopy methods for *in situ* and *ex situ* diagnosis of electrode and separator chemistries. (Aug. 12) **On schedule**

## PROGRESS TOWARD MILESTONES

**Charge distribution:** A 6.6 V, A123 Racing Nanophosphate battery pack was purchased for this study. The pack contained two 1.1 Ah 18650 cells (Fig. 1) rated for discharge at 30 C (continuous), 60 C (pulse). The cells were separated and cycled individually at C/10 to determine their capacity.



**Figure 1.** 1100 mAh 18650 nanophosphate cell.

One cell (1020 mAh) was charged at 400 mA to 3.6 V and held at 3.6 V for 3 h. It was then discharged at 30 A (29.4 C) for 77 s ( $Q_d = 642$  mAh). The voltage (Fig. 2) dropped to 0.53 V, began to rise slightly as the cell became warmer, and recovered rapidly at open circuit to 3.3 V.

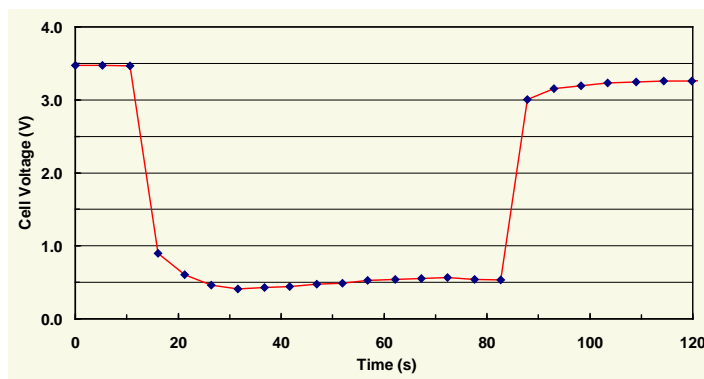


**Figure 2.** Cell voltage during 30 A discharge.

A grinding tool was used to cut open the stainless steel can and the contents were removed without shorting. The double-sided cathode measured 5.6 cm x 70 cm (784 cm<sup>2</sup> total area) and was 200  $\mu$ m thick. A cross section of the dense cathode was obtained by ion milling (Fig. 3).

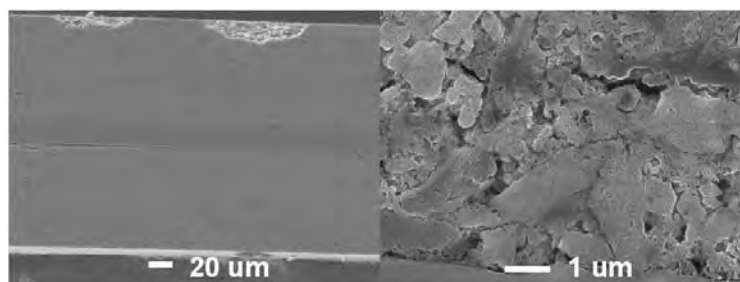


**Figure 3.** SEM cross section of cathode.

The cathode surface was almost uniformly fully discharged, as shown by attenuated total reflectance FTIR measurements at many locations. The in-plane bulk charge distribution was mapped by XRD and by transmission FTIR. Complete results will be reported soon.

A technique for charge distribution mapping using ultrafast laser induced breakdown spectroscopy (LIBS) is in development.

Collaborations: Robert Kosteki, Guoying Chen, Marca Doeff, Vassilia Zorba, Jordi Cabana, Vince Battaglia, the Molecular Foundry, National Center for Electron Microscopy, Advanced Light Source, and the Stanford Synchrotron Radiation Laboratory.

**TASK 1.3 - PI, INSTITUTION:** K. Zaghib, Hydro-Québec (IREQ)

**TASK TITLE PROJECT:** Cell Analysis - Interfacial Processes- SEI Formation and Stability on Cycling

**BASELINE SYSTEMS:** Conoco Philips CPG-8 Graphite/1 M LiPF<sub>6</sub>+EC:DEC (1:2)/Toda High-energy layered (NMC)

**BARRIERS:** Low energy and poor cycle/calendar life

**OBJECTIVES:** Synthesis and evaluation of high voltage cathode (spinel Mn-Ni) with improved electrochemical stability. Reduce the oxidation of the cathode composition, electrolyte, and separator. Find the appropriate alternative anode material composition that meets the requirement for low cost and high energy. Continue the development of binders for the cathode and alternative anode to understand and improve the properties of the SEI layer.

**GENERAL APPROACH:** Our approach is to develop an appropriate method to stabilize the interface reaction of the high voltage oxide (Mn-Ni based like LiMn<sub>1.5</sub>Ni<sub>0.5</sub>O<sub>4</sub>) by surface coating with more stable material like olivine. The emphasis is to improve electrochemical performance at high voltage. Binder type, electrolyte composition, separator will be investigated at this level of voltage. Going with high capacity anode; Si based anode composition will be optimized in terms of particle size (micro vs. nano), graphite and SiO<sub>x</sub> content.

**STATUS OCT. 1, 2011:** Effort is oriented to silicon based anode alloys; LiMn<sub>1.5</sub>Ni<sub>0.5</sub>O<sub>4</sub> based cathode and SEI study and its stabilization. Work will start on these items in August by exploring an appropriate composition of anode material based on carbon coated nano-silicon, SiO<sub>x</sub> and graphite. More work on high voltage cathode will be addressed by reducing its oxidation problem with electrolyte.

**EXPECTED STATUS SEP. 30, 2012:** Due to its low cost and high capacity, the development of silicon-oxide anodes material will continue to achieve the DOE objectives, research will be conducted to find a suitable composition of the Si-based high capacity anode. Different anode composition; pure Si and its mixing with SiO<sub>x</sub> and graphite will be investigated. For the cathode side, as recommended by the DOE, high voltage cathode based on Mn-Ni spinel oxide will be used in this work. In order to reduce the oxidation of the electrolyte at high voltage, some items will be considered; more stable binder, different electrolyte composition, carbon additives and surface coating of this high voltage cathode. With the scope of the work tendency, the investigation of SEI layer on both sides of the anode and cathode is essential. Many parameters will affect this SEI layer; binder type, electrolyte composition, the cathode and anode composition.

**RELEVANT USABC GOALS:** High energy and low cost: 96 Wh/kg (PHEV, 40 miles). Cycle life, calendar life: 15 year life (at 40°C).

**MILESTONES:**

- (a) Identify a candidate of a silicon based composition as anode material. (Mar. 12) **Complete**
- (b) Demonstrate stabilized high-voltage LiMn<sub>1.5</sub>Ni<sub>0.5</sub>O<sub>4</sub> spinel cathode material with surface-coated of ceramic and oxides material. (Sep. 12) **On Schedule**
- (c) Complete the development the *in situ* SEM analysis of the Si-based anode. (Sep. 12) **On Schedule**

## PROGRESS TOWARD MILESTONES

This quarter, the effect of the SiO<sub>x</sub>:graphite ratio on electrode performance was completed; compositions of 50:50, 40:60, 30:70, and 20:80 were studied. These electrodes were prepared with an alginate-based binder. The cycling evaluation was performed in Li cells with EC-DEC-1M LiPF<sub>6</sub> at C/6. A constant voltage (CV) was applied on the discharge step, based on the previous result, where dendrites were formed with cells with CV at 5 mV, the cut-off voltage was fixed at 50 mV. The reversible capacities (mAh/g) were 700, 482, 452, and 420, respectively. However, with a 50 mV cut-off voltage, some capacity, which increased with the graphite content in the electrode, was sacrificed because the capacity associated with the last graphite intercalation stage was still not utilized. The cycling life in Fig. 1 shows quite good stability for some compositions. When the SiO:graphite ratio is higher, the capacity is higher but the cycle life is shorter. This data indicates that a capacity greater than that of graphite can be obtained while avoiding Li dendrite formation. More effort on the anode composition towards optimizing the electrode porosity and performance should be pursued.

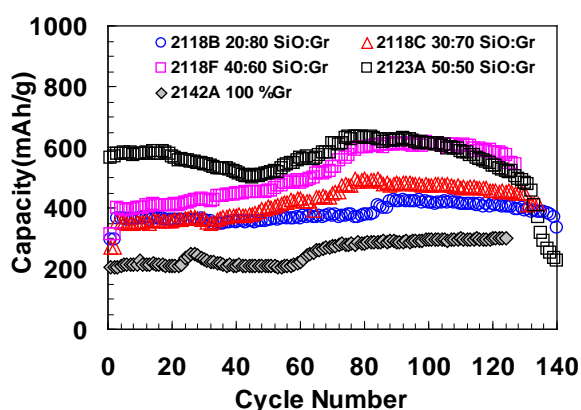


**Figure 1.** Li/EC-DEC-1M LiPF<sub>6</sub>/C-SiO<sub>x</sub>:Gr cells cycled at C/6 at 50 mV cut-off voltages with floating

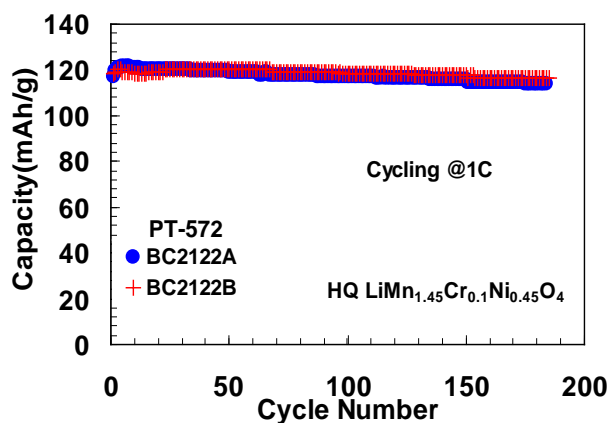


**Figure 2.** Cycling of LiMn<sub>1.45</sub>Cr<sub>0.1</sub>Ni<sub>0.45</sub>O<sub>4</sub>/Li in EC-DEC-LiPF<sub>6</sub>.

Effort was also focussed on doped LiMn<sub>1.5</sub>Ni<sub>0.5</sub>O<sub>4</sub>. To improve cycling, a small amount of Cr, Fe, and Co was substituted for Ni<sup>2+</sup> and Mn<sup>4+</sup> such that the Mn<sup>4+</sup> oxidation state was unchanged (2Cr<sup>3+</sup> = Ni<sup>2+</sup> + Mn<sup>4+</sup>). Neither Co nor Fe doping showed improvement in rate performance or cycleability; however, Cr-doped LMNO showed very good stability. At 25°C, LiMn<sub>1.45</sub>Cr<sub>0.1</sub>Ni<sub>0.45</sub>O<sub>4</sub> obtained by co-precipitation showed outstanding cycleability at 1C. The initial discharge capacity was about 119 mAh/g, and after 185 cycles at a 1C rate it was about 117 mAh/g (Fig. 2). To produce larger batches of this doped material, a solid-state method was adopted, as it possesses a high production yield. The first evaluation of LMnCrNiO from the solid-state method showed slightly lower capacity, but the rate performance was acceptable. Progress continues to improve the synthesis and obtain larger batches for the evaluation by other BATT researchers.

HQ is continuing its collaboration with LBNL researchers Vince Battaglia and Robert Kostecki of the BATT Program. 20 m of laminated film with two different sources of LMNO (NEI and Toda) were coated at HQ and sent to LBNL. LiMnPO<sub>4</sub> and LMNO powders from PNNL were used to prepare LiMnPO<sub>4</sub>-coated LMNO and then returned to PNNL.

**TASK 1.4 - PI, INSTITUTION:** Yet-Ming Chiang, Massachusetts Institute of Technology

**TASK TITLE - PROJECT:** Cell Analysis – New Electrode Design for Ultrahigh Energy Density

**BASELINE SYSTEMS:** Conoco Philips CPG-8 Graphite/1 M LiPF<sub>6</sub>+EC:DEC (1:2)/Toda High-energy layered (NMC)

**BARRIERS:** High energy system: low energy, poor cycle life

**OBJECTIVES:** Develop a scalable high density binder-free low-tortuosity electrode design and fabrication process to enable increased cell-level energy density compared to conventional Li-ion technology for a range of electrode-active materials. Characterize transport properties in high voltage Ni-Mn spinel.

**GENERAL APPROACH:** Fabricate high density sintered cathodes and anodes with controlled pore volume fraction and pore topology. Electrochemically test electrodes in laboratory half-cells and small lithium ion cells (<100 mAh), and model electrode response. Aim to increase cell-level specific energy and energy density by maximizing electrode density and thickness, under operating conditions commensurate with USABC targets for PHEV and EV. Titrate Li content in pure single phase sintered porous electrodes while measuring electronic and ionic transport.

**STATUS OCT. 1, 2011:** 1) Fabrication and testing of at least two cathode materials in the proposed high density low tortuosity electrode approach; 2) Development of methodology for measurement of electronic conductivity vs. Li concentration in porous sintered electrodes.

**EXPECTED STATUS SEP. 30, 2012:** 1) Conclude electrode fabrication and electrochemical testing in at least one targeted cathode compound; 2) Fabrication and testing of high density low tortuosity electrodes of at least one anode compound; 3) Conclude measurement of electronic conductivity vs.  $x$  in sintered undoped Li <sub>$x$</sub> Ni<sub>0.5</sub>Mn<sub>1.5</sub>O<sub>4</sub>

**RELEVANT USABC GOALS:** EV: 200 Wh/kg; 1000 cycles (80% DoD).

**MILESTONES:**

- (a) Demonstrate >80% capacity retention at 2C rate in additive-free low tortuosity LiCoO<sub>2</sub> electrode of >50 vol% density and >200  $\mu$ m thickness. (Oct. 11) **Complete**
- (b) Complete measurement of electronic conductivity vs.  $x$  in sintered undoped Li <sub>$x$</sub> Ni<sub>0.5</sub>Mn<sub>1.5</sub>O<sub>4</sub>. (Jan. 12) **Complete**
- (c) Complete measurement of electronic conductivity vs.  $x$  in sintered Li<sub>4</sub>Ti<sub>5</sub>O<sub>12</sub> anode. (Jan. 12) **Complete**
- (d) Develop tortuosity measurement for freeze-cast/sintered cathodes. (Mar. 12) **Complete**
- (e) Complete process development study for directionally freeze-cast and sintered LiNi<sub>0.5</sub>Mn<sub>1.5</sub>O<sub>4</sub> cathodes. (Jun. 12) **Complete**

## PROGRESS TOWARD MILESTONES

Collaborator: Antoni P. Tomsia (LBNL)

**Accomplishments:** During the present reporting period, progress was made in measuring electronic and ionic transport in  $\text{Li}_{1-x}\text{Ni}_{0.5}\text{Mn}_{1.5}\text{O}_4$ . The approach used was to sinter the starting powders with a maximum firing temperature of 900 or 1000°C, followed by a 24h hold at 650°C in those cases where the ordered phase was desired. Electrochemical delithiation to a range of  $x$  values was conducted, after which the samples were cleaned and dried for *ex situ* measurement. Silver was used as blocking electrodes for the measurement of electronic conductivity and a PEO-based solid polymer electrolyte for the ionic conductivity measurements, the latter being conducted at *ca.* 50°C to ensure sufficient ionic conductivity. Representative results are shown in Fig. 1. In ordered samples, the electronic conductivity increased monotonically with increasing  $x$ , with the exception of an anomalous result for the  $x=0.60$  sample, which may be due to a fractured sample. In delithiated samples, the activation energy decreases to 0.30 to 0.37eV from 0.53eV.

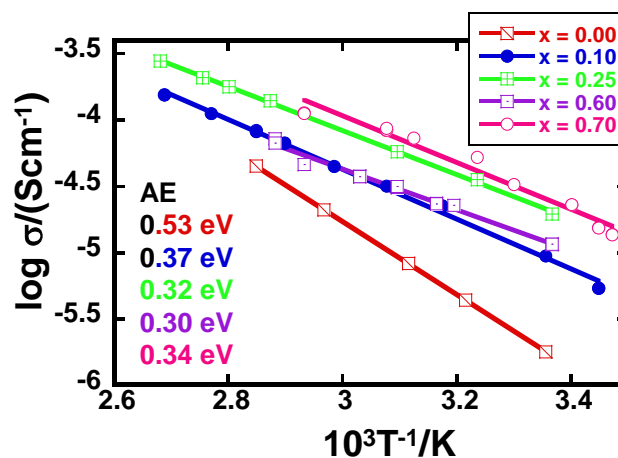


Figure 1.

The ionic conductivity of as-sintered samples of both ordered and disordered spinel (at  $x = 0$ ) was measured using dc polarization (example shown in Fig. 2) and ac impedance spectroscopy. Good agreement was obtained between the two methods, with the ionic conductivity being *ca.*  $4 \times 10^{-8}$  S/cm at *ca.* 50°C, about  $10^3$  times lower than the electronic conductivity at the same temperature. The chemical diffusion coefficient at the same temperature is *ca.*  $10^{-7}$   $\text{cm}^2/\text{s}$ . Within experimental variability, no significant difference was found between the ordered and disordered spinel. These are, to our knowledge, the first direct ionic conductivity measurements of the high voltage spinel in the absence of electrochemical reactions, which in this system is accompanied by a phase transition. The results indicate that, at least at small  $x$ , the chemical diffusion coefficient is limited by ion transport.

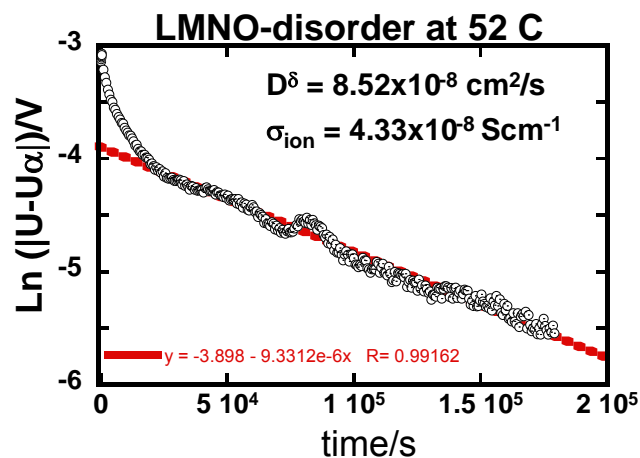


Figure 2.

**TASK 1.5 - PI, INSTITUTION:** Gao Liu, Lawrence Berkeley National Laboratory

**TASK TITLE - PROJECT:** Cell Analysis - Advanced Binder for Electrode Materials

**BASELINE SYSTEMS:** Conoco Philips CPG-8 Graphite/1 M LiPF<sub>6</sub>+EC:DEC (1:2)/Toda High-energy layered (NMC)

**BARRIERS:** High energy system: poor cycle life, high first cycle irreversible capacity, low coulomb efficiency.

**OBJECTIVES:** Develop new conductive polymer binder materials to enable large volume change lithium storage materials to be used in lithium-ion electrode.

**GENERAL APPROACH:** Use functional polymer design and synthesis to develop new conductive polymers with proper electronic properties, strong adhesion and improved flexibility to provide electric pathways in the electrode, and to accommodate large volume/phase change of the active material during lithium insertion and removal.

**STATUS OCT. 1, 2011:** Gained fundamental understanding of the Si particle surface properties to the electrode performance characteristics; developed HF etching process to clean off SiO<sub>2</sub> surface layer for improved initial performance; demonstrated change of porosity of the cycled Si/conductive polymer electrode as a main issue to prevent high loading electrode from stable cycling, demonstrated over 600 cycles of the Si/conductive polymer composite electrode between 0.01-1V vs. Li/Li<sup>+</sup> with less than 15% capacity loss, and demonstrated initial cycling performance of the Sn/conductive binder electrode.

**EXPECTED STATUS SEP. 30, 2012:** Investigate conductive binder properties to Si electrode performance in various electrode compositions and configurations; explore electrolyte and additives to increase coulomb efficiency; and explore the conductive binders in other high capacity material systems.

**RELEVANT USABC GOALS:** PHEV-40: 144 Wh/l, 4000 deep-discharge cycles.

**MILESTONES:**

- (a) Continue to optimize the Sn/conductive binder electrode system to achieve 600 mAh/g-Sn specific capacity cycling. (Mar.12) **Complete**
- (b) Study conductive binder properties to Si electrode performance in various electrode compositions and configurations, aim to achieve 3.5 mAh/cm<sup>2</sup> loading electrode. (Sep. 12) **On schedule**
- (c) Develop one type of electrolyte additives and select Si materials to minimize side reactions, and increase coulombic efficiency to 99.5%. (Sep. 12) **On schedule**

## PROGRESS TOWARD MILESTONES

A systematic study has been performed to characterize the PFFOMB/Sn system. The SEM images of the electrodes with different combinations of PFFOMB/Sn are provided in Fig. 1. Due to the high density ( $7.0 \text{ g/cm}^3$ ) of the Sn particles, 10% polymer by weight is equivalent to over 30% by volume. The SEM images clearly show the 10% PFFOMB/Sn electrode sample has extensive coverage of polymer on the Sn particles. This extensive coverage leads to higher impedance at the interface between the electrolyte and the Sn particles, resulting in fast capacity fade. The 2% PFFOMB sample has a low polymer content and is the main reason the electrode fails rapidly from cycling. The 5% binder performs the best among the three compositions; however, extended cycling of the electrode leads to particle reorganization in the binder and possible Sn aggregation. The reorganization and aggregation leads to separate domain structures that are binder rich and Sn rich. This may create a situation that the binder-rich regions isolate the Sn-rich domains from effective Li-ion access from the electrolyte.

The aggregation of Sn particles is also detected by the TEM analysis of the electrode composite before and after cycling. The Sn particles are spherical before cycling but become irregular after cycling. The cycled particles are also closer to each other than they were before cycling. The dynamic change of the composite electrode during cycling is believed responsible for the capacity fade.

[1] PFFOMB stands for Poly(9,9-dioctylfluorene-co-fluorenone-co-methylbenzoic ester).

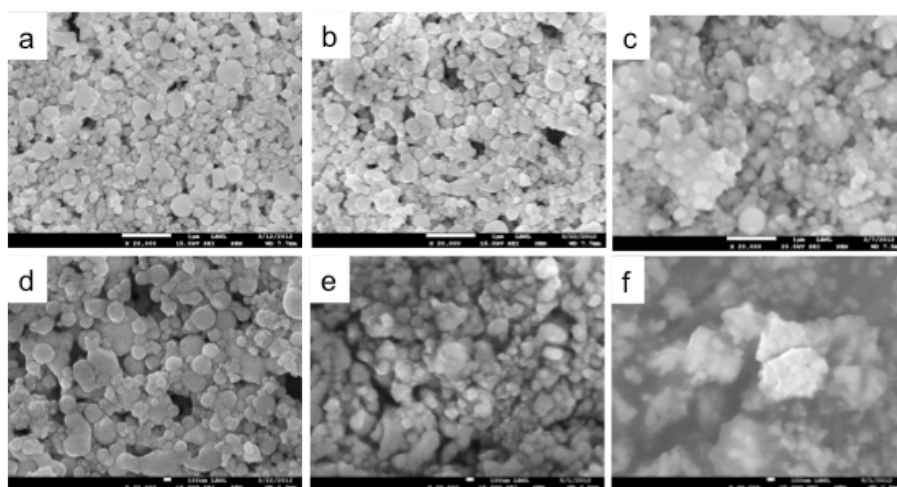


**Figure 1.** SEM images of the new PFFOMB/Sn electrode surface, PFFOMB content by weight is 2% (a); 5% (b); 10% (c); 5% PFFOMB electrode, new (d); after 1 cycle (e); after 10 cycles (f).

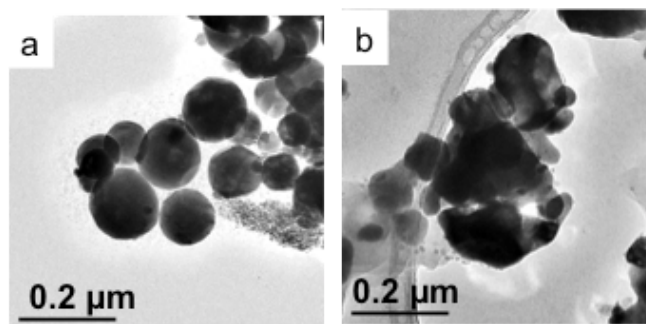


**Figure 2.** TEM image of the Sn particles in the new electrode (a) and after 10 cycles.

**TASK 1.6 - PI, INSTITUTION:** Guoying Chen, Lawrence Berkeley National Laboratory

**TASK TITLE - PROJECT:** Cell Analysis - High-Energy Cathodes - Improving Performance, Safety, and Cycle Life through Structure and Morphology Design

**BASELINE SYSTEMS:** Conoco Philips CPG-8 Graphite/1 M LiPF<sub>6</sub>+EC:DEC (1:2)/Toda High-energy layered (NMC)

**BARRIERS:** Available energy (Goal: 11.6 kWh); Cycle life (Goal: 5,000 cycles/58 MWh).

**OBJECTIVES:** Identify phase transition mechanisms and kinetic barriers of high voltage and high capacity cathode materials. Establish direct correlations between crystal structure, composition, morphology, performance and stability. Provide guidelines to design and fabricate cathode materials with improved energy density, rate capability and safety, especially with regard to thermal stability.

**GENERAL APPROACH:** Prepare well-formed crystals with various structure, composition, size and morphology using wet synthesis routes, such as solvothermal and molten salt methods. Characterize their physical properties and investigate their solid state chemistry using advanced spectroscopic, spectromicroscopic, scanning calorimetry and electron microscopic techniques.

**STATUS OCT. 1, 2011:** Overlithiation in Li<sub>1+x</sub>(Ni<sub>0.33</sub>Mn<sub>0.33</sub>Co<sub>0.33</sub>)<sub>1-x</sub>O<sub>2</sub> (NMC333) was found to increase extractable Li in the structure and energy density of the cathode. Increasing Mn content in the overlithiated NMC333 improves rate capability but decreases the stability of the initial O3 phase, which transforms to P3 structure upon deep Li extraction. The irreversible charging plateau observed at high voltage was attributed to overlithiation in Li<sub>1+x</sub>M<sub>1-x</sub>O<sub>2</sub>. LiNi<sub>0.5</sub>Mn<sub>1.5</sub>O<sub>4</sub> single crystals were synthesized in a variety of sizes and shapes, with the best performance achieved with the octahedral micron-sized crystals. Large crystals with a range of Mn<sup>3+</sup> content were prepared by varying the Ni/Mn ratio in LiNi<sub>x</sub>Mn<sub>2-x</sub>O<sub>4</sub>. Synthesis precursors were found to influence the transition-metal ordering in the prepared spinel.

**EXPECTED STATUS SEP. 30, 2012:** The effect of structural, composition and morphological changes during Li extraction and insertion in Li<sub>1+x</sub>M<sub>1-x</sub>O<sub>2</sub> will have been further evaluated. Oxygen evolution mechanism and kinetics will have been investigated. The effect of particle size and morphology on oxide activation process and electrode stability will have been revealed. The impact of Mn<sup>3+</sup> content on property and performance of LiNi<sub>x</sub>Mn<sub>2-x</sub>O<sub>4</sub> cathode will have been established, and the kinetics of structural disordering in the spinel examined.

**RELEVANT USABC GOALS:** PHEV: 96 Wh/kg, 5000 cycles; EV: 200 Wh/kg; 1000 cycles (80% DoD)

**MILESTONES:**

- (a) Investigate the kinetics of order/disorder transitions in LiNi<sub>x</sub>Mn<sub>2-x</sub>O<sub>4</sub>. (Mar. 12) **Complete**
- (b) Determine the effect of Mn<sup>3+</sup> content on property and performance of the spinels. (Jun. 12) **Complete**
- (c) Investigate the mechanism and kinetics of delithiation/relithiation on oxide crystals. (Aug. 12) **On schedule**
- (d) Synthesize at least four oxide crystal samples with different physical characteristics. (Sep. 12) **On schedule**

## PROGRESS TOWARD MILESTONES

**Ni/Mn Spinels:** Previously, a series of 2- $\mu\text{m}$  sized, octahedral  $\text{LiNi}_x\text{Mn}_{2-x}\text{O}_4$  ( $0.3 \leq x \leq 0.5$ ) single crystals were prepared and their structural and kinetic properties were compared. The team demonstrated that FTIR is an effective qualitative technique to measure transition-metal ordering in Ni/Mn spinels, with validation provided by  $^6\text{Li}$  MAS NMR. In this quarter, the effect of  $\text{Mn}^{3+}$  content on structure, redox properties, and rate capabilities of the spinels was evaluated by varying the cycling rate of  $\text{LiNi}_x\text{Mn}_{2-x}\text{O}_4$  ( $0.3 \leq x \leq 0.5$ ) half-cells between 3.0 and 5.0 V. In the integrated capacity and voltage profiles (Fig. 1a), the peak separations between the  $\text{Ni}^{2+}/\text{Ni}^{3+}$  and  $\text{Ni}^{3+}/\text{Ni}^{4+}$  redox couples at 4.7 V were 20, 21, and 27 mV for  $x=0.5, 0.45,$  and  $0.4,$  respectively. The separation increased to 60 and 63 mV for  $x=0.35$  and  $0.3,$  suggesting a rapid decrease in transition metal ordering below a critical Ni content. The results are consistent with our FTIR and  $^6\text{Li}$  MAS NMR observations and demonstrated the excellent correlation between the three techniques. At  $x=0.3$  and  $0.35,$  the two peaks at 4.7 V were largely asymmetric, and significant lower-voltage peak broadening was observed. This suggests the existence of a solid-solution region during low SOC Li intercalation and deintercalation in the disordered spinels. While the structurally more ordered spinels transform through two 2-phase transitions, indicated by the two sets of sharp redox peaks at 4.7 V, the disordered only go through one 2-phase transition. These differences dramatically affect transport properties, as evidenced by the rate capability study (Fig. 1b). The disordered spinels consistently delivered higher capacities than the more ordered ones, and the best performance was obtained from  $x=0.30$  with the highest  $\text{Mn}^{3+}$  content. Among the three ordered spinels, the sample with  $x=0.5$  and the lowest  $\text{Mn}^{3+}$  content showed the best performance at nearly all rates tested, suggesting  $\text{Mn}^{3+}$  may play a different role in the ordered spinels. By eliminating the influences of crystal size and morphology in this single-crystal study, the significance of structural ordering, phase transformation mechanism is clearly shown.

Broad peaks at 4.1 V, which are characteristic of the  $\text{Mn}^{3+}/\text{Mn}^{4+}$  redox couple (Fig. 1a), were integrated to estimate the  $\text{Mn}^{3+}$  content in the crystals. The  $\text{Mn}^{3+}$  concentrations were 1.5, 4.0, 9.0, 15 and 19.3% for  $x=0.5, 0.45, 0.4, 0.35,$  and  $0.3$  respectively. The results correlate well with the peak ratio of 620/590 in the FTIR patterns (Fig. 1c), suggesting that FTIR may also be used to estimate  $\text{Mn}^{3+}$  content. This report completes the work toward milestone (b) in FY2012.

**Collaborations this quarter:** Richardson, Grey, Cabana, Kostecki, Doeff, Battaglia, Chiang, Lucht, and NCEM.

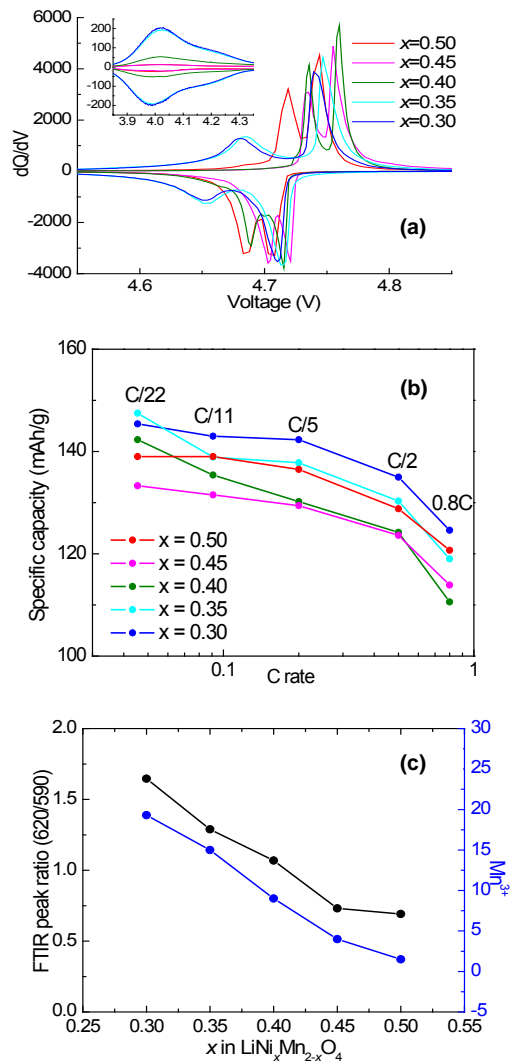


**Figure 1.** a) Integrated capacity and voltage profiles obtained at C/22, b) rate capability comparison, and c) relationship between the FTIR peak ratio and  $\text{Mn}^{3+}$  content in  $\text{LiNi}_x\text{Mn}_{2-x}\text{O}_4$  crystals.

## **BATT TASK 2** **ANODES**

**Task 2.1-PI, INSTITUTION:** Jack Vaughey, Argonne National Laboratory

**TASK TITLE:** Anodes: Novel Anode Materials

**BASELINE SYSTEMS:** Conoco Philips CPG-8 Graphite/1 M LiPF<sub>6</sub>+EC:DEC (1:2)/Toda High-energy layered (NMC)

**BARRIERS:** Low energy, poor low-temperature operation, and abuse tolerance limitations

**OBJECTIVES:** To address and overcome the electrochemical capacity limitations (both gravimetric and volumetric) of conventional carbon anodes by designing electrode architectures containing main group metal, metalloid or intermetallic components that can tolerate the volumetric expansion of the materials and provide an acceptable cycle life.

**GENERAL APPROACH:** Our approach is to search for anode materials or formulations that provide an electrochemical potential a few hundred mV above the potential of metallic Li. Effort will be predominantly on Sn- and Si-based systems. A major thrust will be to design new electrode architectures in which an electrochemically active species is attached to the surface of a porous current collector providing a strong connection from the active species to the substrate. Such an approach minimizes the need for conductive additives and increases the power capabilities of these high energy anodes.

**STATUS OCT. 1, 2011:** A series of new electrode structures will have been synthesized and evaluated that use elemental silicon and tin as the active material. The energy and power advantages of three-dimensional electrode architectures when compared to two dimensional anode structures will be quantified. Electrodes that utilize metallic copper as both the binder and conductive additive will have been evaluated. Methods to create the three dimensional copper current collector around the active materials, notably silicon, will have been developed.

**EXPECTED STATUS SEP. 30, 2012:** The interfacial structure of silicon-based electrodes bound to the substrate using metallic binders will have been determined. Studies will have been initiated on the deposition of silicon and tin into porous substrates and developed characterization tools to study active material/current collector interactions and their effect on cycle life and fade rate.

**RELEVANT USABC GOALS:** 200 Wh/kg (EV requirement); 96 Wh/kg, 316 W/kg, 3000 cycles (PHEV 40 mile requirement). Calendar life: 15 years. Improved abuse tolerance.

### **MILESTONES:**

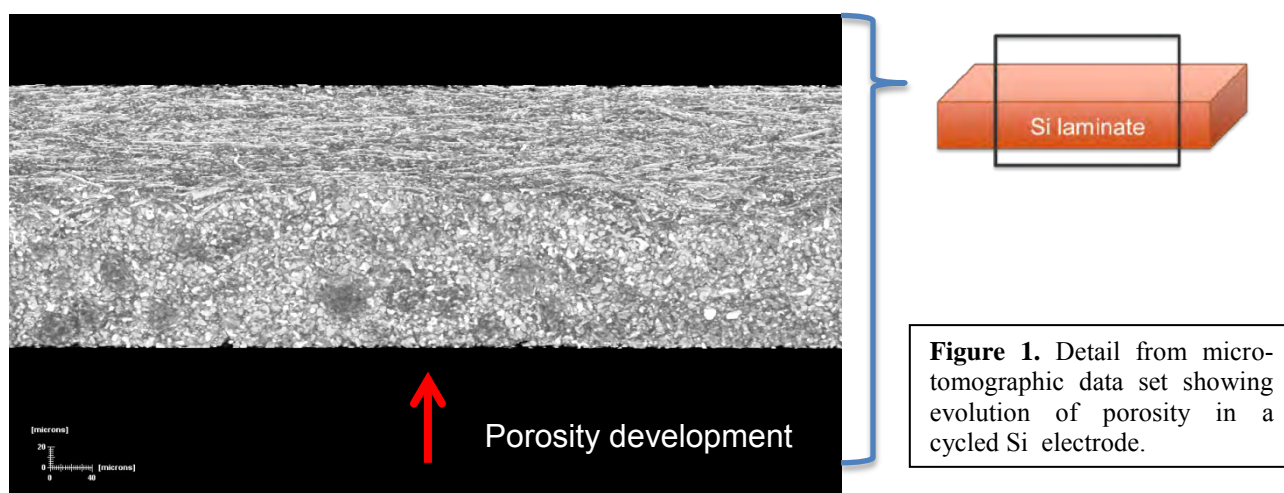
- (a) Complete characterization of the interfacial region in Cu-Si metallic electrodes. (Mar. 12) **Complete**
- (b) Characterize the phases formed and extent of electrode homogeneity for a series of electrodeposited Sn-based electrodes. (Sep. 12) **On schedule**
- (c) Assess the role of electrolytes and irreversible capacity and SEI formation in three-dimensional electrode structures. (Sep. 12) **On schedule**
- (d) Demonstrate the benefit of polymeric surface coatings on the cycle life of three-dimensional electrode structures. (Sep. 12) **On schedule**

## PROGRESS TOWARD MILESTONES

Team: Fikile Brushett, Fulya Dogan, Lynn Trahey, Jack Vaughey (ANL)

As part of our study into the relationship between three-dimensional electrode structure and cycling, the team is developing several tomographic tools to look for the effects of electrochemical testing. In the previous report, a description of the instrumentation and testing procedures developed by the team were described. Building on the advances made earlier, a review was performed of a series of Si-based electrodes fabricated following industry-based standards: 20  $\mu\text{m}$  commercial Si powders (70%), 15% PVdF binder, and 15% carbon black conductive additive. These electrodes were cycled using a 20  $\mu\text{A}$  current and Gen2 (1.2M  $\text{LiPF}_6$  3:7 EC/EMC) electrolyte in the range of 0 to 2V. Cycling behavior was typical of Si-based electrodes.

For the study, Si laminates were imaged before and after cycling in order to look for changes resulting from cycling on overall electrode structure. After several cycles, observations could be made that related to the utility of the electrode formulations. One of the most relevant observations, Fig. 1, was the front surface of the electrode which had developed a higher level of porosity than the middle or rear of the electrode. This evolution in porosity may result from the more rapid lithiation of the surface particles compared to the bulk, resulting in faster local volume expansion with all the resulting stresses built up being released as particle pulverization. This may even occur in cells cycled to a limited capacity (below theoretical capacity) as formation of  $\text{Li}_{15}\text{Si}_4$ , the crystalline end member of the cycling process. Similar stresses and preferential lithiation of the surface *versus* the bulk has been observed for various Li-Mn-O spinels. The results to date lead us to believe that re-formulating the electrode lamination process would be beneficial to the overall performance.



One direction presently being pursued, in association with Gao Liu (LBNL), is to use nanoparticle Si. These materials are below the size threshold where the strain and stress of lithiation will break apart the particles, thus stabilizing the binder connectivity. However, as these smaller particles are much more air sensitive, their electrochemical activity is more variable and difficult to control. This is in addition to issues with binders being able to control particle movement unless utilized at much lower active material levels. In association with this study, methods to look at these laminates *in situ* while cycling are underway. Preliminary effort has shown that under these conditions, the electrolyte has been sufficiently stable to the beam to warrant further tool development.

**TASK 2.2 - PI, INSTITUTION:** Stanley Whittingham, Binghamton University

**TASK TITLE - PROJECT:** Anodes – Metal-based High Capacity Li-ion Anodes

**BASELINE SYSTEMS:** Conoco Philips CPG-8 Graphite/1 M LiPF<sub>6</sub>+EC:DEC (1:2)/Toda High-energy layered (NMC)

**BARRIERS:** Cost, safety and volumetric capacity limitations of lithium-ion batteries

**OBJECTIVES:** To replace the presently used carbon anodes with safer materials that have double the volumetric energy density, and will be compatible with low cost layered oxide and phosphate cathodes and the associated electrolyte.

**GENERAL APPROACH:** Our anode approach is to synthesize, characterize and develop inexpensive materials that have a potential around 500 mV above that of pure lithium (to minimize risk of Li plating and thus enhance safety) and have higher volumetric energy densities than carbon. Emphasis will be placed on simple metal alloys/composites at the nano-size. Tin will initially be emphasized, building on what was learnt from our studies of the tin-cobalt anode, the only commercial anode besides carbon. All materials will be evaluated electrochemically in a variety of cell configurations, and for thermal, kinetic and structural stability to gain an understanding of their behavior.

**STATUS OCT. 1, 2011:** It has been shown that bulk crystalline metals have a high capacity, react readily with lithium but that their capacity faded rapidly after several deep cycles in carbonate-based electrolytes; their behavior was no better under shallow cycling. In contrast, it has been shown that amorphous nano-size tin alloys, unlike pure tin, have a high capacity and maintain it on deep or shallow cycling, when stabilized with elements like cobalt. A nano-tin material that shows electrochemical behavior comparable to that of the Sn-Co alloy but without the need for cobalt was successfully formed by mechanochemical synthesis. It has also been shown that small amounts of silicon enhance the cyclability of aluminum.

**EXPECTED STATUS SEP. 30, 2012:** Our proposed work will result in the development of durable metal-based Li-ion battery anodes with volumetric energy densities that approach double those of the state-of-the art carbons. Nano-tin materials will have been synthesized by at least two different approaches and then characterized, to determine their morphology and electrochemical behavior. Clues as to how to control the SEI on such materials to optimize lifetime will have been gathered.

**RELEVANT USABC GOALS:** 5000 deep and 300,000 shallow discharge cycles, abuse tolerance to cell overcharge and short circuit, and maximum system volume.

**MILESTONES:**

- (a) Synthesize a nano-size Sn material by a second method. (Dec. 11) **Complete**
- (b) Have the nano-size Sn meet the gravimetric capacity of the Sn-Co-C electrode and exceed the volumetric capacity of the Conoco Philips CPG-8 Graphite. (Mar. 12) **Complete**
- (c) Determine the limitations to the electrochemical behavior of the mechanochemical Sn; characterize these materials and determine their electrochemical behavior. (Sep. 12) **On schedule**
- (d) Determine the electrochemistry of a new synthetic nano-Si material. (Sep. 12) **On schedule**

## PROGRESS TOWARD MILESTONES

The goal of this project is to synthesize new tin- and silicon-based anodes that have double the volumetric capacity of the present carbons, without a loss of gravimetric capacity.

**Milestone (d):** This quarter reports a synthesis of a new synthetic nano-Si material and initial electrochemical measurements on it. A low-cost Al-Si engine-block alloy was used as the starting material. The powder was etched in aqueous HCl acid, resulting in the selective dissolution of the Al. The XRD pattern showed just peaks from the Si phase. The nanostructured porous Si sphere was retained after the etching as indicated in Fig. 1 (left). Overnight etching with vigorous stirring caused these spheres to break. The average crystallite size of the Si in both the initial Al-Si powder and the etched sample is around 20 nm, as determined using the Scherrer Equation, and hence showing no change in size during the Al removal.

The electrochemical behavior of this porous Si material is shown in Fig. 1 (right). On Li insertion, 2.8 Ah of Li were inserted per gram of Si spheres and 2.1 Ah of the Li was removed in the first cycle. The capacity dropped to 1.5 Ah/g in the first 3 cycles, but then stabilized. After more than 60 cycles, the capacity was still 1.15 Ah/g. The coulombic efficiency of the broken Si, as indicated in the figure, was 76.5% in the first cycle and rose to 99% after 10 cycles.

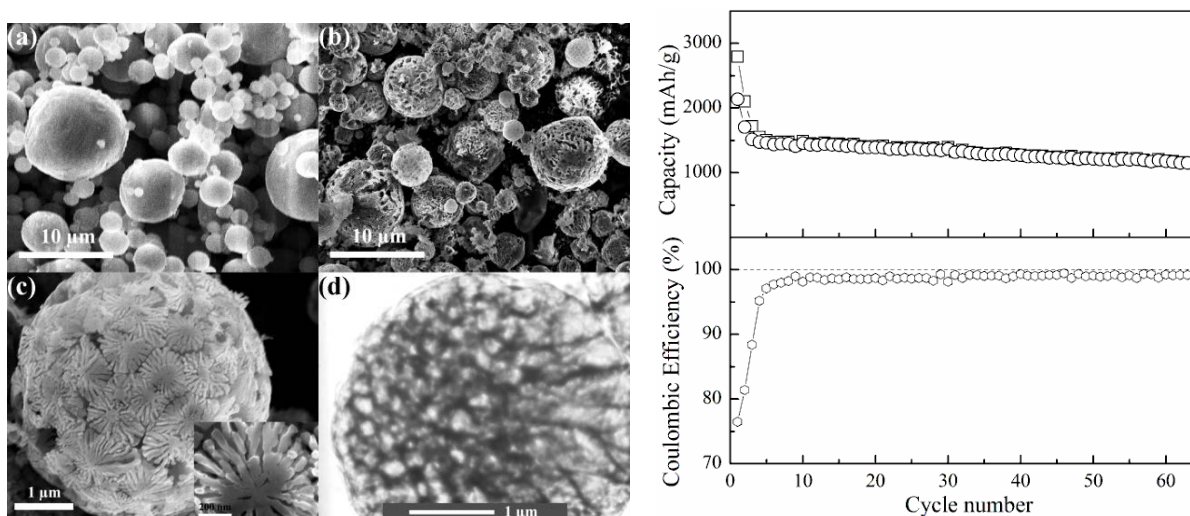


**Figure 1.** (left) SEM of (a) initial Al-Si, and of (b) and (c) porous Si spheres; (d) TEM of the Si spheres; (right) Electrochemical cycling of the porous Si spheres material at  $0.5 \text{ mA/cm}^2$  between  $0.01 \text{ V} \sim 1.5 \text{ V}$ . First cycle current density was  $0.3 \text{ mA/cm}^2$ . The electrodes were made of Si, carbon black additive, and binder in a weight ratio of 70:20:10. Capacities were calculated based on the weight of Si ( $2 \text{ to } 3 \text{ mg/cm}^2$ ).

**Further plans to meet or exceed milestones:** None

**Reason for changes from original milestones:** None

### Publications and Presentations:

1. Wenchao. Zhou, Ruigang Zhang, Shailesh Upreti, and M. Stanley Whittingham, "Sn-Fe Nano-Materials as Anodes for Li-Ion Batteries," Materials Research Society, San Francisco, April 2012.

**Task 2.3-PI, INSTITUTION:** Prashant N. Kumta, University of Pittsburgh

**TASK TITLE:** Anodes – Nanoscale Heterostructures and Thermoplastic Resin Binders: Novel Li-ion Anode Systems

**BASELINE SYSTEMS:** Conoco Philips CPG-8 Graphite/1 M LiPF<sub>6</sub>+EC:DEC (1:2)/Toda High-energy layered (NMC)

**BARRIERS:** Low specific energy and energy density, poor cycle life and coulombic efficiency, large irreversible loss, poor rate capability, and calendar life.

**OBJECTIVES:** To identify new alternative nanostructured anode materials to replace graphite that will provide higher gravimetric and volumetric energy density. The objective is to replace carbon with an inexpensive nanostructured composite exhibiting higher capacity (1200 mAh/g) than carbon while exhibiting similar irreversible loss (<15%), coulombic efficiency (>99.9%), and cyclability. The project addresses the need to improve the capacity, specific energy, energy density, rate capability, cycle life, coulombic efficiency, and irreversible loss limitations of silicon based electrodes.

**GENERAL APPROACH:** Our approach is to search for inexpensive silicon, carbon, and other inactive matrix based composites (powders rather than thin films) that provide 1) an electrochemical potential a few hundred mV above the potential of Li, and 2) a capacity of 1200 mAh/g or greater (>2600 mAh/ml). Research will be focused on exploring novel economical methods to generate nanoscale heterostructures of various Si nanostructures and different forms of C derived from graphitic carbon, nanotubes (CNT) and new binders. Other electrochemically inactive matrices will also be explored. Promising electrodes will be tested in half cells against Li and compared to graphite as well as in full cells. Electrode structure, microstructure, rate capability, long and short term cyclability, coulombic efficiency, SEI origin and nature will also be studied.

**STATUS OCT. 1, 2011:** Nano-scale electrodes comprising Si-graphitic carbon-polymer derived C, and CNT related systems have been successfully synthesized and analyzed in half cells. The nano-composite Li-Si-C hetero-structures exhibit stable capacities of 700-3000 mAh/g.

**EXPECTED STATUS SEP. 30, 2012:** Efforts will continue to generate nano-composite ‘core-shell’, random, and aligned structures of varying nanoscale Si morphologies, boron (B), and C nanotubes exhibiting 1500 mAh/g and higher capacities. Research will be conducted to generate novel binders, study the synthesis conditions, nano-scale microstructure affecting the energy density, rate capability, first cycle irreversible loss and coulombic efficiency, characterize the SEI layer, and outline steps to yield stable capacity, reduce irreversible loss and increase coulombic efficiency.

**RELEVANT USABC GOALS:** Available energy for CD Mode, 10 kW Rate: 3.4 kWh (10 mile) and 11.6 kWh (40 mile); Available Energy for CS Mode: 0.5 kWh (10 mile) and 0.3 kWh (40 mile); 10s peak pulse discharge power: 45 kW (10 mile) and 38 kW (40 mile); Peak Regen Pulse Power (10 sec): 30 kW (10 mile) and 25 kW (40 mile); Cold cranking power at -30°C, 2sec-3 Pulses: 7kW; Calendar life: 15 years (at 40°C); CS HEV Cycle Life, 50 Wh Profile: 300,000 Cycles

**MILESTONES:**

(a) Achieve stable reversible capacity of 1500 mAh/g or higher (Mar. 12). **Reversible capacity achieved, stability on schedule for Sep. 12**

(b) Achieve irreversible loss ( $\leq 15\%$ ) and efficiency ( $\geq 99.95\%$ ) to match carbon (Sep. 12). **On schedule**

## PROGRESS TOWARD MILESTONES

In earlier reports (Q2, 2012) hierarchical structures comprised of vertically aligned carbon nanotubes (VACNTs), a thin layer of an additive serving as an interface control agent (ICA), and Si was studied in order to see improvements of the interfacial strength of the Si/VACNT materials. Briefly, VACNTs were grown on quartz substrates using a floating catalyst-based liquid injection chemical vapor deposition method (LICVD). The ICA (10 nm thick) was deposited onto these VACNTs using e-beam evaporation. Finally, Si was deposited by thermal decomposition of silane ( $\text{SiH}_4$ ) in a low pressure CVD system. Raman spectra obtained on the Si film (Fig. 1) shows the presence of a broad peak at *ca.*  $470\text{ cm}^{-1}$  that corresponds to the transverse optical (TO) mode of amorphous Si. An absence of a sharp peak at  $520\text{ cm}^{-1}$ , which is a characteristic of TO mode for crystalline Si, confirms that the deposited Si is completely amorphous. Electrochemical cyclic response (Fig. 2) of the obtained CNT/ICA/Si heterostructures, cycled at a discharge/charge rate of *ca.*  $300\text{ mA/g}$  in the potential window between  $0.02$  to  $1.2\text{ V}$  vs.  $\text{Li}^+/\text{Li}$ , shows a first discharge capacity of *ca.*  $3240\text{ mAh/g}$  with a very low first-cycle irreversible loss of *ca.*  $12\%$ . At the end of 25 cycles, a reversible capacity *ca.*  $2500\text{ mAh/g}$  capacity was obtained with a very low fade in capacity of *ca.*  $0.3\%$  loss per cycle and high coulombic efficiency (*ca.*  $99.8\%$ ). Studies are currently on-going to ascertain the effect of the ICA upon the cycling behavior, coulombic efficiency, and adhesion of Si films to the VACNTs. A detailed high-resolution TEM study will be performed on CNT/ICA/Si to understand the origin of the low first-cycle irreversible (FIR) loss (possibly due to stable SEI) observed in the present system, which will enable the design of the surface structure and morphology of the other high capacity, long cycle life anodes.

Despite showing promise, direct, low-cost, large-scale synthesis of (*a/nc*)-Si/ICA/CNT is a major challenge. Hence, composites based on (*a/nc*)-Si/ICA/ $\text{MO}_x$  where  $\text{MO}_x$  is a metal oxide with varying stoichiometry has been suggested for future study to alleviate the high cost of CNT production. In this report, preliminary results on the synthesis of (*a/nc*)-Si/ $\text{MO}_x$  by low-cost mechano-chemical reduction and the electrochemical response of the (*a/nc*)-Si/ $\text{MO}_x$  has been presented. As an example, the team has successfully synthesized *nc*-Si/ $\text{MO}_x$  by direct mechanochemical reduction of SiO with the metallic component, M, as follows:  $x\text{SiO} + \text{M} \rightarrow x\text{Si} + \text{MO}_x$ . Similarly, a composite based on *a*-Si/ $\text{Li}_2\text{O}$  has been synthesized by mechano-chemical reduction of SiO with Li, as reported in an earlier report. The electrochemical cycling response of *a*-Si/ $\text{Li}_2\text{O}$ , cycled at  $160\text{ mA/g}$  in the potential window of  $0.02\text{ V}$  to  $1.2\text{ V}$ , shows a 1<sup>st</sup> discharge capacity *ca.*  $1620\text{ mAh/g}$ . However, the composite shows rapid fade in capacity (*ca.*  $3\%$ ) and large 1<sup>st</sup> cycle irreversible loss ( $42\%$ ). In the near future, ICA will be introduced into this composite, *in situ* by mechanochemical reduction, to improve the mechanical properties, and, as a result, the cyclability and stability of the composite.

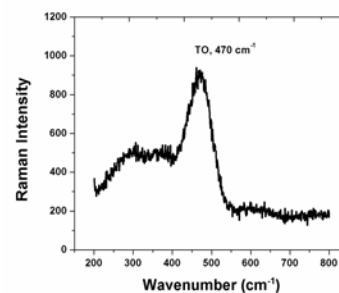


**Figure 1.** Raman spectra of Si deposited on CNT/ICA.

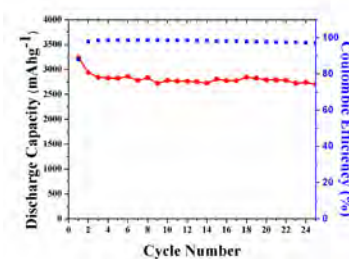


**Figure 2.** Charge-discharge plot of Si/ICA/VACNTs cycled at  $300\text{ mA/g}$  between  $0.02$ - $1.2\text{ V}$  vs.  $\text{Li}^+/\text{Li}$ .

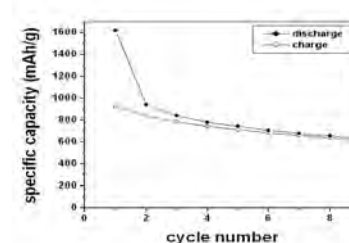


**Figure 3.** Capacity vs. cycle number of *a*-Si/ $\text{Li}_2\text{O}$  composite.

**TASK 2.4: PRINCIPAL INVESTIGATOR, INSTITUTION:** Ji-Guang (Jason) Zhang and Jun Liu, Pacific Northwest National Laboratory

**TASK TITLE – PROJECT:** Anodes.-.Development of Silicon-based High Capacity Anodes

**BASELINE SYSTEMS:** Conoco Philips CPG-8 Graphite/1 M LiPF<sub>6</sub>+EC:DEC (1:2)/Toda High-energy layered (NMC)

**BARRIERS:** Low energy density, high cost, limited cycle life

**OBJECTIVES:** To develop high-capacity, low-cost electrodes with good cycle stability and rate capability to replace graphite in Li-ion batteries

**GENERAL APPROACH:** Our approach is to manipulate the nano-structure and conductivity of silicon (Si)-based anodes to improve their mechanical and electrical stability. Si-based nanostructures, including micro-sized Si particles with nano-pore structures and core-shell Si composite materials will be investigated. Interactions between Si-based anode and binders also will be investigated. PNNL's capabilities in *in situ* characterization (including *in situ* TEM and NMR) and modeling will be leveraged to investigate the fundamental fading mechanism in Si-based anodes.

**STATUS OCT. 1, 2011:** Porous Si with micrometer particle sizes and different nano-pore sizes have been investigated for anode applications. The electrochemical performances of micro-sized Si particles with larger nano-pores have demonstrated improved performance. The porous Si powders have been coated with a thin layer (~6% in weight) of carbon by chemical vapor deposition (CVD) to increase their electrical conductivities. The porous structure of Si helps to accommodate the large volume variations that occur during Li-insertion/extraction processes. An initial capacity of ~1200 mAh/g (based on the full electrode) and capacity retention of ~800 mAh/g over 30 cycles were obtained at a 0.1C rate. In another effort, a SiC/SiO/C core-shell composite was developed. An initial capacity of ~1000 mAh/g (based on the full electrode) and capacity retention of ~600 mAh/g over 100 cycles were obtained.

**EXPECTED STATUS SEP. 30, 2012:** Micro-sized Si particles with large nano-pores will be prepared. An initial capacity of >1000 mAh/g (based on electrode) and capacity retention of ~700 mAh/g over 100 cycles will be obtained. A SiC/Si/C (or SiC/SiO/C) core-shell composite will be investigated further to improve its performance with a targeted initial capacity of >1200 mAh/g (based on the full electrode) and capacity retention of ~700 mAh/g over 100 cycles. The initial capacity loss of the electrodes will be minimized, and their coulomb efficiency during cycling will be increased further by selection of electrolytes and additives. The structure and evolution of the solid electrolyte interface (SEI) will be investigated by *in situ* microscopic analysis.

**RELEVANT USABC GOALS:** > 96 Wh/kg (plug-in hybrid electric vehicles [PHEV]), 5000 deep-discharge cycles, 15-year calendar life, improved abuse tolerance, and less than 20% capacity fade over a 10-year period.

**MILESTONES:**

- (a) Identify the main failure mechanisms of the Si-based anode. (Mar. 12) **Complete**
- (b) Improve the performance of Si based anode with a capacity-retention of >700 mAh/g over 150 cycles. (Sep. 12) **On schedule**
- (c) Select binders and electrolyte additive to improve the coulombic efficiency of Si-based anodes to more than 99%. (Sep. 12) **On schedule**

## PROGRESS TOWARD MILESTONES

The electrospin method was used to form a more flexible Si-based anode with an extra carbon coating applied to the rigid skeleton-supported Si composite. More specifically, the anode consists of nano-Si formed *in situ* on boron carbide (B<sub>4</sub>C) fibers followed by a graphite coating synthesized through ball-milling (see details in last quarterly report). These composite fibers were prepared as an anode (with a Si loading of up to *ca.* 0.5 mg/cm<sup>2</sup>) and tested in a coin-cell between 0.05 V and 1.5 V at a current density of *ca.* 1 A·g<sup>-1</sup> (the first three formation cycles are tested at a current density of 100 mA/g). The samples demonstrated a stable cycling behavior with a specific capacity of *ca.* 860 mAh·g<sup>-1</sup> (based on the whole electrode weight, including binder and conductive carbon) over 24 cycles (see Fig. 1a). Long term cycling stability and rate performance are still under evaluation.

In a separate approach, the hollow core-shell-structure (instead of a rigid skeleton-supported, porous Si-C nanocomposite) was further modified by sandwiching it between graphene layers in an effort to further improve the cycling stability. The coin cell was tested between 0.05 and 1.5 V at a current density of *ca.* 1 A·g<sup>-1</sup> (the first three formation cycles are tested at a current density of 100 mA/g). Stable cycling with a specific capacity of *ca.* 640 mAh·g<sup>-1</sup> (based on the whole electrode weight, including binder and conductive carbon) for over 50 cycles was obtained (Fig. 1b). Long-term cycling stability and rate performance are still under investigation.

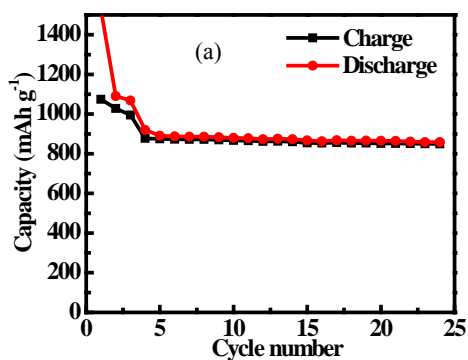


**Figure 1a.** Stable cycling of the electrospin fibers of the rigid skeleton supported Si composite.

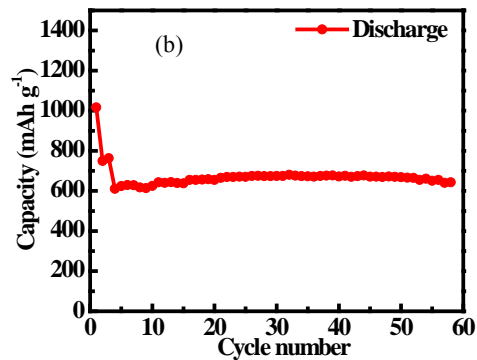


**Figure 1b.** Stable cycling of the hollow core-shell structured porous Si-C nanocomposite sandwiched between graphene sheets.

Further optimization of these two types of composite structures will be performed to improve the cycling stability. The electrode thickness, structure, porosity, binder, and electrolyte additives will be further investigated. Fundamental understanding of the structure of the SEI layer with electrolyte additives will be systematically investigated.

**Collaborations:** I.A. Aksay, Princeton University, and Vorbeck Inc. have provided the graphene for this work.

### Publications:

1. "Hollow Core-Shell Structured Porous Si-C Nanocomposites for Li-Ion Battery Anodes," Xiaolin Li, Praveen Meduri, Xilin Chen, Wen Qi, Mark H. Engelhard, Wu Xu, Fei Ding, Jie Xiao, Wei Wang, Chongmin Wang, Ji-Guang Zhang, and Jun Liu, *J. Mater. Chem.*, **22**, 11014-11017 (2012).
2. "Enhanced performance of graphite anode materials by AlF<sub>3</sub> coating for lithium-ion batteries," Fei Ding, Wu Xu, Daiwon Choi, Wei Wang, Xiaolin Li, Mark H. Engelhard, Xilin Chen, Zhenguo Yang, and Ji-Guang Zhang, *J. Mater. Chem.*, **22** (25), 12745–12751 (2012).

**TASK 2.5 - PI, INSTITUTION:** Anne Dillon, National Renewable Energy Laboratory

**TASK TITLE - PROJECT:** Anodes – Atomic Layer Deposition for Stabilization of Amorphous Silicon Anodes

**BASELINE SYSTEMS:** Conoco Philips CPG-8 Graphite/1 M LiPF<sub>6</sub>+EC:DEC (1:2)/Toda High-energy layered (NMC)

**BARRIER:** Cost, low gravimetric and volumetric capacities, safety

**OBJECTIVES:** In this work, an inexpensive and scalable hot wire chemical vapor deposition (HWCVD) technique for the production of either amorphous silicon (a-Si) or nano-Si powders and/or doped a-Si or nano-Si will continue to be used. Novel atomic layer deposition (ALD) coatings that will enable durable cycling to be achieved for the high volume expansion Si materials (~ 400 %) will also be developed. Coatings and electrode design may also be demonstrated with commercially available crystalline nano-Si particles.

**GENERAL APPROACH:** The a-Si or nano-Si powders will be fabricated with HWCVD *via* silane decomposition on a hot filament. Growth parameters will be explored to optimize yield as well as incorporate dopants to produce more conductive a-Si as well as additives to improve cycling stability. Conventional electrodes containing active material, conductive additive and binder will be fabricated and subsequently coated *via* ALD that will serve as an artificial solid electrolyte interphase (SEI) and will importantly help minimize degradation upon volume expansion.

**STATUS OCT. 1, 2011:** This award was initiated at NREL in FY11. The University of Colorado was funded as of January 1, 2011. Collaborations with both Prof. M. Stanley Binghamton and Prof. Arumugam Manthiram, as well as with General Motors and LG Chem, are in place. Samples were sent to Prof. Clare Grey to perform *in situ* NMR studies to provide mechanistic information about our ALD coatings.

**EXPECTED STATUS SEP. 30, 2012:** A thick Si anode with an ALD coating will be demonstrated to have a high durable capacity as well as high rate capability. Both gravimetric and volumetric capacities will be optimized.

**RELEVANT USABC GOALS:** 200 Wh/kg (EV requirement); 96 Wh/kg, 316 W/kg, 3000 cycles (PHEV 40 mile requirement). Calendar life: 15 years. Improved abuse tolerance.

#### **MILESTONES**

- (a) Demonstrate mechanistic information about ALD coatings *via in situ* techniques including Raman spectroscopy, nuclear magnetic resonance and/or Time of Flight Secondary Ion Mass Spectrometry. (Jan. 12) **Complete**
- (b) Send an optimized thick electrode ( $\geq 15 \mu\text{m}$ ) with a reversible capacity of at least 2000 mAh/g at C/20 to Dr. Vince Battaglia at LBNL for verification. (May 12) **Complete**
- (c) Demonstrate an ALD coating with rate performance of  $\geq C/5$  for a thick Si anode. (Jul. 12) **Complete**
- (d) Demonstrate at least 50 cycles at a minimum of C/3 rate. (Sep. 12) **On schedule**

## PROGRESS TOWARD MILESTONES

A novel Si anode coated with a unique carbon composite has been demonstrated to have a highly durable capacity at C/10 and C/5 with a coulombic efficiency  $\geq 99\%$ . Milestones (b) “Demonstrate an ALD coating with rate performance of  $\geq C/5$  for a thick Si anode” and (c) “Send the electrode ( $\geq 15 \mu\text{m}$ ) to Dr. Vince Battaglia at LBNL for verification” have been achieved by fabricating thick anodes composed of the core-shell Si nanostructures.

The Si core-shell nanostructure demonstrates stable cycling performance with minor degradation with cycling. The plotting of the differential capacity as a function of voltage confirms the structural stability after the first lithiation process, and shows highly reversible Li-alloying/dealloying over 50 cycles without degradation, as indicated in Fig. 1. All of the electrochemical data were collected in coin-cells with Li metal as counter electrode. An electron-energy-loss-spectroscopy (EELS) overlay mapping image of the Si-C core-shell nanostructure, insert in Fig. 1, displays the carbon shell covering the Si core. The optimization of the synthesis conditions has been performed recently on thick electrodes to reduce the irreversible capacity loss and improve the cycling stability. The synthesis temperature has shown to have an important effect on the irreversible capacity loss and mechanical strength. Electrodes annealed at  $300^\circ\text{C}$  have a high reversible capacity and good mechanical properties. Figure 2 exhibits the hardness of the carbon shell at different synthesis temperatures. An abrupt increase in hardness occurs at  $300^\circ\text{C}$ , doubling the hardness measured at lower temperatures (Fig. 2). The nano-Si-C core-shell structure obtained at  $300^\circ\text{C}$  also exhibits a specific charge capacity of nearly  $1500 \text{ mAh g}^{-1}$  after 150 cycles and shows sustainable cycling performance upon replacement of the Li metal counter electrode. The greatly improved cyclability and coulombic efficiency are attributed to the uniformity of the carbon coating, which ensures good electronic conductivity and superior mechanical resiliency.

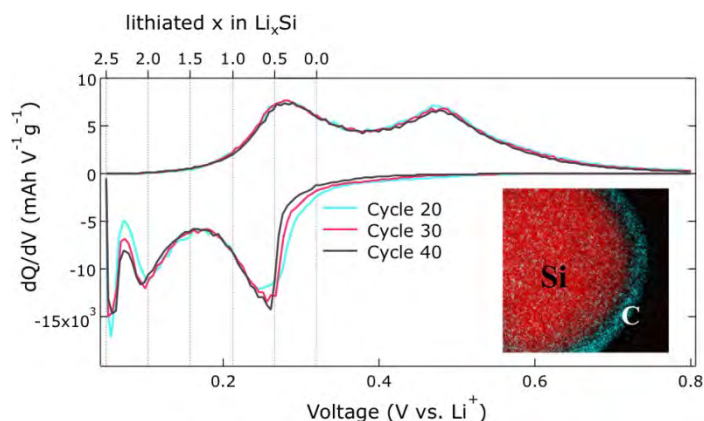


**Figure 1.** Differential capacity vs. voltage curves represent the Li-Si alloying/dealloying with cycling, the inset shows EELS mapping image of Si/C core-shell structure.

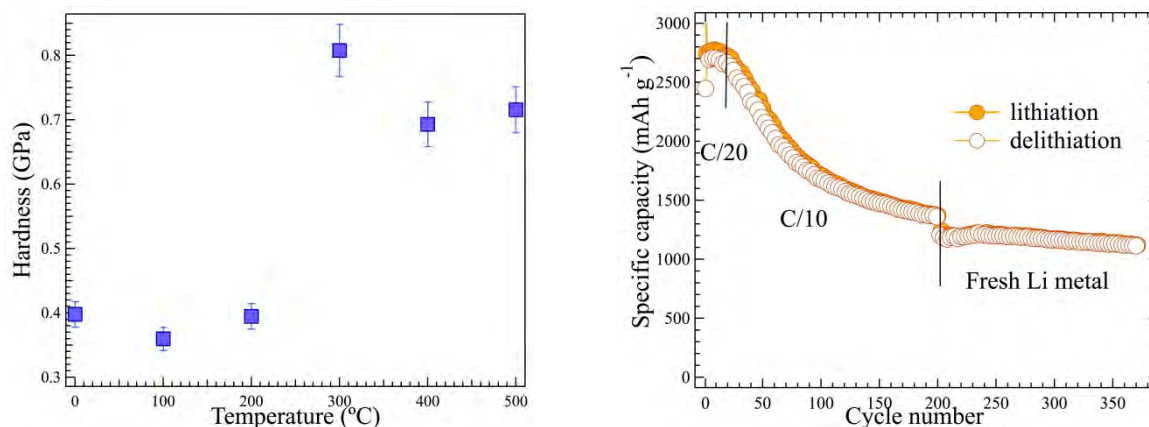


**Figure 2.** The effect of synthesis temperature on the hardness of the carbon shell (left); the sustainable cycling of Si-C core shell nanostructure (right).

**TASK 2.6 - PI, INSTITUTION:** Yury Gogotsi and Michel Barsoum, Drexel University

**TASK TITLE - PROJECT:** Anodes – New Layered Nanolaminates for Use in Lithium Battery Anodes

**BASELINE SYSTEMS:** Conoco Philips CPG-8 Graphite/1 M LiPF<sub>6</sub>+EC:DEC (1:2)/Toda High-energy layered (NMC)

**BARRIERS:** Needs increased life, capacity and improved safety.

**OBJECTIVES:** Replace graphite with a new material. Layered ternary carbides and nitrides known as MAX phases - may offer combined advantages of graphite and Si anodes with a higher capacity than graphite, lesser expansion, longer cycle life and potentially, a lower cost than Si nanoparticles.

**GENERAL APPROACH:** Since at this time the relationship between capacity and MAX phase chemistry is unknown; a rapid screening of as many MAX phases as possible will be carried out to determine the most promising chemistry, by testing their performance in lithium ion batteries. This will be guided by *ab initio* calculations. Reducing particle size, selective etching of an A element out from the MAX structure, and exfoliation of these layered structure will also be investigated to increase the Li<sup>+</sup> uptake by these structures and improve the Faradaic efficiency.

**STATUS OCT. 1, 2011:** Based on the selection of the most promising MAX phases from the 60-phase family (guided by *ab initio* calculations) perform the testing of the binder-less material as Li-ion battery anodes. Reduce the particle size to < 1 μm and evaluate the effect of the particle size. Exfoliate MAX phases into nanolayers and conduct preliminary electrochemical studies using coin and swagelok-type cells.

**EXPECTED STATUS SEP. 30, 2012:** MAX-phase based anode formulation providing an optimum performance (capacity and cyclability) in a coin cell configuration.

**RELEVANT USABC GOALS:** 200 Wh/kg (EV requirement); 96 Wh/kg, 316 W/kg, 3000 cycles (PHEV 40 mile requirement). Calendar life: 15 years. Improved abuse tolerance.

**MILESTONES:**

- (a) Reduce the particle size of MAX phase to submicrometer level and demonstrate a correlation between the particle size and the Li uptake capacity. (Mar. 12) **Canceled due to change in research direction**
- (b) Partially/and or fully remove the A-group layer from the MAX phase (fully removing “A” layer resulted in exfoliation of MAX phases into graphene-like 2-D structure which were labeled "MXene") and study its effect on electrochemical behavior as anodes Li-ion batteries. (Sep. 12) **On schedule**
- (c) Produce anodes from MAX and/or MXene with the capacity of about 80% of the commercial graphite anodes. (Sep. 12) **On schedule**
- (d) Investigate the effect of different carbon additives on the performance of MXene anodes and define the best additive conditions (Sep. 12) **On schedule**

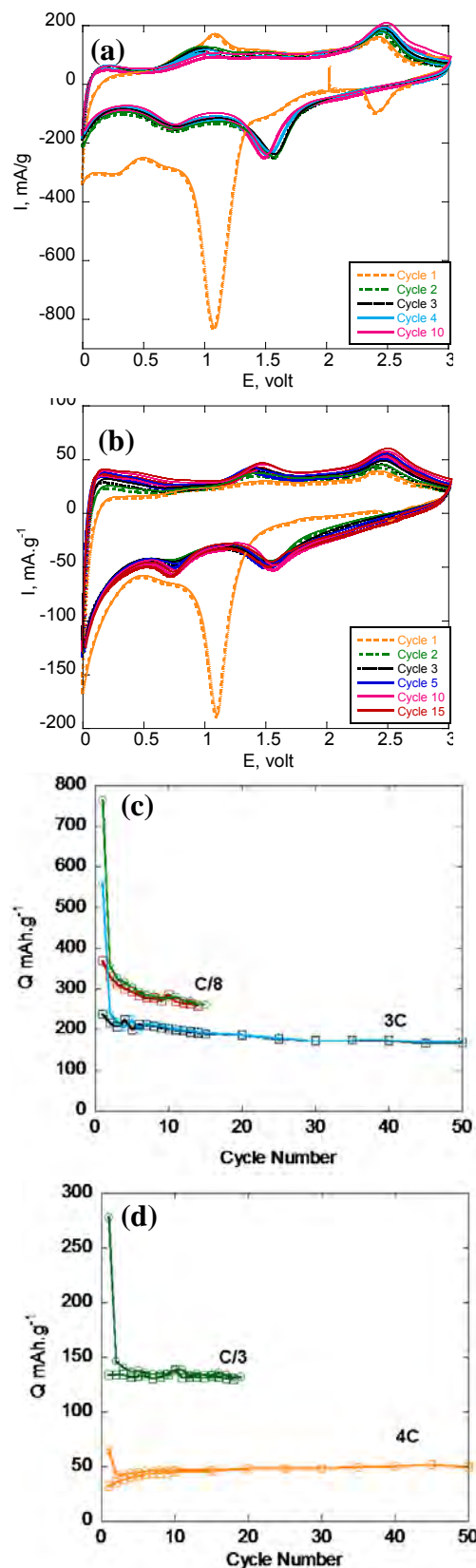
## PROGRESS TOWARD MILESTONE

More MXenes, with different compositions, have been tested as anode materials in LIBs. This document reports on the performance of  $\text{Ti}_3\text{CN}$  and  $\text{Ta}_4\text{C}_3$ . The CV curves for both  $\text{Ti}_3\text{CN}$  (Fig. 1a) and  $\text{Ta}_4\text{C}_3$  (Fig. 1b) show large first-cycle irreversible lithiation peaks around 1 V. This can be explained by the presence of F on the surface of the MXene layers after the exfoliation process that involves HF. Similar irreversible reactions were reported for transition metal fluorides due to the decomposition of fluoride and the irreversible formation of LiF during the first cycle. After the first cycle, reversible capacity was obtained in both systems. So, controlling the surface chemistry of MXene and producing F free MXenes should help in minimizing the 1<sup>st</sup> cycle irreversibility.

The specific capacity vs. cycle number at different C rates calculated from galvanostatic (GV) tests are shown in Figs. 1c and 1d for  $\text{Ti}_3\text{CN}$  and  $\text{Ta}_4\text{C}_3$ , respectively. As shown in Fig. 1c, at C/8, a stable capacity of more than 250  $\text{mAhg}^{-1}$  was obtained for  $\text{Ti}_3\text{CN}$  and, at 3C, a stable capacity of 170  $\text{mAhg}^{-1}$  was obtained after 50 cycles.

For  $\text{Ta}_4\text{C}_3$  (Fig. 1d) a stable capacity of 140  $\text{mAhg}^{-1}$  was obtained at C/3, while at 4C a stable capacity of 50  $\text{mAhg}^{-1}$  was obtained for 50 cycles. Although the specific capacities for  $\text{Ta}_4\text{C}_3$  are relatively low, volumetrically those capacities translate to *ca.* 1400 and 500  $\text{mAhcm}^{-3}$  at C/3 and 4C, respectively, which are relatively high volumetric capacities at such cycling rates.

**Figure 1.** a) Cyclic voltammetry curves for  $\text{Ti}_3\text{CN}$ , and b)  $\text{Ta}_4\text{C}_3$ . c) specific lithiation (circles) and delithiation (squares) capacities (per mass of active material) vs. cycle number at different rates for  $\text{Ti}_3\text{CN}$ , and d) the same as c) but for  $\text{Ta}_4\text{C}_3$ .



**Task 2.7-PI, INSTITUTION:** Donghai Wang and Michael Hickner, Pennsylvania State University

**TASK TITLE - PROJECT:** Anodes – Synthesis and Characterization of Polymer-coated Layered SiO<sub>x</sub>-graphene Nanocomposite Anodes

**BASELINE SYSTEMS:** Conoco Philips CPG-8 Graphite/1 M LiPF<sub>6</sub>+EC:DEC (1:2)/Toda High-energy layered (NMC)

**BARRIERS:** Low energy, poor capacity cycling, large initial irreversible capacity.

**OBJECTIVES:** To seek mitigation of the electrochemical limitations of SiO<sub>x</sub> anodes during charge/discharge by designing novel SiO<sub>x</sub>-graphene nanocomposite and polymer binders to tolerate volume change, improve electrode kinetics, and decrease initial irreversible capacity loss. The new materials proposed and optimized fabrication strategies will improve the performance of SiO<sub>x</sub>-based anodes.

**GENERAL APPROACH:** Our approach is to synthesize SiO<sub>x</sub>-graphene nanocomposites to tolerate volume change upon lithiation/delithiation while maintaining Li-ion conductivity. Novel polymer binders will be developed with controlled elastic properties, ion-conductive moieties, and SiO<sub>x</sub> surface binding functionality, in order to stabilize and bridge SiO<sub>x</sub> particles. To improve the initial coulombic efficiency, SiO<sub>x</sub>-graphene nanocomposites to compensate for Li consumption upon irreversible conversion of SiO<sub>x</sub> into Li<sub>2</sub>O and Li silicates will be prelithiated.

**STATUS OCT. 1, 2011:** Si nanoparticles with controlled particle sizes and Si-graphene nanocomposites have been successfully synthesized via a solution approach. Several types of polymer binders with controlled SiO<sub>x</sub> binding groups and Li-conducting blocks have been synthesized. Processing parameters that control Si nanoparticle size and polymer functionality will be determined. Formation of SiO<sub>x</sub>/Si nanoparticles by coating SiO<sub>x</sub> layer onto Si nanoparticles and the corresponding SiO<sub>x</sub>-graphene nanocomposites will be also demonstrated.

**EXPECTED STATUS SEP. 30, 2012:** Evaluation of electrochemical performance of Si nanoparticles and Si-graphene nanocomposites will be completed. Processing parameters that control SiO<sub>x</sub> coating on Si nanoparticles and polymer functionality will be determined. The electrochemical properties of SiO<sub>x</sub>/Si nanoparticles and the novel polymer binders will be optimized, and their compositions and cycling protocols will be evaluated at LBNL BATT partner labs to confirm the initial results.

**RELEVANT USABC GOALS:** 200 Wh/kg (EV requirement); 96 Wh/kg, 316 W/kg, 3000 cycles (PHEV 40 mile requirement). Calendar life: 15 years. Improved abuse tolerance.

**MILESTONES:**

- (a) Demonstrate Si nanoparticles and Si-graphene nanocomposites that can achieve a reversible capacity of at least 1200 mAh/g and a cycle life of at least 50 cycles. (Dec. 11) **Complete**
- (b) Synthesize and characterize SiO<sub>x</sub>/Si nanoparticles, SiO<sub>x</sub>/Si-graphene nanocomposites, and binders with multiple functionalities. (May 12) **Complete**
- (c) Demonstrate SiO<sub>x</sub>/Si-graphene nanocomposite anode coated with novel binder with a reversible capacity of at least 1500 mAh/g within 100 cycles. (Sep. 12) **Complete**

## PROGRESS TOWARD MILESTONES

**Si-based anode materials:** A novel  $\text{SiO}_x$  anode material was synthesized and demonstrated long cycle life in a Li-ion battery. XPS investigations show that the major surface composition of the material is  $\text{SiO}_x$  (Fig. 1A). The  $\text{SiO}_x$  materials were further characterized and their physical properties probed through a variety of methods such as TEM, EDS, and FTIR spectroscopy. Without further surface modification, the  $\text{SiO}_x$  material showed long cycle stability. The first cycle discharge capacity of the  $\text{SiO}_x$  materials was 2190 mAh/g and stabilized at *ca.* 650 mAh/g for the cycles thereafter (Fig. 1B). After the initial cycle, the electrode showed good capacity retention after 100 cycles (>90%) and 350 cycles (>85%). The coulombic efficiency after 30 cycles reached 99% and grew to >99.5%. The  $\text{SiO}_x$  also showed excellent cycling stability at different current densities. Further studies are undergoing to improve cycling capacity and first cycle coulombic efficiency.

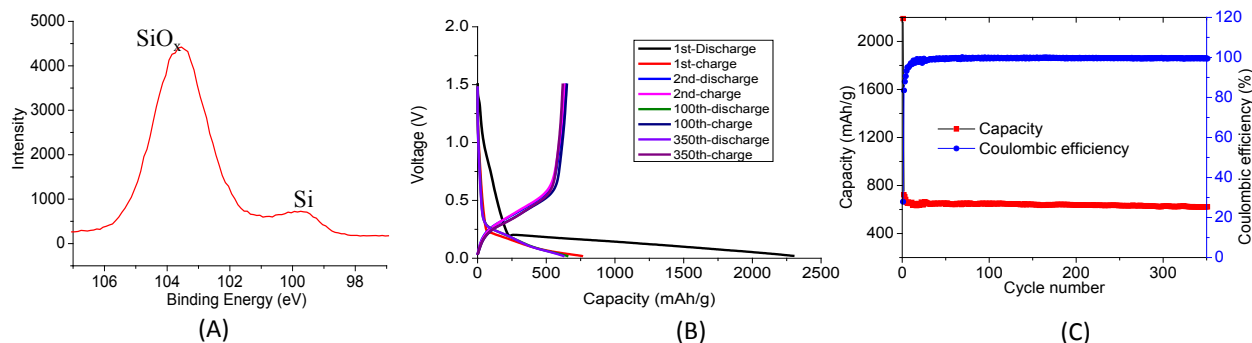


**Figure 1.** (A) XPS spectroscopy of the  $\text{SiO}_x$  materials. (B) Charge/discharge voltage profiles of the  $\text{SiO}_x$  materials. (C) Discharge capacity and coulombic efficiency of 350 cycles between 0.01 and 1.5V.

**Polymer binders:** Controlled crosslinking was achieved in a series of polymers to limit the electrolyte uptake of the binder. Sulfonated Radel with IEC 2.5 meq/g was mixed with hydroxyl terminated PEO and heated to affect crosslinking between the sulfonate groups and hydroxyl endgroups of the PEO. The general structure of the crosslinked polymer is shown in Fig. 2.

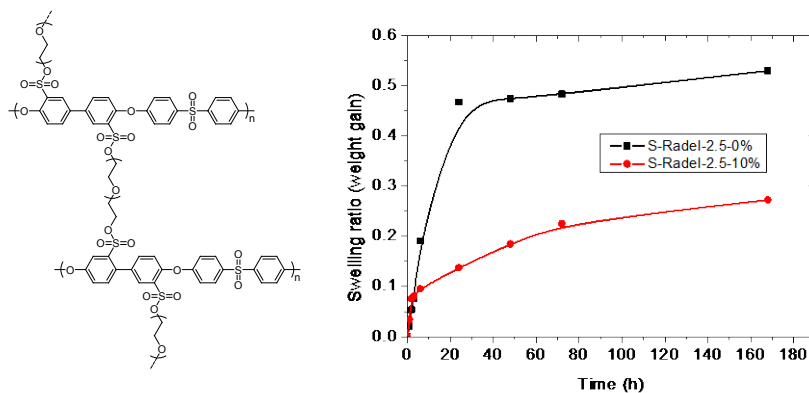


**Figure 2.** Chemical structure of S-Radel/PEO crosslinks and swelling of crosslinked and uncrosslinked samples in EC:DMC.

With 10 wt% crosslinker, the swelling of the polymer in EC:DMC was reduced by a factor of two. These types of crosslinked binders are currently being tested in cells with commercial Si nanopowder-based anodes.

**TASK 2.8 - PI, INSTITUTION:** Yi Cui, Stanford University

**TASK TITLE - PROJECT:** Anodes – Wiring up Silicon Nanoparticles for High Performance Lithium-ion Battery Anodes

**BASELINE SYSTEMS:** Conoco Phillips CPG-8 Graphite/1 M LiPF<sub>6</sub>+EC:DEC (1:2)/Toda High-energy layered (NMC)

**BARRIERS:** Low energy density, low efficiency, short cycle life, and safety issues

**OBJECTIVES:** To overcome the charge capacity limitations of conventional carbon anodes by designing optimized nano-architected silicon electrodes 1) fabricate novel nanostructures that show improved cycle life, and 2) develop methods to study the lithiation/delithiation process to understand volume expansion for higher efficiency.

**GENERAL APPROACH:** This project explores new types of Si nanostructures to be used as lithium ion battery anodes. Specifically, a variety of hollow and porous nanostructures will be fabricated, and their performance will be compared with other nanostructures such as nanowires. These hollow/porous nanostructures could act to minimize external volume expansion and produce stable SEI layers that will lead to more efficient long-term cycling. In addition, separate efforts will be dedicated to understanding the fundamentals of volume expansion in Si nanostructures through single nanostructure observation. This project was initiated January 1, 2011.

**STATUS OCT. 1, 2011:** A variety of spherical, one-dimensional, tubular, and porous Si nanostructures will have been fabricated and incorporated into Si anode architectures. Critical size for fracture of various nanostructure geometries during lithiation/delithiation will be established.

**EXPECTED STATUS SEP. 30, 2012:** Anode cycle life, Coulombic efficiency, first cycle irreversible capacity loss, specific capacity, and mass loading will be optimized by varying synthesis conditions. Effect of hollow/porous structure on volume expansion and Coulombic efficiency will be identified. A detailed understanding of how volume expansion depends on nanostructure geometry will be advanced.

**RELEVANT USABC GOALS:** 200 Wh/kg (EV requirement); 96 Wh/kg, 316 W/kg, 3000 cycles (PHEV 40 mile requirement). Calendar life: 15 years. Improved abuse tolerance.

**MILESTONES:**

- (a) Fabricate hollow/porous nanostructured anode with high reversible capacity and high Coulombic efficiency. (Jan. 12) **Complete**
- (b) Determine effect of hollow structure on volume expansion, compare to non-hollow nanostructures. (Apr. 12) **Complete**
- (c) Optimize nanostructure design for high mass loading and long cycle life (>1000 cycles). (Jul. 12) **Complete**
- (d) Develop fundamental understanding of the features that control volume expansion/contraction in Si nanostructures (*i.e.*, Li diffusivity, Si mechanical properties). (Sep. 12) **On schedule**

## PROGRESS TOWARD MILESTONES

### A Novel Yolk-Shell Design for Stable Cycling of Si Nanoparticles.

It is desirable to create high-performance, Si-based, nanostructured anodes that do not have significant additional processing costs compared to conventional anode materials. With this in mind, the team has designed a yolk-shell structure based on Si nanoparticles that is fabricated primarily with solution-based methods. This yolk-shell structure consists of Si nanoparticles encapsulated within a thin (*ca.* 30 nm) carbon shell with empty space between the Si particle and the shell. This empty space is rationally designed to accommodate the volume expansion that occurs during lithiation. An example TEM image of this structure is shown in Fig. 1, where the Si particles (darker contrast) are seen to be surrounded by the outer carbon shell. This structure is fabricated *via* a sacrificial templating method: Si nanoparticles are first coated with *ca.* 100 nm of SiO<sub>2</sub> *via* a TEOS decomposition in solution, and then the carbon coating is applied. Finally, the SiO<sub>2</sub> layer is removed with HF etching, leaving the yolk-shell structure behind.

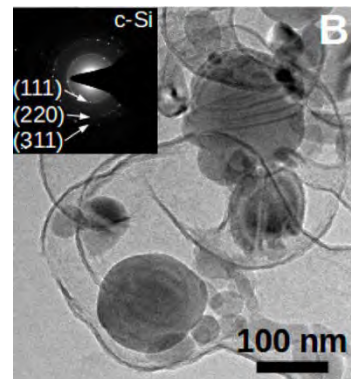


**Figure 1** Yolk-shell structure.

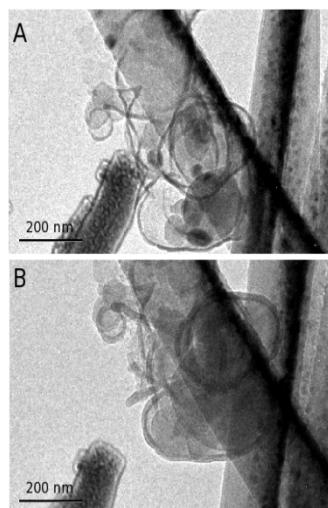


**Figure 2.** *In situ* TEM. A, Before lithiation. B, After lithiation.

The idea behind this structure is that when it is used as the active material in a Li battery anode, the electrolyte will only contact the outer carbon surface, while the Si particles can expand and contract within the hollow pockets *via* Li diffusion through the outer carbon layers. In this way, the surface in contact with the electrolyte (the carbon coating) undergoes only minor mechanical deformation, which allows for a stable, compact SEI to grow on the outer carbon layer. This design overcomes problems associated with volume changes in traditional Si electrodes, which commonly result in very thick SEI films and poor coulombic efficiency. To demonstrate this lithiation process, we carried out *in situ* TEM experiments to visualize lithiation of these structures in real time. TEM images before and after lithiation are shown in Fig. 2; it is evident that the Si nanoparticles within the carbon shells expand to fill most of the empty space, but the carbon shells do not fracture.

The yolk-shell material shows excellent electrochemical behavior when tested in half cells. Example data are shown in Fig. 3. Here, a Si nanoparticle yolk-shell electrode was cycled 1000 times at 1C with little capacity decay. Although, during the first 100 cycles the average

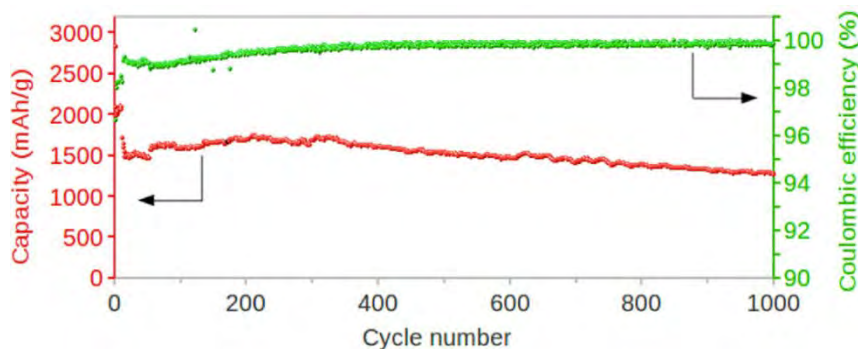


**Figure 3.** Electrochemical cycling data from a half cell test.

average coulombic efficiency is about 99%, from cycle 500 to 1000, the average coulombic efficiency increases to 99.84%. The success of the yolk-shell design indicates that rational engineering of nanostructured anodes to manage volume changes and control SEI growth can lead to improvements in performance.

**TASK 2.9 - PI, INSTITUTION:** Kwai Chan and Michael Miller, Southwest Research Institute

**TASK TITLE - PROJECT:** Anodes – Synthesis and Characterization of Silicon Clathrates for Anode Applications in Lithium-ion Batteries

**BASELINE SYSTEMS:** Conoco Phillips CPG-8 Graphite/1 M LiPF<sub>6</sub>+EC:DEC (1:2)/Toda High-energy layered (NMC)

**BARRIERS:** Low energy density, low-power density, and short calendar and cycle lives

**OBJECTIVES:** The objectives are to synthesize and characterize silicon clathrate anodes designed to exhibit small volume expansion during lithiation, high specific energy density, while avoiding capacity fading and improving battery life and abuse tolerance.

**GENERAL APPROACH:** Our approach is to synthesize guest-free Type I silicon clathrate (Si<sub>46</sub>, space group  $Pm\bar{3}n$ ) using high-pressure and high-temperature experimental methods, including a newly-developed arc-melt technique. Concurrently, an investigational route for direct synthesis of guest-free clathrate will be explored, and *ab initio* and classical molecular dynamics (MD) computations to identify lithiation pathways will be performed. The silicon clathrates will be utilized to fabricate prototype silicon clathrate anodes. Electrochemical characterization will be performed to evaluate and improve, if necessary, anode performance including cyclic stability. The final year of the program will be directed at the design, assembly, and characterization of a complete (anode/cathode) small-scale, prototype battery suitable for concept demonstration.

**STATUS OCT. 1, 2011:** Batch quantities (1-2 grams) of Type I silicon clathrates will have been fabricated by down-selecting and adopting at least two synthetic approaches. Furthermore, computational results will have been obtained using first principles and classical theories to identify possible reaction pathways for the formation of clathrates, Li<sub>x</sub>Si<sub>46</sub>, and Li<sub>15</sub>Si<sub>4</sub>. Several half cells of clathrate anodes will have been fabricated.

**EXPECTED STATUS SEP. 30, 2012:** The most viable method of synthesizing Type I silicon clathrate will have been selected and optimized in terms of yield and purity. Scale-up of synthesis from small quantities (1-2 grams) to hundreds of grams via one or two methods will have been completed. Three different approaches to fabricating clathrate anodes on suitable substrates would have been explored and one selected for laboratory-scale measurements. The intrinsic electrochemical properties of these anodes will have been characterized using a half-cell test apparatus. Classical and *ab initio* computations will have continued with the aim of assessing the effects of metal alloying on Li<sup>+</sup> occupancy and lattice expansion, while identifying possible reaction pathways for intercalation and deintercalation of lithium.

**RELEVANT USABC GOALS:** 200 Wh/kg (EV requirement); 96 Wh/kg, 316 W/kg, 3000 cycles (PHEV 40 mile requirement). Calendar life: 15 years. Improved abuse tolerance.

**MILESTONES:**

- (a) Select one synthetic pathway. (Dec. 11). **Complete**
- (b) Predict the Li<sup>+</sup> occupancy and lattice expansion potential of Type I metal-silicon clathrate alloys using classical and *ab initio* calculations. (Mar. 12) **Complete**
- (c) Identify possible reaction pathways for the formation of empty clathrates □Si<sub>46</sub>, Li<sub>x</sub>Si<sub>46</sub>, Li<sub>15</sub>Si<sub>4</sub>, and Li<sub>x</sub>M<sub>y</sub>Si<sub>46-y</sub>. (Jun. 12) **Complete**
- (d) Synthesize hundreds of grams of Type I silicon clathrates and/or metal-silicon Type I clathrate alloys with complementary determination of structural purity. (Sep. 12) **On schedule**

## PROGRESS TOWARD MILESTONES

### Task 1 – Synthesis of Guest-Free Type I Silicon Clathrate

*Batch Synthesis via Soft Oxidation of NaSi.* The present quarter focused on exercising a revised synthetic procedure in which the much more reactive NaSi, compared with BaSi<sub>2</sub>, was employed for the synthesis of guest free Si clathrate (□Si<sub>46</sub>). This fuel-grade silicide was milled to a fine powder, then combined with the liquid-eutectic ionic salt dodecyltrimethylammonium bis(trifluoromethylsulfonyl)imide under relatively mild conditions (*ca.* 300°C) in an inert environment. The determination of product yield and structural purity is currently underway.

### Task 2 – Molecular Modeling of Silicon Clathrates

The appropriate amounts of Ba and Al additions to attain a stable alloyed Si-clathrate structure with limited volume expansion during Li insertion were identified through first-principles computations *via* the CPMD code. Two clathrate compositions, Ba<sub>6</sub>Li<sub>x</sub>Al<sub>8</sub>Si<sub>38</sub> and Ba<sub>6</sub>Li<sub>x</sub>Al<sub>16</sub>Si<sub>30</sub>, have been found to allow Li insertion without Ba removal. Both exhibit small increases in the lattice constant upon insertion of up to 24 Li atoms, as shown in Fig. 1a. The corresponding energy change is negative (Fig. 1b), indicating that lithiation is energetically feasible and relatively easier compared to delithiation.

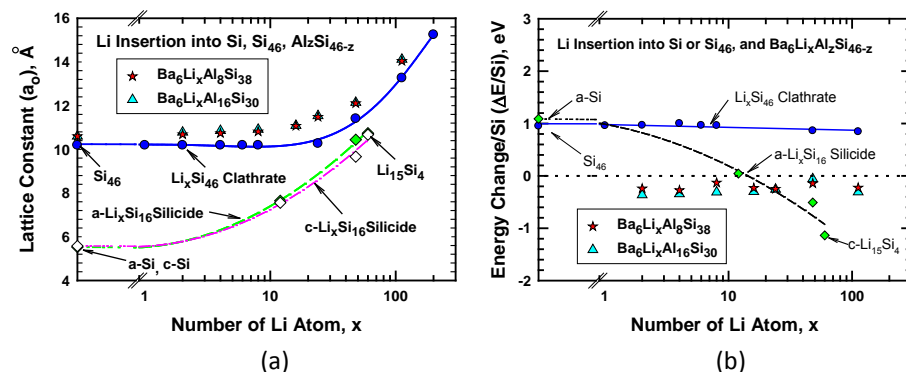


**Figure 1.** Comparisons of computed lattice constant and energy change as a function of Li insertion in Ba<sub>6</sub>Li<sub>x</sub>Al<sub>8</sub>Si<sub>38</sub>, Ba<sub>6</sub>Li<sub>x</sub>Al<sub>16</sub>Si<sub>30</sub>, Li<sub>x</sub>Si<sub>46</sub>, and Li<sub>x</sub>Si<sub>4</sub>: (a) lattice constant, and (b) energy change/Si atom.

### Task 4 – Half-Cell Electrochemical Characterization

Electrochemical measurements during this reporting period were aimed at exploring the effects of binder and conductive additives on the net capacity, cycle loss, and SEI formation of the anode when combined with the intermetallic clathrate Ba<sub>8</sub>Al<sub>8</sub>Si<sub>38</sub> previously synthesized by the vacuum arc-melting technique. Overall, the results suggest that the compounded anodes formed by mechanical compression into free-standing disks (1 cm diam. × 3 μm thick) tend to be diffusionally constrained at rates  $\geq C/14$ , particularly on intercalation of Li<sup>+</sup>, with a first-cycle net (irreversible) loss of 24% of the theoretical capacity (259 mAh/g, exemplary cycles shown in Fig. 2). Additionally, potential and/or current fluctuations during anodic deintercalation of Li<sup>+</sup> point to instabilities in SEI formation that persist beyond the second cycle. To overcome these gaps in half-cell performance, future cycling measurements will employ anodes formed by casting slurry compositions with a higher porosity. The stability of the electrolyte and its SEI formation may be significantly improved by including fluoroethylene carbonate (FEC) in the electrolyte formulation as either binary or tertiary mixtures with EC and DMC.

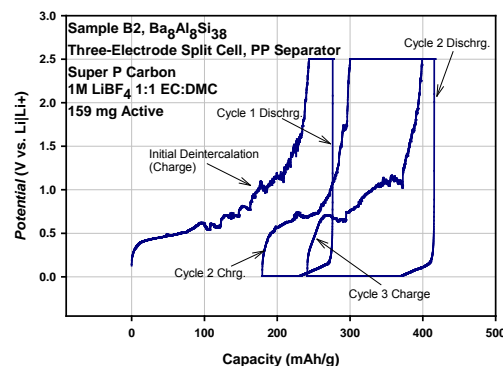


**Figure 2.** Half-cell voltage profiles for the first few delithiation-lithiation cycles of clathrate anode.

## **BATT TASK 3** **ELECTROLYTES**

**TASK 3.1 - PI, INSTITUTION:** Nitash Balsara, Lawrence Berkeley National Laboratory

**TASK TITLE - PROJECT:** Electrolytes – Development of Polymer Electrolytes for Advanced Lithium Batteries

**BASELINE SYSTEMS:** Conoco Philips CPG-8 Graphite/1 M LiPF<sub>6</sub>+EC:DEC (1:2)/Toda high-energy layered (NMC)

**BARRIERS:** Needs improved cycle life, energy density and safety.

**OBJECTIVES:** Characterize PS-PEO electrolytes with LiTFSI against Li-metal anodes in symmetric cells, sulfur, and air cathodes. Use block copolymers to create mesoporous battery separators for conventional liquid electrolytes.

**GENERAL APPROACH:** Synthesize and characterize dry PS-PEO (and PS-PEO-PS) polymer electrolytes. Continue to characterize salt/polymer mixtures by AC impedance spectroscopy, and make DC measurements with Li|polymer electrolyte|Li cells to obtain Li transference numbers. Collaborate with members of the BATT Program to test stability of the electrolyte against electrodes (Li metal, sulfur, and air). Synthesize and characterize porous PS-PE polymer separators by synthesizing a block copolymer, blending with a homopolymer, and washing out the homopolymer to yield a porous block copolymer.

**STATUS OCT. 1, 2011:** Complete study of morphology on solubility of Li<sub>2</sub>S<sub>x</sub> in PS-PEO copolymers. Use membrane casting device to create Li|SEO| air cells. Identify ideal molecular weight of homopolymer for creating block copolymer-based separators. Cycle cells with an electronically and ionically conducting polymer binder in the cathode. Obtain conductivity-morphology relationships in block copolymer-based separators with well-defined pores.

**EXPECTED STATUS SEP. 30, 2012:** Complete study of effect of morphology on transference number in PS-PEO copolymers. Quantify dendrite resistance of SEO electrolytes in symmetric and full cells. Study polysulfide dissolution in Li|SEO/LiTFSI|S cells. Cycle Li|SEO|air cells. Optimize conductivity-morphology relationships in block copolymer-based separators with well-defined pores. Obtain conductivity-morphology relationships in block copolymer-based separators with well-defined pores. Build Li/SEO/FePO<sub>4</sub> cells with an electronically and ionically conducting polymer binder in the cathode with active loading greater than 50 wt%.

**RELEVANT USABC GOALS:** EV applications goals are a specific energy of 200 Wh/kg and a specific pulse power of 400 W/kg.

### **MILESTONES:**

- (a) Complete transference number measurement as a function of morphology of SEO. (Dec. 11) **Complete**
- (b) Quantify improvement in dendrite resistance due to nanostructuring. (Mar. 12) **Complete**
- (c) Report on improving cathode loading in Li/SEO/FePO<sub>4</sub> cells with electronically and ionically conducting binder. Target active material loading: 65 wt%. (Jun. 12) **Delayed to Sep. 12**
- (d) Report cycling characteristics of Li/SEO/S and Li/SEO/air cells. (Sep. 12) **On schedule**
- (e) Report on conductivity and morphology of second generation porous block copolymer separators and demonstrate performance comparable to Celgard. Target conductivity: 0.4 mS/cm. (Sep. 12) **On schedule**

## PROGRESS TOWARD MILESTONES

Milestone 3.1 (a) was completed December 2011.

Milestone 3.1 (b) has been completed. A manuscript is currently in preparation.

Completion of milestone 3.1 (c) is delayed to September 2012. Figure 1 shows the cycling data for ten cells with 70 wt% loading of  $\text{LiFePO}_4$  active material. Average cell capacities for the first 10 cycles approach the theoretical value for  $\text{LiFePO}_4$ , indicating good contact/conductivity between the particles and the polymer matrix. Further analysis of data obtained from varied C rates is necessary to determine cathode stability at higher currents.

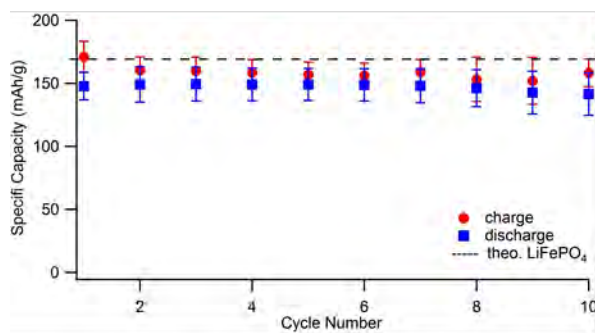


**Figure 1.** Cycling data for lithium battery with 70 wt%  $\text{LiFePO}_4$ .

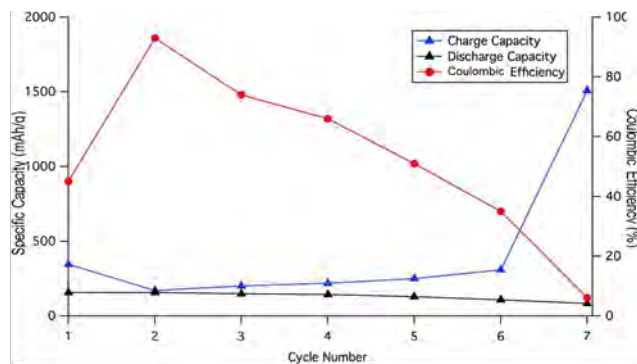


**Figure 2.** Cycling data for Li/SEO/S battery at 25 wt% sulfur.

For milestone 3.1 (d), preliminary data for Li/SEO/S cells with over 25 wt% sulfur in the cathode show evidence of significant polysulfide diffusion into the SEO electrolyte (Fig.2). When cycled at  $40 \mu\text{A}$ , low values are observed for coulombic efficiency, yet no significant decrease in the cell capacity. This indicates a high rate of self-discharge that could be due to the polysulfide shuttle mechanism. Future work will be on cells cycled at higher currents, which may reduce the influence of the polysulfide shuttle on the data. Li/SEO/air battery studies remain on schedule. Cell designs are being developed to determine the cathode reaction(s) using XPS and IR.

Work toward milestone 3.1 (e) is ongoing and on schedule. A manuscript discussing the characterization of the morphology of the SES battery separators using Resonant Soft X-Ray Scattering (RSoXS) is under preparation. Separators with the highest conductivity from each synthesized block copolymer are being tested in coin cells. These data will be compared to tensile strength tests to demonstrate the decoupling of the mechanical properties from the conductivity.

### Publications:

1. Simultaneous Conduction of Electronic Charge and Lithium Ions in Block Copolymers. Patel, S.N.; Javier, A.E.; Stone, G.M.; Mullin, S.A.; Balsara, N.P. *ACS Nano*, **6** (2), 1589–1600 (2012).
2. Relationship between Morphology and Conductivity of Block-Copolymer Based Battery Separators. Wong, D.T.; Mullin, S.A.; Battaglia, V.S.; Balsara, N.P. *J. Membrane Science*, **394-395**, 175-183 (2012).

**TASK 3.2 - PI, INSTITUTION:** John Kerr, Lawrence Berkeley National Laboratory

**TASK TITLE - PROJECT:** Electrolytes – R&D for Advanced Lithium Batteries

**BASELINE SYSTEMS:** Conoco Philips CPG-8 Graphite/1 M LiPF<sub>6</sub>+EC:DEC (1:2)/Toda High-energy layered (NMC)

**BARRIERS:** Poor cycle and calendar life, low power and energy densities, particularly at low temperatures (-30°C).

**OBJECTIVES:**

- Determine the role of electrolyte structure upon bulk transport and intrinsic electro-chemical kinetics and how it contributes to cell impedance (Energy/ power density).
- Determine chemical and electrochemical stability of electrolyte materials to allow elucidation of the structure of and the design of passivating layers (*e.g.*, SEI).

**APPROACH:** A physical organic chemistry approach is taken to electrolyte design, where the molecular structure is varied to provide insight into the processes that may affect the performance of the battery. This involves model compounds as well as synthesis of new materials to test hypotheses which may explain battery behavior.

**STATUS OCT. 1, 2011:** Initial studies on composite electrodes using single-ion conductor binders will be complete with the focus area materials: High voltage Ni-Mn Spinel cathodes and Conoco Philips CPG-8 Graphite anodes. Experiments will be complete on the use of modified multiwalled carbon nanotubes and carbon blacks for preparation of improved composite electrodes. The TGA/GC/MS system will be used to identify SEI components. Work on high volume expanding anodes with single-ion conducting binders and modified conducting additives will be extended to Si-based alloys. Dry polymer systems will be tested with LiFePO<sub>4</sub> and non-lithium metal anodes.

**EXPECTED STATUS SEP. 30, 2012:** Carbon nanotubes and other carbonaceous conducting elements will be further modified with a broader range of chemical groups (PEGs, imide and malonato-difluoroborate anions) and the effects on composite electrode performance determined. Combination of these modifications with variations of binder polymers will be studied to determine how electrode ink formulation affects the electrode morphology and electrode performance particularly for thick, high energy electrodes.

**RELEVANT USABC GOALS:** *Available energy:* 56 Wh/kg (10 mile) and 96 Wh/kg (40 mile); *10 s discharge power:* 750 W/kg (10 mile) and 316 W/kg (40 mile); *Cycle life:* 5000 cycles (10 mile) and 3000 cycles (40 mile); *Calendar life:* 15 years (at 40°C); cold cranking capability to -30°C; abuse tolerance.

**MILESTONES:**

- (a) Determine the benefits of conducting element modifications on electrode performance. (Apr. 12). **Complete**
- (b) Determine the role of electrode ink properties (*e.g.*, viscosity, stability, *etc.*) on electrode coating morphology and effects on electrode performance. (Sep. 12). **On schedule**

## PROGRESS TOWARD MILESTONES

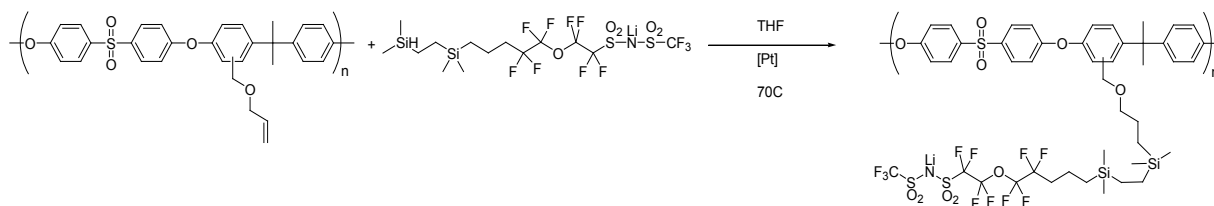


**Figure 1.** Synthetic scheme for preparation of Imide functionalized polysulfone binders.

Effort has been focused on preparation of more imide groups and polymers with a higher degree of functionalization so that the concentration of fixed ions in the resulting single-ion conductor can be increased. The completion of the first task was delayed due to supply of the expensive starting material but adequate supplies are now in preparation. The preparation of more highly functionalized polymers is a slow process, taking over a week of reaction time to double the concentration of functionalities. Efforts have been made to accelerate this process but with little success so far. Preparation of polyether polymers is also underway to provide more elastic binding materials for high volume expansion electrodes.

Attempts have been made to increase the concentration of functionalities on the conducting carbon materials and this has been successful as judged by the thermogravimetric analyses. Little improvement is seen on the performance of the composite electrodes with the use of hydroxyl-modified carbons prepared; however, functionalization with imide anions should result in significant differences and these will be tested in the coming year.

In preparation for fabricating full cells with a single-ion conductor, cells were first prepared with  $\text{LiFePO}_4$  cathodes and  $\text{TiO}_2$  anodes containing functionalized multiwalled carbon nanotubes (MWCNT). The electrodes performed well in half-cell tests against Li metal, as shown in Fig. 2; however, the performance in the full cell was not as expected. This indicates that there is much to learn as to how to balance these electrodes.

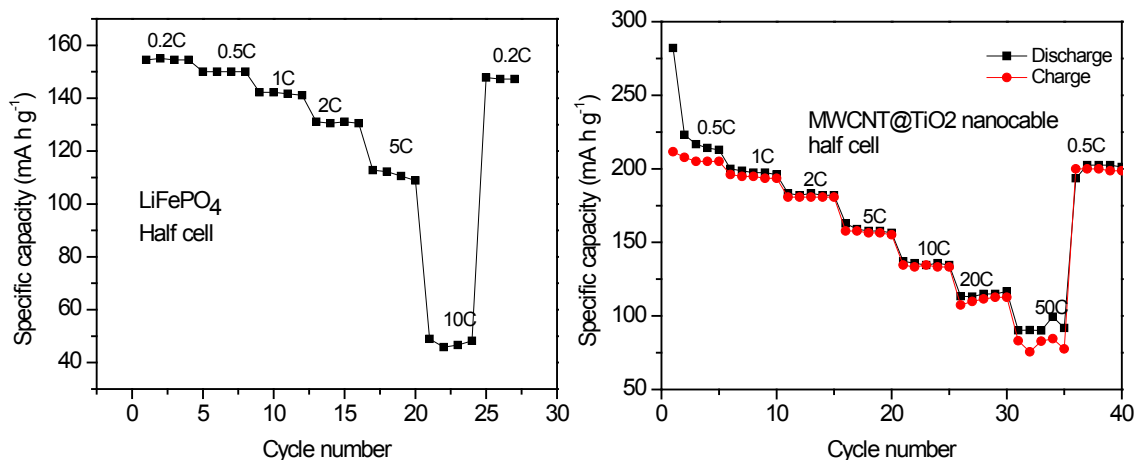


**Figure 2.** Half-cell testing of anodes and cathodes with functionalized MWCNT.

**TASK 3.3 - PI, INSTITUTION:** Dmitry Bedrov, Feng Liu, University of Utah, and Oleg Borodin, Army Research Laboratory

**TASK TITLE - PROJECT:** Modeling – Molecular Modeling of Electrolytes and Electrolyte/Electrode Interfaces

**BASELINE SYSTEMS:** Conoco Philips CPG-8 Graphite/1 M LiPF<sub>6</sub>+EC:DEC (1:2)/Toda High-energy layered (NMC)

**BARRIERS:** Poor low temperature operation, transport through SEI layer and cycle life. High interfacial resistance. Low energy and power density.

**OBJECTIVES:** Prediction of low energy surface structures and electrolyte reactivity for high voltage cathodes. Prediction and understanding of properties of novel high voltage electrolytes and additives including oxidative stability and degradation products on the cathode. Improved understanding of electric double layer structure, capacitance and transport as a function of electrode potential and temperature for high voltage cathode. Prediction and investigation of structure and formation of the SEI at high voltage cathodes using reactive molecular dynamics (MD) simulations.

**GENERAL APPROACH:** Utilize DFT methodologies to investigate low energy surfaces of high voltage cathodes, investigate electrolyte reactions at cathode surfaces and investigate oxidative stability of electrolyte components. Develop reactive and non-reactive MD force fields and simulation methods to simulate high voltage novel electrolytes. Utilize reactive force field (ReaxFF) methods to study oxidation reactions and SEI formation at model cathodes with emphasis on additives and electrolyte oxidation at model cathodes.

**STATUS OCT. 1, 2011:** Investigation of electric double layer structure and charge transfer resistance as a function of electrode potential for model electrodes, investigation of conductivity of novel high voltage electrolytes, investigation study of SEI formation and role of additives for model anodes completed.

**EXPECTED STATUS SEP. 30, 2012:** Prediction of low energy surface structures and electrolyte reactivity for high voltage cathodes will be completed. Prediction and understanding of properties of novel high voltage electrolytes and additives including oxidative stability and degradation products on the cathode will be completed for initial electrolytes and additives and compared with experiment. Prediction and investigation of structure and formation of the SEI at high voltage cathodes using reactive MD simulations will be completed for initial electrolyte compounds.

**RELEVANT USABC GOALS:** 10 s discharge power: 750 W/kg (10 mile) and 316 W/kg (40 mile)

**MILESTONES:**

- (a) Predict low energy surface structures and electrolyte reactivity for high voltage cathodes. (Jan. 12) **Complete**
- (b) Predict and understand properties of novel high voltage electrolytes and additives including oxidative stability and degradation products on the cathode. (Mar. 12) **Complete**
- (c) Perform MD simulations of electric double-layer structure, capacitance and transport as a function of electrode potential and temperature for high voltage cathode. (Jun 12) **Complete**
- (d) Predict and investigate structure and formation of the SEI at high-voltage cathodes using reactive MD simulations. (Sep 12) **On schedule**

## PROGRESS TOWARD MILESTONES

During this quarter, DFT studies of  $\text{LiNi}_{0.5}\text{Mn}_{1.5}\text{O}_4$  spinel surface energies were completed; DFT studies of the interactions of EC with  $\text{LiNi}_{0.5}\text{Mn}_{1.5}\text{O}_4$  were initiated.

MD simulations of the  $\text{Li}_2\text{BDC}$  ( $\text{Li}(\text{O}_2\text{COCH}_2\text{CH}_2)_2$ ) SEI component and  $\text{Li}_2\text{BDC}||\text{EC}:\text{DMC}(3:7)/\text{LiPF}_6$  interface were extended to lower temperatures. Transport and structural properties were obtained.

In collaboration with I. Halalay, GM, D. Aurbach and M. Levy, Israel, oxidative stability, initial decomposition reactions, transport and structural properties of *N-N*-Dimethylmethanesulfonamide, (DMMSA)/LiTFSI, electrolyte were investigated and compared with those for carbonate electrolyte, as described below. The DMMSA-based electrolytes showed quite different oxidative decomposition behavior compared to carbonates with LiTFSI and LiFSI salts. DFT calculations performed at B3LYP/6-311++G(d) on a single DMMSA, DMMSA dimer, and DMMSA/anions showed that while oxidation stability of DMMSA is about 70kJ/mol (0.7V)

lower than that for carbonate solvents (EC and PC), the barrier for the DMMSA decomposition is significantly higher than that for EC, EC<sub>2</sub>, PC, and PC/ClO<sub>4</sub> (Fig. 1). Therefore, the oxidized-DMMSA species will have a long life before they decompose, suggesting that DMMSA-based electrolytes operating above their oxidative stability limit will act as a redox shuttle.

MD simulations of DMMSA/LiTFSI and DMMSA/LiFSI were performed to investigate mechanisms of ion mobility in these electrolytes and potential pathways to improve their low-temperature conductivity through eutectic mixing of DMMSA/LiTFSI and DMMSA/LiFSI electrolytes. In collaboration with Halalay, the focus has been on the prediction and analysis of thermodynamic and transport properties of these mixtures with 4:1 (solvent:salt) compositions. MD simulations of DMMSA/LiTFSI mixtures showed very good agreement of the transport properties with available experimental data. Systematic analysis of mechanisms and strategies on how to improve Li mobility in these types of electrolytes is currently underway.

Another direction the team pursued is the understanding of nitrile and dinitrile-based electrolytes. In this quarter, the many-body polarizable force field was developed and validated for acetonitrile (AN)-based electrolytes. Predictions of MD simulations were validated for a series of AN-based electrolytes doped with LiDFOB, LiTFSI, LiFSI, and LiPF<sub>6</sub> salts in collaboration with Prof. Henderson (NCSU). A detailed comparison of AN-LiTFSI, AN-LiFSI, and AN-LiPF<sub>6</sub> structural properties extracted from MD simulations with those from Raman spectroscopy has been completed and summarized in two joint publications with Prof. Henderson's group: "Electrolyte Solvation and Ionic Association (II): Acetonitrile-Lithium Salt Mixtures - Highly Dissociated Salts," *J. Electrochem. Soc.* (JES-12-0583R) and "Li<sup>+</sup> cation coordination by acetonitrile - Insights from crystallography," *RSC Adv.*, DOI:10.1039/C2RA21290K. Analysis of AN-LiDFOB simulations and comparison with experiments is ongoing. The developed force field also predicts very good agreement of ion mobility and conductivity in AN/Py<sub>13</sub>TFSI/LiTFSI and EC/Py<sub>13</sub>TFSI/LiTFSI mixtures with experimental data. A manuscript summarizing these results has been submitted to *J. Phys. Chem. B*.

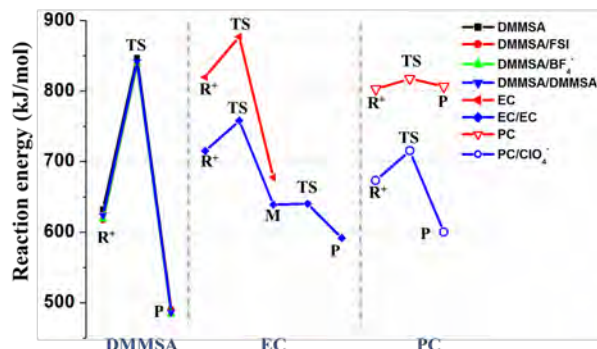


**Figure 1.** Reaction energy (kJ/mol) profile for the oxidized DMMSA, EC, and PC in various environments. R<sup>+</sup> defines the oxidized solvent, P is the final decomposition product, M - denotes intermediate compounds, TS is the transition state.

**TASK 3.4 - PI, INSTITUTION:** Khalil Amine and Larry Curtiss, Argonne National Laboratory

**TASK TITLE - PROJECT:** Electrolytes - Advanced Electrolyte and Electrolyte Additives

**BASELINE SYSTEMS:** Conoco Philips CPG-8 Graphite/1 M LiPF<sub>6</sub>+EC:DEC (1:2)/Toda High-energy layered (NMC)

**BARRIERS:** Cycle/calendar life, abuse tolerance

**OBJECTIVES:** Develop advanced quantum chemical models to predict functional additives that form stable SEI on carbon anodes and cathodes and redox shuttles for overcharge protection. Synthesize suitable additives predicted by model, characterize and perform extensive cycle and calendar life tests.

**GENERAL APPROACH:** Search for new electrolytic additives that react in a preferential manner to prevent detrimental decomposition of other cell components using experiment and theory. Use quantum chemical screening to predict oxidation and reduction potentials and decomposition pathways that form desirable coatings for testing by experiment, Use density functional studies of graphite surface reactions to determine mechanisms for protective film formation from additives.

**STATUS OCT. 1, 2011:** Promising additive candidates obtained from our reduction potential screening will have been further investigated computationally for the initial decomposition step in formation of the SEI. Experimental testing and characterization of selected additives will be performed. Oxidation potentials for potential redox shuttles will have been calculated.

**EXPECTED STATUS SEP. 30, 2012:** Exploration of full decomposition pathways for selected additive candidates will be carried out using advanced quantum chemical techniques. Experimental testing and characterization of the additives will be performed. Quantum chemical studies of the reaction energies for decomposition of shuttle candidates and experimentally testing.

**RELEVANT USABC GOALS:** 10-s discharge power: 750 W/kg (10 mile) and 316 W/kg (40 mile)

**MILESTONES:**

- (a) Use quantum chemical predictions of reaction energies for decomposition of redox shuttle candidates selected based on calculated oxidation potentials (Feb. 12) **Delayed to Jun. 12**
- (b) Explore full decomposition pathways to formation of SEI for additive candidates based on salts, anhydrides, and carbonates will be carried out using advanced quantum chemical techniques. (Apr. 12) **Complete**
- (c) Perform experimental testing of carbonate based additive candidates predicted from our computational model (May 12) **Complete**
- (d) Perform experimental synthesis and testing of redox shuttles for overcharge protection. (Jul. 12). **On schedule**
- (e) Synthesize, characterize, and test selected carbonate-based additives from theoretical prediction. Identify at least one additive that significantly improves the cycle and calendar life. (Sep. 12). **On schedule**

## PROGRESS TOWARD MILESTONES

A database of new electrolyte additives for SEI formation is being developed through the screening of reduction potentials by use of accurate density functional methods. The database also contains information on the mechanism of decomposition through investigation of various reaction pathways. Our database of additives has increased to over 375 species, all of which have been screened for reduction potentials with a subset further studied for decomposition pathways to form SEI components. The theoretical results are used to help identify compounds for experimental investigation in a battery cell.

Density functional calculations have been carried out on anhydride analogs including thiazolidinedione, oxazolidinedione, oxadiazolidinedione, and maleimide derivatives to gauge their suitability as SEI additives for Li-ion batteries. The maleimide species are analogs of maleic anhydrides, which are good additives, while thiazolidinedione, oxazolidinedione, and oxadiazolidinedione are substituted analogs of succinic anhydrides, and are also considered good additives. The anion radical of these species is stabilized by conjugation. Maleimide has a somewhat smaller reduction potential than maleic anhydride. Replacing the imide NH hydrogen or CH hydrogens in the maleimide ring can influence the reduction potential. The oxadiazolidinedione species (with an extra nitrogen in the ring) has a larger reduction potential than oxazolidinedione due to a larger electron affinity. An extra nitrogen in the ring of the sulfur-containing species also increases the reduction potential. The sulfur-containing species (*e.g.*, thiazolidinedione) have smaller reduction potentials than the corresponding oxygen-containing species (*e.g.*, oxazolidinedione) and open spontaneously upon reduction. Substituting imino C=NH for carbonyl C=O lowers the reduction potentials. Two extra nitrogens in the ring also decreases the reduction potential. All have higher reduction potentials than succinic anhydride so they should be good SEI additive candidates.

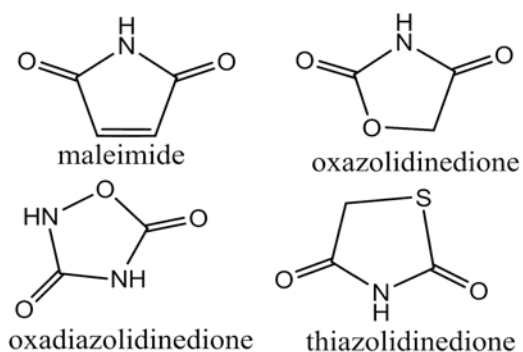


**Figure 1.** Structures of the of the anhydrides investigated as SEI additives.

Decomposition pathways for the anhydride analogs were investigated based on ring opening. The ring-opening decomposition reactions of anion radicals of three maleic anhydrides and three succinic anhydrides were studied using our density functional model. The maleic anhydride anion radicals had significant barriers for ring opening and the open structures were less stable than the corresponding ring species. In contrast, the succinic anhydrides' rings opened spontaneously. The 3-oxabicyclohexane-2,4-dione species was investigated experimentally as a possible additive. A new peak is observed at 2.25 V upon addition of a small amount of 3-oxabicyclohexane-2,4-dione. However, traditional SEI is not formed, indicating the formation of a new SEI at higher reduction potential than the Gen 2 carbonate electrolytes. This may involve a polymerization of the reduced 3-oxabicyclohexane-2,4-dione anion radical with EC.

The decomposition pathways for carbonates that were identified previously in our database with good reduction potentials were also investigated. Theoretically, cyclic carbonate electrolytes such as EC break a C-O bond to form an open anion radical. There is sometimes an energy barrier associated with this ring opening. Anion radical decomposition reactions were examined for a number of carbonates, including ones having the functional groups: hexadiene, cyclopropenyl, cyclopropyl, methylene cyclopropene, cyclobutadiene, divinylethylene, naphthalene, ditertbutylethylene, butadienylethylene, cyclopentadienyl, and allene. All were found to spontaneously open upon reduction except for cyclopropylethylene and 1,1-di-tert-butylethylene and thus, potentially, are good candidates for electrolyte additives.

**TASK 3.5 - PI, INSTITUTION:** Brett Lucht, University of Rhode Island

**TASK TITLE - PROJECT:** Electrolytes - Development of Electrolytes for Lithium-ion Batteries

**BASELINE SYSTEMS:** Conoco Philips CPG-8 Graphite/1 M LiPF<sub>6</sub>+EC:DEC (1:2)/Toda High-energy layered (NMC)

**BARRIERS:** Cell performance, life, cost: Calendar life: 40°C, 15 yrs; Survival Temp Range: -46 to +66°C; Unassisted Operating & Charging Temperature Range, -30 to +52°C.

**OBJECTIVES:** Develop novel electrolytes with superior performance to SOA (LiPF<sub>6</sub> in carbonates). Develop and understanding of the source of performance fade in LiNi<sub>1.5</sub>Mn<sub>0.5</sub>O<sub>4</sub> cathodes cycled to high voltage (4.9 V vs. Li). Develop an electrolyte formulation that allows for superior performance of LiNi<sub>0.5</sub>Mn<sub>1.5</sub>O<sub>4</sub> cathodes.

**APPROACH:** Optimize properties of LiPF<sub>4</sub>C<sub>2</sub>O<sub>4</sub>/carbonate electrolytes in small Li-ion cells at low temperature (-30°C) after accelerated aging. Investigate electrode surface films for cells cycled with LiPF<sub>4</sub>(C<sub>2</sub>O<sub>4</sub>) to determine source of performance differences. Investigate cathode film forming additives for high voltage (> 4.5 V) cathode materials. Investigate the surface of cathodes and anodes cycled with novel electrolytes, with or without additives, to develop a mechanistic understanding of interface formation and degradation.

**STATUS OCT. 1, 2011:** Additional cathode film forming additives was developed for high voltage cathodes. An understanding of the source poor first efficiency for LiPF<sub>4</sub>(C<sub>2</sub>O<sub>4</sub>) electrolytes on graphite anodes was developed. The low-temperature performance of LiPF<sub>4</sub>(C<sub>2</sub>O<sub>4</sub>)/PC electrolytes after accelerated aging was investigated. Novel electrolytes to improve performance of Si-based alloy anodes were investigated.

**EXPECTED STATUS SEP. 30, 2012:** An LiPF<sub>4</sub>(C<sub>2</sub>O<sub>4</sub>) electrolyte with optimized performance at low temperature after accelerated aging will have been developed. A better understanding of the role of electrolytes in the poor cycling efficiency and capacity fade of LiNi<sub>0.5</sub>Mn<sub>1.5</sub>O<sub>4</sub> cathodes will have been developed. Novel electrolyte formulations which optimize the performance of LiNi<sub>0.5</sub>Mn<sub>1.5</sub>O<sub>4</sub> cathodes cycled to high voltage (4.9 V vs. Li) will have been designed.

**RELEVANT USABC GOALS:** Calendar life: 40°C, 15 yrs; Survival Temp Range: -46–52°C; Cold cranking power at -30°C; Cycle life; Peak Pulse Discharge Power, 10 sec.

**MILESTONES:**

- (a) Develop an understanding of the role of electrolytes in capacity fade and poor cycling efficiency of LiNi<sub>0.5</sub>Mn<sub>1.5</sub>O<sub>4</sub> cathodes. (Mar. 12) **Complete**
- (b) Design electrolyte formulations to improve performance of high voltage Ni-Mn spinel cathode materials. (Jul. 12) **Complete**
- (c) Optimize a LiPF<sub>4</sub>(C<sub>2</sub>O<sub>4</sub>) electrolyte for graphite/LiNi<sub>x</sub>Co<sub>1-2x</sub>Mn<sub>x</sub>O<sub>2</sub> cells for high and low temperature performance. (Sep. 12) **On schedule**

## PROGRESS TOWARD MILESTONES

With regards to milestone (a): As indicated in our Q2 report, an understanding of the role of electrolyte in capacity fade and poor efficiency has been developed for Li/LiNi<sub>0.5</sub>Mn<sub>1.5</sub>O<sub>4</sub> cells. However, the performance of graphite/LiNi<sub>0.5</sub>Mn<sub>1.5</sub>O<sub>4</sub> cells cycled at 55 °C is much worse than Li/LiNi<sub>0.5</sub>Mn<sub>1.5</sub>O<sub>4</sub> cells. Our efforts will focus on developing a strong understanding of the role of electrolyte in this difference in FY13.

With regards to milestone (b): The team is designing electrolyte formulations to optimize the performance of LiNi<sub>0.5</sub>Mn<sub>1.5</sub>O<sub>4</sub> cathodes cycled to 4.9 V (*vs.* Li). An investigation of two primary types of additives is being conducted: Lewis basic additives, which inhibit Mn dissolution, and cathode film forming additives, which inhibit electrolyte oxidation on the cathode surface. As reported in our previous quarterly reports, the incorporation of three different additives: LiBOB, a Lewis base, and a cathode film former, decrease the capacity fade by 50% and improve the efficiency (>99%) for Li/ LiNi<sub>0.5</sub>Mn<sub>1.5</sub>O<sub>4</sub> cells cycled to 4.9 V. Experiments have been initiated with these same additives in graphite/LiNi<sub>0.5</sub>Mn<sub>1.5</sub>O<sub>4</sub> cells. While preliminary investigations suggest incorporation of additives can improve the performance of graphite/LiNi<sub>0.5</sub>Mn<sub>1.5</sub>O<sub>4</sub> cells cycled to high voltage, more detailed experiments will be conducted in FY13.

With regards to milestone (c): Lithium-ion coin cells were constructed with 1.2 M LiPF<sub>6</sub> in 3:7 EC/EMC, 1.2 M LiPF<sub>6</sub> in 2:2:6 EC/EMC/MB (Methyl Butyrate), and 1.2 M LiFOP in 2:2:6 EC/EMC/MB with natural graphite/LiNi<sub>1/3</sub>Co<sub>1/3</sub>Mn<sub>1/3</sub>O<sub>2</sub> electrodes to probe low temperature performance. The first-cycle efficiency of all cells was similar (*ca.* 85%). After initial formation cycles, the cells with MB electrolytes have a similar cycling performance, which is slightly higher than the EC/EMC cells (Fig. 1). When the cells were cooled to -10°C for low-temperature discharging, the discharge capacities of all three sets of coin cells decreased, but cells containing MB outperformed the EC/EMC cells. Then cells were stored at 55°C for one week to simulate accelerated aging. After aging, the RT-cycling performance was comparable to the initial RT performance. Upon cycling at -10°C after aging, all sets of cells had similar performance, although the cell with LiPF<sub>6</sub> and MB had the highest discharge capacity. Upon dropping the temperature further (-30°C), the differences in performance were greater. Cells containing LiPF<sub>6</sub> and MB provided the best performance, followed by LiPF<sub>6</sub> in carbonates, while LiFOP with MB gave the worst performance at -30°C. Similarly, poor low-temperature performance was observed for LiFOP electrolytes with PC after aging. Surface analysis of the electrodes is in progress to better understand these differences.

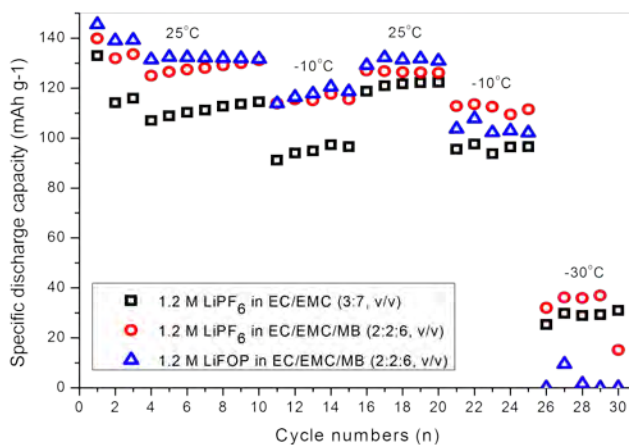


**Figure 1.** Cycling performance of different electrolytes with graphite/LiNi<sub>1/3</sub>Co<sub>1/3</sub>Mn<sub>1/3</sub>O<sub>2</sub>.

**Collaborations:**, M. Smart (NASA-JPL), V. Battaglia and G. Chen (LBNL), O. Borodin (ARL), W. Li (S. China Univ. Tech.), A. Garsuch (BASF), and Spinel Focus Group.

**TASK 3.6 - PI, INSTITUTION:** Daniel Scherson and John Protasiewicz, Case Western Reserve University

**TASK TITLE - PROJECT:** Electrolytes - Bifunctional Electrolytes for Lithium-ion Batteries

**BASELINE SYSTEMS:** Conoco Philips CPG-8 Graphite/1 M LiPF<sub>6</sub>+EC:DEC (1:2)/Toda High-energy layered (NMC)

**BARRIERS:** Abuse tolerance

**OBJECTIVES:** Design, synthesize, and characterize physical, electrochemical, and interfacial characteristics of functionalized Li-salt anions containing phosphorus moieties known to impart materials with flame retardant properties (Flame Retardant Ions or FRIONS) and additional functional redox active groups capable of providing overcharge protection. Develop and implement ATR-FTIR spectroscopic methods for monitoring *in situ* the nature of products generated at Li-ion battery anodes under highly controlled conditions.

**GENERAL APPROACH:** Develop methods for the chemical functionalization of anions known to improve the performance of Li-ion batteries with covalently linked groups displaying flame retardant and/or overcharge protection attributes. Establish guidelines for the rational design and synthesis of optimized FRIONS and FROPs based on the analysis of results of testing in actual Li-ion batteries. Develop new *in situ* tactics for the application of attenuated total reflection Fourier transform infrared ATR-FTIR for the characterization of solution products generated at Li-ion battery anodes and solid electrolyte interfaces formed therein.

**STATUS OCT. 1, 2011:** Synthesis and purification of three cyclic triol borate (CTB) and one bicyclic borate phosphine oxide (CBPO) salts and determination of their flammability. Develop methods for the preparation of 100g of CTB-type compound for testing in actual batteries. Collect data using the *in situ* IRAS-FTIR cell for monitoring *in situ* the composition of the electrolyte and surface films on ultrapure Li metal in selected alkyl carbonate-salt formulations.

**EXPECTED STATUS SEP. 30, 2012:** Complete synthesis and characterization of three additional CTB-type and CBPO-type materials including flammability and electrochemical testing. Establish structure-electrochemical performance relationships within the CTB and CBPO anion families. Explore monocyclic FRION frameworks. Explore other synthetic routes towards Li-BOBPHO-R (R = Ph), especially those involving larger scale methods. Systematic *in situ* ATR-FTIR spectroscopic studies involving selected solvent formulations incorporating Case FRIONS both as main salts and additives.

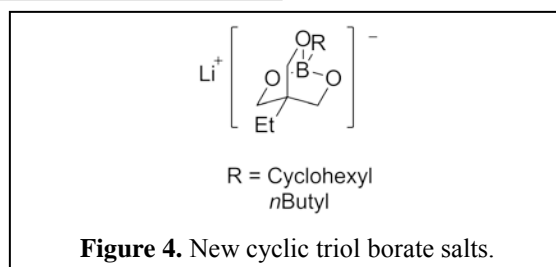
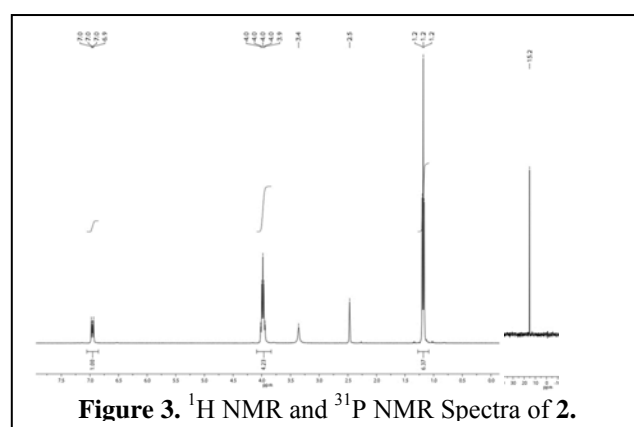
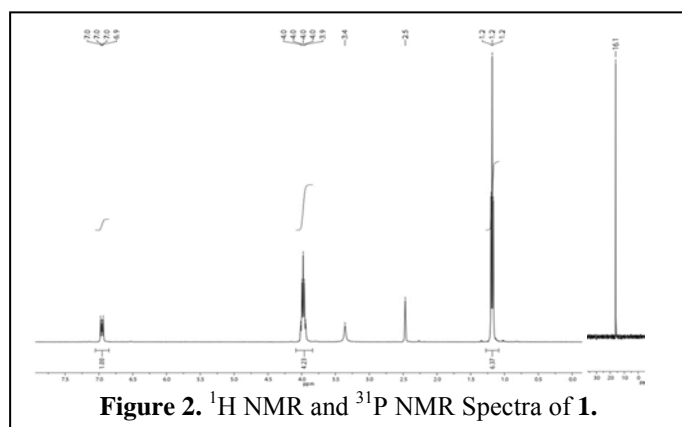
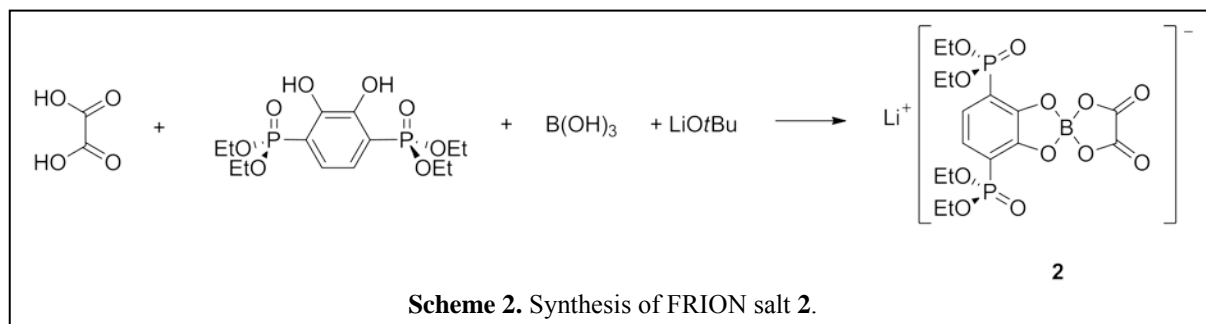
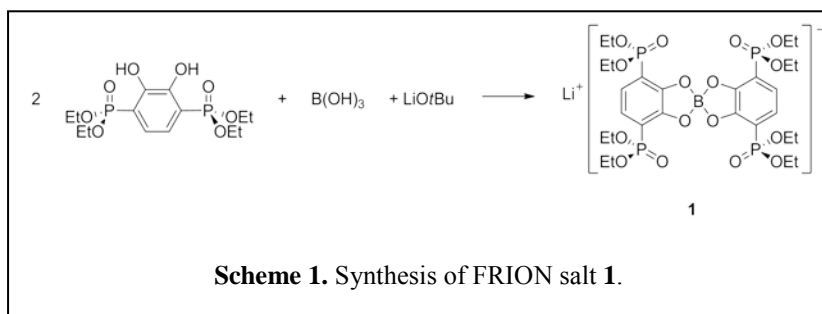
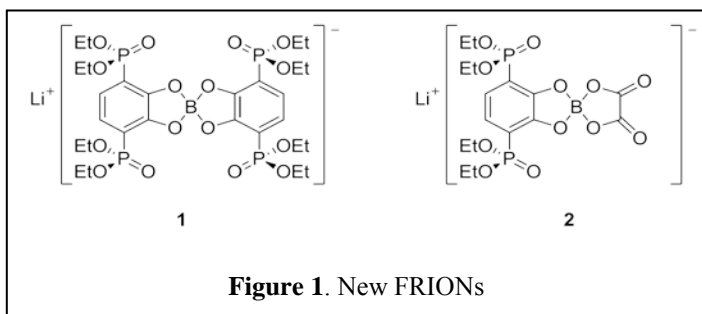
**ELEVANT USABC GOALS:** No fire or rapid disassembly of cells during abuse conditions.

**MILESTONES:**

- (a) Prepare and fully characterize the electrochemical and flammability properties characteristics of three CTB-type compounds and one CBPO-type compound. (Oct. 11) **Complete**
- (b) Expand the CTB-type and CBPO-type libraries of compounds. (Mar. 12) **Complete**
- (c) Synthesize and characterize a monocyclic FRION. (Sep. 12) **On schedule**
- (d) Complete design, construction and testing of cell for *in situ* new infrared reflection absorption (IRAS) spectroscopy and impedance measurements with first (Oct. 11) **Delayed, due Jul. 12;** and two additional Case electrolytes. (Sep. 12) **On schedule**
- (e) Perform full testing of three Case salts as full fledged electrolytes and as additives in actual batteries at Novolyte (Oct 11), and LBNL and ANL. (Sep 12) **On schedule**
- (f) Improve cycling by at least 15% to reach the same decay/end of life *vs.* the control electrolyte. (Sep 12) **On schedule**

## PROGRESS TOWARD MILESTONES

c) Synthesis and characterization of FRIONS – Two new FRION salts have been prepared (Fig. 1) and characterized by NMR spectroscopy (Figs. 2 and 3). Salt **1** was prepared using two equivalents of a diphosphorylated catechol, boric acid, and lithium t-butoxide (Scheme 1). For salt **2**, one equivalent of oxalic acid replaced one equivalent of the diphosphorylated catechol (Scheme 2) to make a lower molecular weight oxalatoborate salt. These FRION salts show promise of being more soluble in organic solvents than previous FRIONS and cyclic triol borate salts, and large scale synthesis is underway for solubility and electrochemical testing. Two new cyclic triol borate salts, similar in structure to those in previous reports, have been prepared (Fig. 4). Cyclohexyl and *n*butyl groups have been attached to boron of the borate salts. These cyclic triol borate salts will be useful for solubility and electrochemical testing, as they are aliphatic salts (both cyclic and straight chain).



**TASK 3.7 - PI, INSTITUTION:** Wesley Henderson, North Carolina State University

**TASK TITLE - PROJECT:** Electrolytes - Inexpensive, Nonfluorinated (or Partially Fluorinated) Anions for Lithium Salts and Ionic Liquids for Lithium Battery Electrolytes

**BASELINE SYSTEMS:** Conoco Philips CPG-8 Graphite/1 M LiPF<sub>6</sub>+EC:DEC (1:2)/Toda High-energy layered (NMC)

**BARRIERS:** Low cost cell materials, abuse tolerance, low temperature performance

**OBJECTIVES:** Develop new anions as replacements for PF<sub>6</sub><sup>-</sup> or as additives for electrolytes

**GENERAL APPROACH:** Synthesize and fully characterize two classes of nonfluorinated (or partially fluorinated) anions: 1) chelated and non-chelated organoborate anions (related to bis(oxalato)borate (BOB<sup>-</sup>)), and 2) Hückle-type anions in which the charge is stabilized on a 5-member azole ring and noncyclic cyanocarbanions. Characterize the physical properties of these new anions, incorporated in both Li salts and ionic liquids, by examining the thermal phase behavior (phase diagrams); thermal, chemical and electrochemical stability; transport properties; interfacial properties; molecular interactions and cell performance. These salts will be compared with widely used salts such as LiPF<sub>6</sub> and LiBOB and ionic liquids based upon the bis(trifluoromethanesulfonyl)imide anion.

**STATUS OCT. 1, 2011:** Several synthesis procedures for new lithium salts have been developed. The characterization of the salts is in progress. Ionic liquids (ILs) have been prepared with *N*-alkyl-*N*-methylpyrrolidinium cations and the difluoro(oxalato)borate (DFOB<sup>-</sup>) anion. These ILs have been characterized as additives to electrolyte formulations.

**EXPECTED STATUS SEP. 30, 2012:** Extensive characterization of solvent-LiFSI and -LiDFOB mixtures will be completed. Several new lithium salts will be reported along with a comparison of their properties with conventional salts such as LiBF<sub>4</sub> and LiPF<sub>6</sub>. ILs will have been prepared from these anions and tested in IL-LiX and IL-LiX-solvent mixtures, as well as for use as additives to conventional electrolyte formulations.

**RELEVANT USABC GOALS:** Available energy: 56 Wh/kg (10 mile) and 96 Wh/kg (40 mile); 10-s discharge power: 750 W/kg (10 mile) and 316 W/kg (40 mile); cycle life: 5000 cycles (10 mile) and 3000 cycles (40 mile); calendar life: 15 years (at 35°C); cold cranking capability to -30°C; abuse tolerance.

**MILESTONES:**

- (a) Determine the phase behavior/properties of solvent-LiPF<sub>6</sub> mixtures. (Apr. 12) **Complete**
- (b) Determine the phase behavior/properties of solvent-LiFSI and -DFOB mixtures. (Sep. 12) **On schedule**
- (c) Prepare/characterize lithium salts with partially fluorinated cyanocarbanions and dianions. Conduct half/full-cell electrochemical testing (graphite and NMC electrodes) using the salts as replacements for LiPF<sub>6</sub> or as additives, in parallel with the control electrolyte with LiPF<sub>6</sub>, to demonstrate improved cycling behavior performance over 200+ cycles. (Sep. 12) **On schedule**
- (d) Prepare/characterize ILs with DFOB<sup>-</sup> and partially fluorinated cyanocarbanions. Conduct half/full-cell electrochemical testing (graphite and NMC electrodes) using the salts as replacements for aprotic solvents or as additives, in parallel with the control electrolyte with LiPF<sub>6</sub>, to demonstrate improved cycling performance over 200+ cycles. (Sep. 12) **On schedule**

## PROGRESS TOWARD MILESTONES

**Raman Characterization of Ionic Association of Solvent-LiDFOB Mixtures:** Solvent-lithium difluoro(oxalato)borate (LiDFOB) mixtures are consistently found to have a comparable or higher ionic conductivity than analogous  $\text{LiBF}_4$  mixtures (Fig. 1) – this despite the fact that lithium bis(oxalato)borate (LiBOB) mixtures are typically less conductive than  $\text{LiBF}_4$  mixtures, especially at low temperature. To explain this, it is necessary to understand the ionic association interactions of the ions in solution. Solvates with LiDFOB have been analyzed to aid in discerning the manner in which the  $\text{DFOB}^-$  anion coordinates  $\text{Li}^+$  cations and how such coordination manifests itself in the Raman spectra of the solvates. This work has been complemented with a quantum chemical analysis of the vibrational bands of the  $\text{DFOB}^-$  anion through a collaboration with Patrik Johansson. This information is sought to improve the understanding of how anion structure influences the transport properties of electrolyte solutions.

**Anion Synthesis/Characterization:** Lithium 4,5-dicyano-2-(trifluoromethyl)imidazolid (LiTDI) readily forms highly aggregated solvates, but it is also able to form very stable (high  $T_m$ ) solvates with uncoordinated anions, such as a 2/1 diglyme/LiTDI solvate (*i.e.*,  $(\text{G}2)_2\text{LiTDI}$ ) (Fig. 2). This indicates that the salt is much less associated in solution than the corresponding lithium dicyanotriazolate (LiDCTA) salt. As for the LiDFOB solvates, the evaluation of LiTDI solvates by Raman spectroscopy has been completed to assign vibrational band positions to specific forms of  $\text{TDI}\dots\text{Li}^+$  cation coordination.

**Collaborations:** Oleg Borodin/Richard Jow (Army Research Laboratory), Patrik Johansson (Chalmers University of Technology, Sweden), Yuri Andreev/Peter Bruce (St. Andrews University, Scotland), Marshall Smart (Jet Propulsion Laboratory) and Brett Lucht (University of Rhode Island).

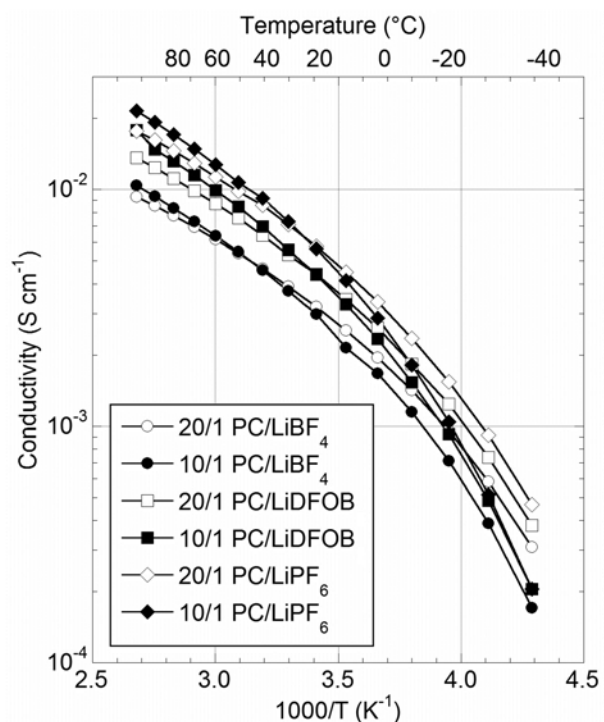


**Figure 1.** Ionic conductivity of  $(\text{PC})_n\text{-LiX}$  solutions.

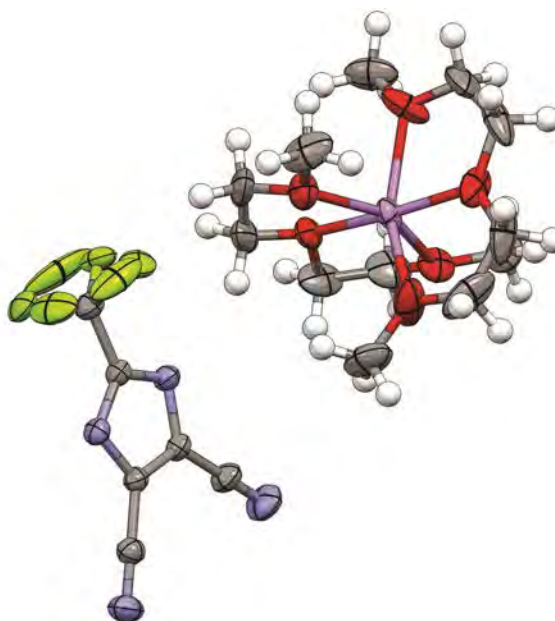


**Figure 2.** Ion coordination in the crystal structure of the  $(\text{G}2)_2\text{-LiTDI}$  solvate (Li-purple, O-red, N-blue, F-green).

**TASK 3.8 - PI, INSTITUTION:** Austen Angell, Arizona State University

**TASK TITLE - PROJECT:** Electrolytes – Sulfones with Additives as Electrolytes

**SYSTEMS:** Conoco Philips CPG-8 Graphite/1 M LiPF<sub>6</sub>+EC:DEC (1:2)/Toda High-energy layered (NMC)

**BARRIERS:** Increased oxidation resistance, decreased ionic resistance, and improved safety.

**OBJECTIVES:** Devise new electrolyte types (sulfone mixtures and superionic glasses or plastic solid derivatives) that will permit cell operation at high voltages without solvent oxidation and with adequate overcharge protection, and provide optimized nanoporous supporting membranes.

**GENERAL APPROACH:** Twofold: (i) A suite of electrolyte studies, beginning with cell-performance testing of recently developed sulfone electrolytes and extending to the design of novel Li<sup>+</sup>-conducting media, are planned. The latter will retain the high oxidation resistance known for noncyclic sulfones, and conductivity of EC-DMC solutions, but will have Li<sup>+</sup> transport number unity. Novel Li<sup>+</sup>-conducting thiophosphate solids (known  $\sigma > 10$  S/cm) and rubbery polymers (developing) will be tested for compatibility with the chosen Li(Ni,Mn) spinel cathode. Some ionic liquid electrolytes will be tested. (ii) Further development of the “Maxwell slats” approach to synthesis of nanoporous supports. A hot water-soluble reversibly-self-assembling net has already been developed as model, and a stronger-bonded model that self-assembles in hot ionic liquid solvents, is the next target.

**STATUS OCT. 1, 2011:** Half-cell and full-cell tests with the Li(NiMn) high-voltage cathode using our newly developed graphite-compatible all-sulfone, and part sulfone electrolyte solvents, were completed, and relative merits assessed. Tests of fluorinated sulfone FPMS, with DMC co-solvent in similar half-cell and full cell modes were done. The crystal structures of one of our self-assembling open-network structures (and its pore space fraction) is known, and XRD of its nearest glass-forming analog is available for comparison. Studies to expand the glassy range and mechanical properties are in progress.

**EXPECTED STATUS SEP. 30, 2012:** A go-no-go point will have been passed on sulfone-solvent-based high voltage cell development. An alternative solvent system of even higher voltage window and comparable conductivity, based on “ionic liquid” solvents, will have been tested for performance with the Li(Ni,Mn)O<sub>4</sub> cathode, and variants of the superionic glass and metastable crystal variety will have been examined. The best cases of the latter will be tested with the Li(Ni,Mn)O<sub>4</sub> cathode and the expected absence of side reactions verified. The nanoporosity of aqueous self-assembling models of the Maxwell slat concept will have been assessed, and study of more practical (stronger-bonding) variants will have been commenced.

**RELEVANT USABC GOALS:** 1000 cycles (80% DoD); 10 year life. An electrolyte with electrochemical window 5.2 volts and conductivity 20 mS/cm

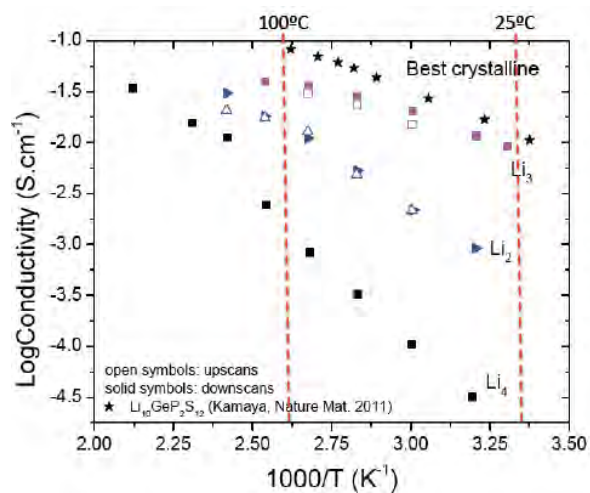
**MILESTONES:**

- (a) Complete full evaluation of sulfone solvent-based high voltage cells. (Dec. 11) **Complete**
- (b) Complete development of water-soluble self-assembling models of “Maxwell slat” porous solids for creation of self-supporting nanoporous membranes. (Dec. 11) **Complete**
- (c) Complete evaluation of ionic liquid-based, and hybrid, solvent electrolytes. (Apr. 12) **Delayed to Sep. 12**
- (d) Test and compare Li(Ni,Mn) spinel cells using ionic liquid-based electrolyte. (May 12) **Delayed to Sep. 12**
- (e) Test and compare glass and glass-stuffed polymer electrolyte types in cells. (Jun. 12) **Complete**
- (f) Develop covalent-bonded equivalents of the self-assembling nets. (Jul. 12) **On schedule**

## PROGRESS TOWARD MILESTONES

### (c) Complete evaluation of ionic-liquid-based, and hybrid, solvent electrolytes (Mar. 2012)

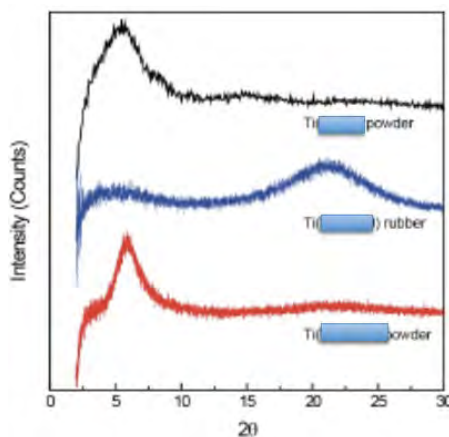
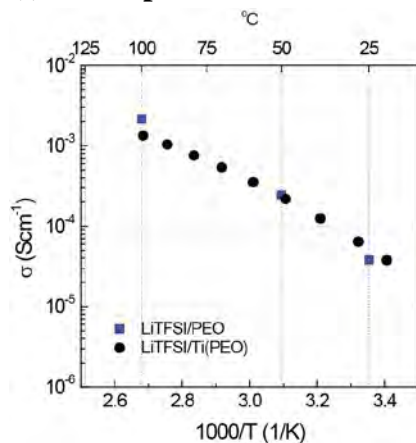
Investigation of novel inorganic salts that favor de-trapping of the Li cation from its anion environment to maximize Li mobility are under development. The effort includes new syntheses that should have lower total cohesive energies than those presented in the second quarterly report. The adjacent figure shows how closely the record set for solids by  $\text{Li}_{12}\text{GeP}_2\text{S}_{12}$  has now been approached by new plastic crystals prepared in the ASU labs. These contain variably charged (2-, 3-, and 4-) bulky anions that spin on their lattice sites, allowing low energy pathways for  $\text{Li}^+$  transport. Solid solutions of these salts will permit optimization of their conductivities in future work.



**(d) Test and compare Li(Ni,Mn) spinel cells using ionic-liquid-based electrolytes.** This part of the program has been put on hold until the electrochemistry postdoc who performed our earlier work on sulfone electrolytes (now being published) and half-cell tests described in earlier reports can be replaced.

**(e) No reports (b) Completed**

**(f) Develop covalent-bonded equivalents of the self-assembling nets.**



The work on amorphous versions of the popular MOF "microporous" solids (actually nanoporous) has continued successfully. Introduction of flexible struts to reduce the brittleness of the films, yields rubbery nets that are highly conducting when containing dissolved LiTFSI.

Conductivities equal to those obtained with viscous liquid PEO solvents shown in the work of Armand are displayed in the Arrhenius plot (above left).

The rubbery character can be controlled by the length of the flexible link. The third figure shows XRD patterns for powder and rubbery forms of networks prepared using different length flexible struts. Short length struts maintain and refine the nanoporosity, as shown by the sharp low angle peak in the third XRD pattern (above right, lowest curve). This contrasts sharply with the pattern obtained for the longer flexible struts which act more like conventional polymer solvents. Combinations of rubbery, nanoporous structures can then be obtained and the mechanical properties controlled by mixing the short-strut and long-strut materials together. This should lead to the avoidance of brittleness found in earlier preparations.

Flexible nets containing the materials of section (b) above are awaited with interest.

## **BATT TASK 4** **CATHODES**

**Task 4.1 - PI, INSTITUTION:** Michael Thackeray, Argonne National Laboratory

**TASK TITLE:** Cathodes – Novel Cathode Materials and Processing Methods

**SYSTEMS:** Conoco Philips CPG-8 Graphite/1M LiPF<sub>6</sub>+EC:DEC(1:2)/Toda NMC  
Conoco Philips CPG-8 Graphite/High voltage electrolyte/Li-Ni-Mn-O spinel

**BARRIERS:** Low energy, cost and abuse tolerance limitations of Li-ion batteries

**OBJECTIVE:** To develop low cost, high-energy and high-power Mn-oxide-based cathodes.

**APPROACH:** Li<sub>2</sub>MnO<sub>3</sub>-stabilized composite electrode structures, such as ‘layered-layered’ xLi<sub>2</sub>MnO<sub>3</sub>•(1-x)LiMO<sub>2</sub> (M=Mn, Ni, Co), ‘layered-spinel’ xLi<sub>2</sub>MnO<sub>3</sub>•(1-x)LiM<sub>2</sub>O<sub>4</sub> and more complex ‘layered-layered-spinel’ y{xLi<sub>2</sub>MnO<sub>3</sub>•(1-x)LiMO<sub>2</sub>}•(1-y)LiM<sub>2</sub>O<sub>4</sub> systems are receiving international attention because they can provide rechargeable capacities between 200 and 250 mAh/g between 4.6 and 2.0 V vs. lithium. These electrodes suffer from voltage decay and surface instability on cycling, thereby compromising the energy and power of the lithium-ion cells and preventing their implementation in practical systems. A novel, simple and versatile processing technique, using Li<sub>2</sub>MnO<sub>3</sub> as a precursor, to synthesize composite electrode structures is advocated; it offers the possibility of tailoring composite electrode structures and enhancing their electrochemical properties to meet Li-ion battery performance targets for PHEVs and EVs.

**STATUS OCT. 1, 2011:** This is a new project. During the last six months of FY2011, progress was made in exploiting a new synthesis approach in which Li<sub>2</sub>MnO<sub>3</sub> was used as a precursor to fabricate structurally-integrated lithium-metal-oxide composite electrode materials, including ‘layered-layered’, ‘layered-spinel’, ‘layered-rocksalt’ and more complex types. This technique showed promise for stabilizing high capacity (250 mAh/g) lithium-metal-oxide cathodes to cycling over a wide voltage window and, in particular, for combating voltage decay phenomena.

**EXPECTED STATUS SEP. 30, 2012:** Progress will have been made in enhancing the electrochemical and structural stability of ‘layered-layered’ xLi<sub>2</sub>M’O<sub>3</sub>•(1-x)LiMO<sub>2</sub> electrodes at high potentials, with improvements in rate capability and cycle life.

**RELEVANT USABC GOALS:** 200 Wh/kg (EV requirement); 96 Wh/kg, 316 W/kg, 3000 cycles (PHEV 40 mile requirement). Calendar life: 15 years. Improved abuse tolerance.

### **MILESTONES:**

- (a) Evaluate a new processing route to fabricate stabilized xLi<sub>2</sub>M’O<sub>3</sub>•(1-x)LiMO<sub>2</sub> (‘layered-layered’) electrode structures with a high Mn content using Li<sub>2</sub>MnO<sub>3</sub> as a precursor (Sep. 12)  
**On schedule**
- (b) Use atomic layer deposition and other methods to stabilize the surface of electrode particles at high charging potentials. (Sep. 12) **On schedule**
- (c) Model surface structures and interfacial phenomena of coated electrodes. (Sep. 12) **On schedule**

## PROGRESS TOWARD MILESTONES

Milestone (a) addressed: Evaluate a new processing route to fabricate stabilized  $x\text{Li}_2\text{M}'\text{O}_3 \bullet (1-x)\text{LiMO}_2$  electrode structures with a high Mn content using  $\text{Li}_2\text{MnO}_3$  as a precursor

Despite the growing attention received by  $x\text{Li}_2\text{MnO}_3 \bullet (1-x)\text{LiMO}_2$  ( $M = \text{Ni}, \text{Mn}, \text{and Co}$ ) composite electrode materials, the ability to utilize their exceptionally high capacities (*ca.* 250 mAh/g) in practical applications is hindered largely because of a voltage decay phenomenon during cycling. Electrochemical ‘activation’ above *ca.* 4.4 V alters the structure of these electrode materials and sets in motion a gradual phase transformation that lowers the discharge voltage of the cells, thereby lowering their energy and power output. In an attempt to combat this voltage decay, a new synthesis technique to fabricate  $x\text{Li}_2\text{MnO}_3 \bullet (1-x)\text{LiMO}_2$  electrode materials with greater resilience to internal phase transformations is being explored.

For example, the use of  $\text{Li}_2\text{MnO}_3$  as a layered Li and Mn ‘template’ is being explored for its potential in creating unique and promising structures. As can be seen in Fig. 1(a), the performance of a  $0.5 \text{Li}_2\text{MnO}_3 \bullet 0.5 \text{LiMn}_{0.5}\text{Ni}_{0.5}\text{O}_2$  cathode synthesized *via* a  $\text{Li}_2\text{MnO}_3$  precursor shows very high capacities of just over 250 mAh/g at *ca.* C/15 and maintaining *ca.* 200 mAh/g at close to 1C rates. Remarkably, for these materials the voltage profiles quickly stabilize with respect to the initial 10 cycles. For example, Fig. 1(b) shows charge and discharge curves to 35 cycles between 4.6 and 2.0 V for a Li half-cell at room temperature. This material displays striking stability and capacity retention over extended cycling to high voltage. EXAFS data of fresh cathode materials compared to cathodes cycled up to 50 times (between 4.6 and 2.0 V) reveal clues into the stability of the materials. First, Mn K-edge EXAFS (not shown) show that Mn atoms are present in a predominantly  $\text{Li}_2\text{MnO}_3$ -like environment and that significant changes to local structure occur during initial cycles. Interestingly, from the Ni K-edge EXAFS shown in Fig. 1(c) it is observed that the local Ni environment is virtually unchanged after 50 cycles with respect to its original structure. Thus, the  $\text{Li}_2\text{MnO}_3$  template may allow the formation of a unique ordering of Mn and Ni conducive to the structural stability of local domains. Furthermore, it seems likely that the voltage fade is directly related to the activation process of the  $\text{Li}_2\text{MnO}_3$  component and set in motion by the structural/chemical changes which occur during that process.

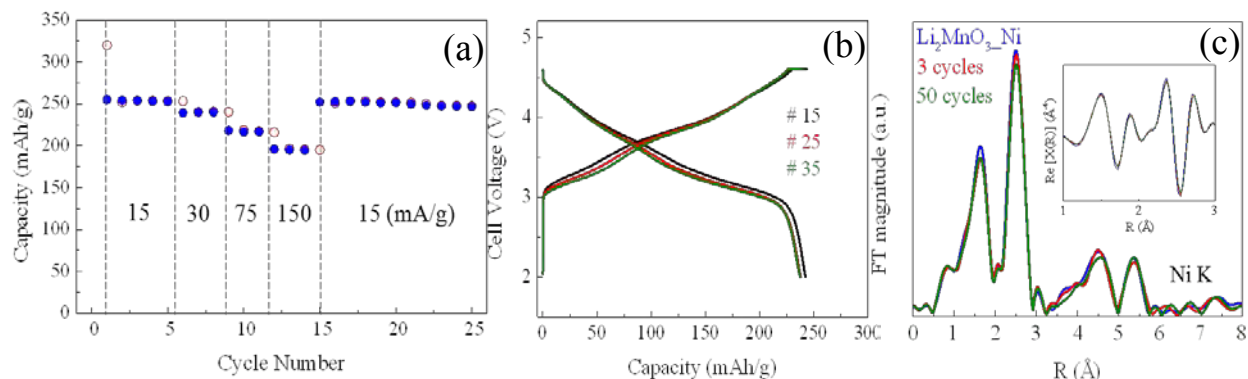


**Figure 1.** (a) Rate data of a  $\text{Li}_2\text{MnO}_3$ -based  $0.5\text{Li}_2\text{MnO}_3 \bullet 0.5\text{LiMn}_{0.5}\text{Ni}_{0.5}\text{O}_2$  cathode. (b) Voltage profiles of the cell in (a) up to 35 cycles (15 mA/g). (c) Ni K-edge EXAFS of a fresh cathode *versus* cycled cathodes revealing the stability of the local nickel environment.

Collaborators: J.R. Croy, M. Balasubramanian

**TASK 4.2: - PI, INSTITUTION:** Marca Doeff, Lawrence Berkeley National Laboratory

**TASK TITLE:** Cathodes – Design of High Performance, High Energy Cathode Materials

**SYSTEMS:** Conoco Philips CPG-8 Graphite/1 M LiPF<sub>6</sub>+EC:DEC (1:2)/Toda High-energy layered (NMC)

**BARRIERS:** Cost, power and energy density, cycle life

**OBJECTIVES:** To develop high energy, high performance cathode materials including composites and coated powders, using spray pyrolysis and related synthesis techniques.

**GENERAL APPROACH:** High energy cathodes such as modified NMCs and LiNi<sub>0.5</sub>Mn<sub>1.5</sub>O<sub>4</sub> (LNMS) are synthesized via spray pyrolysis, as well as composites containing these materials, and coated particles. An array of physical and electrochemical techniques are used to characterize their behavior, in conjunction with members of the diagnostics team. Emphasis is placed on increasing energy density without sacrificing stability and cycle life.

**STATUS OCT. 1, 2011:** Phase-pure samples of LiNi<sub>0.5</sub>Mn<sub>1.5</sub>O<sub>4</sub> spinel (LNMS) have been produced by spray pyrolysis. Structural characterization of cycled Li[Ni<sub>0.45</sub>Co<sub>0.1-y</sub>Al<sub>y</sub>Mn<sub>0.45</sub>]O<sub>2</sub>; y=0, 0.05 electrodes was completed. Structural and electrochemical characterization of high capacity Li[Ni, Co, Ti, Mn]O<sub>2</sub> compounds will continue.

**EXPECTED STATUS SEP. 30, 2012:** Hierarchically structured LNMS with differing primary and secondary particle sizes will be produced by spray pyrolysis, and optionally provided to interested members of the high voltage spinel discussion group. Work on NMCs will be directed towards understanding the mechanism of improvement in capacities and cycling behavior observed in some compounds when Ti is partially substituted for Co.

**RELEVANT USABC GOALS:** High energy, thermal stability, cycle life, cost (EV, PHEV).

**MILESTONES:**

- (a) Complete electrochemical characterization of hierarchically structured LNMS made by spray pyrolysis and compare to results obtained on conventional samples and simple particles made by spray pyrolysis. (Sep. 12). **On schedule**
- (b) Make a go/no go decision on Ti-substitution in NMCs as an approach for increasing energy density and improving cycle life. (Sep. 12). **On schedule**



**TASK 4.3 - PI, INSTITUTION:** Arumugam Manthiram, University of Texas at Austin

**TASK TITLE - PROJECT:** Cathodes – High-capacity, High-voltage Cathode Materials for Lithium-ion Batteries

**BASELINE SYSTEM:** Conoco Philips CPG-8 Graphite/1 M LiPF<sub>6</sub>+EC:DEC (1:2)/Toda High-energy layered (NMC)

**BARRIERS:** Cost, energy density, power density, cycle life, and safety

**OBJECTIVES:** To develop (i) low-cost cathodes based on polyanions that can offer a combination of high energy and power with excellent thermal stability and safety, and (ii) low-cost, high-voltage spinel cathodes that can offer high power and energy along with long cycle life.

**GENERAL APPROACH:** Focus is on the design and development of cathode materials based on polyanions that have the possibility for reversibly inserting/extracting more than one Li<sup>+</sup> ion per transition metal ion M<sup>n+</sup> and/or operating above 4.3 V. Some example systems to be pursued are Li<sub>2</sub>MSiO<sub>4</sub> and Li<sub>2</sub>MP<sub>2</sub>O<sub>7</sub> (M = Mn, Fe, Co, and Ni). However, there are technical challenges in achieving the theoretical energy densities of many of these cathode materials. Synthesis and processing conditions play a critical role in realizing the full capacities of these polyanion cathodes with more than one Li<sup>+</sup> ion per M<sup>n+</sup> ion. Novel solution-based synthesis approaches such as microwave-assisted solvothermal methods that can offer controlled nanomorphologies are pursued to maximize the electrochemical performances. The synthesized nanostructured polyanion cathodes are characterized by a variety of techniques including *ex situ* and *in situ* XRD, electron microscopy (SEM, TEM, and STEM), X-ray photoelectron spectroscopy (XPS), time of flight – secondary ion mass spectroscopy (ToF-SIMS), and in-depth electrochemical measurements. In addition, the role of cation doping, segregation of certain doped cations to the surface, cation ordering, and morphology on the electrochemical properties of 4.7 V spinel cathodes will be investigated. Based on the characterization data gathered, a fundamental understanding of structure-composition-property-performance relationships will be developed.

**STATUS OCT. 1, 2011:** Understanding of the self-surface segregation of cations during the synthesis process of high-voltage (4.7 V) spinel oxide cathodes through advanced characterization methodologies, development of novel solution-based synthesis approaches to obtain high-capacity nanostructured polyanion (silicate and phosphate) cathodes, and an investigation of their structure-composition-property-performance relationships.

**EXPECTED STATUS SEP. 30, 2012:** Development of (i) novel synthesis approaches to obtain high-capacity, high-voltage polyanion (silicate and phosphate) cathodes with unique nanomorphologies, (ii) an understanding of the factors that control the performance of high-voltage (4.7 V) spinel oxide cathodes, and (iii) an understanding of their structure-composition-property-performance relationships.

**RELEVANT USABC GOALS:** 300,000 shallow discharge cycles, 10-year life, <20% capacity fade over a 10-year period

**MILESTONES:**

- (a) Understand the role of cation doping, surface modification, and morphology on the electrochemical properties of 4.7 V spinel cathodes. (Dec.11) **Complete**
- (b) Perform surface characterization of LiFe<sub>1-x</sub>Co<sub>x</sub>PO<sub>4</sub> with various x by XPS and ToF-SIMS. (Jun. 12) **Complete**
- (c) Perform novel synthesis and characterization of Li<sub>2</sub>MSiO<sub>4</sub> and their solid solutions. (Sep. 12) **On schedule**

## PROGRESS TOWARD MILESTONES

$\text{LiM}_{1-x}\text{Fe}_x\text{PO}_4$  ( $M = \text{Mn}$  and  $\text{Co}$ ) solid solution cathodes were synthesized previously and it was found that the substitution of small amounts of Fe for Mn or Co greatly improve electrochemical performance. Recognizing that the segregation of dopant ions like  $\text{Fe}^{3+}$  in the high-voltage  $\text{LiMn}_{1.5}\text{Ni}_{0.5-x}\text{M}_x\text{O}_4$  ( $M = \text{Cr}$ ,  $\text{Fe}$ , and  $\text{Ga}$ ) spinel segregates to the surface and enhances the electrochemical performance, the  $\text{LiM}_{1-x}\text{Fe}_x\text{PO}_4$  phosphate cathodes were revisited to determine if surface segregation occurs in them as well. Through ToF SIMS and XPS, it was determined that segregation of  $\text{Fe}^{2+}$  to the surface does not occur in  $\text{LiM}_{1-x}\text{Fe}_x\text{PO}_4$  ( $M = \text{Mn}$  and  $\text{Co}$ ). Figure 1 shows the surface to bulk ratio of iron in the Fe-substituted  $\text{LiCo}_{1-x}\text{Fe}_x\text{PO}_4$  as a function of sputtering time. As indicated, the Fe concentration remains the same throughout the depth of the particle. Thus, segregation of  $\text{Fe}^{2+}$  to the surface is not occurring, unlike in the case of the high-voltage spinel  $\text{LiMn}_{1.5}\text{Ni}_{0.5-x}\text{Fe}_x\text{O}_4$ . Therefore, the improvement in the electrochemical performances of  $\text{LiM}_{1-x}\text{Fe}_x\text{PO}_4$  ( $M = \text{Mn}$  and  $\text{Co}$ ) is not due to the segregation of Fe to the surface, but may be associated with the different affinities of transition metals to form carbides during the carbon-coating process. For example, any iron carbide formed may enhance electronic conductivity and provide a better electrode-electrolyte interface. Future work will focus on determining whether or not iron carbide is formed during the carbon-coating process of  $\text{LiM}_{1-x}\text{Fe}_x\text{PO}_4$ .

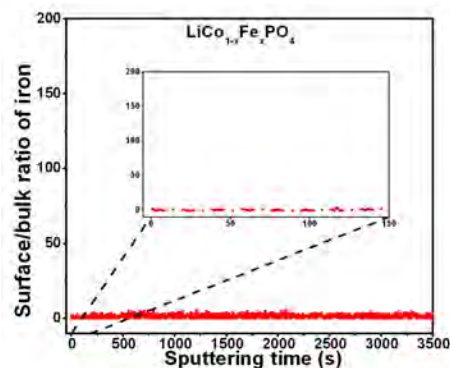


**Figure 1.** Surface to bulk ratio of iron in  $\text{LiCo}_{1-x}\text{Fe}_x\text{PO}_4$  as a function of sputtering time.

The undoped high-voltage spinel  $\text{LiMn}_{1.5}\text{Ni}_{0.5}\text{O}_4$  cathode is known to exhibit capacity fade, especially at elevated temperatures. It was shown that cationic substitutions in  $\text{LiMn}_{1.5}\text{Ni}_{0.42}\text{M}_{0.08}\text{O}_4$  ( $M = \text{Cr}$ ,  $\text{Fe}$ ,  $\text{Ga}$ ) improves the electrochemical performance significantly; current work is focused on developing an in-depth understanding of the factors that influence the electrochemical properties.

This quarter, the focus was the phases formed and the lattice parameter changes occurring during the charge-discharge process of undoped and doped samples. The cathode materials were charged to a specific state of charge and then examined by XRD. Figure 2 shows the variations of lattice parameters with depth of charge for  $\text{LiMn}_{1.5}\text{Ni}_{0.5}\text{O}_4$  and  $\text{LiMn}_{1.5}\text{Ni}_{0.42}\text{M}_{0.08}\text{O}_4$  ( $M = \text{Fe}$  and  $\text{Ga}$ ). While the undoped  $\text{LiMn}_{1.5}\text{Ni}_{0.5}\text{O}_4$  forms three cubic phases with a larger lattice parameter difference among them, the doped samples form only two cubic phases with a smaller lattice parameter difference. The better performance of some of the doped samples could also be related to the small instantaneous change in lattice parameters in addition to the overall change.

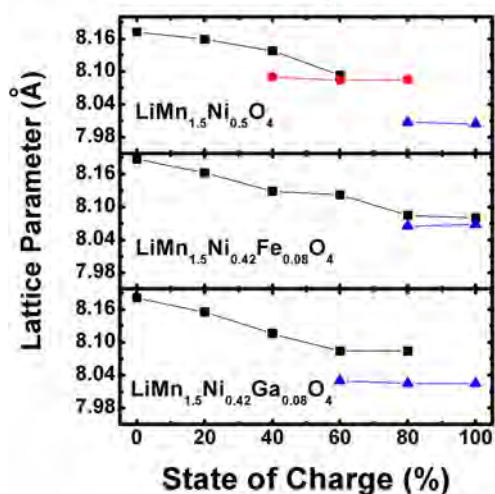


**Figure 2.** Variations of lattice parameters with state-of-charge of undoped and doped high-voltage spinel cathodes.

**TASK 4.4 – PI, INSTITUTION:** Ji-Guang (Jason) Zhang and Jie Xiao, Pacific Northwest National Laboratory

**TASK TITLE:** Cathodes – Development of High Energy Cathode Materials

**BASELINE SYSTEM:** Conoco Philips CPG-8 Graphite/1 M LiPF<sub>6</sub>+EC:DEC (1:2)/Toda High-energy layered (NMC)

**BARRIERS:** Low energy density, high cost, limited cycle life

**OBJECTIVES:** To develop high-energy, low-cost, and long-life cathode materials.

**GENERAL APPROACH:** Our approach is to develop high-energy cathode materials through a cost effective synthesis process. Appropriate doping, surface treatment and the identification of the electrolytes/additives will be used to improve the electrochemical performance of high voltage LiNi<sub>0.5</sub>Mn<sub>1.5</sub>O<sub>4</sub> based cathode. This high voltage cathode will be further combined with layer cathode to form a composite electrode with ‘layered-spinel’ structure. The experience and technologies developed in the high-capacity composite cathode will be used to further improve the capacity and stability of composite cathode.

**STATUS OCT. 1, 2011:** High-voltage LiNi<sub>0.5</sub>Mn<sub>1.5</sub>O<sub>4</sub> doped with Cr has been synthesized by a facile approach suitable for mass production. The reversible capacity is around 130mAh/g from the doped spinel, which exhibits a stable cycling for more than 100 cycles in half cells. The thermal stability investigation for electrochemically cycled LiMnPO<sub>4</sub> electrodes has been completed. The MnPO<sub>4</sub> reduction to Mn<sub>2</sub>P<sub>2</sub>O<sub>7</sub> with oxygen evolution was observed only at a temperature higher than 490°C, while the charged MnPO<sub>4</sub> undergoes structure distortion at above 180°C, possibly because of the Jahn-Teller effect accompanied by the decomposition of the passivation film formed on the cathode surface. Investigation of the electrochemical performance of non-stoichiometric LiMnPO<sub>4</sub> will be completed.

**EXPECTED STATUS SEP. 30, 2012:** High-energy cathodes for Li-ion battery applications will be further explored. Using rheological phase reactions that involve only milling and heating processes and are suitable for scale up, layered composite cathodes based on xLi<sub>2</sub>MnO<sub>3</sub>•(1-x)LiMO<sub>2</sub> (M=Mn, Ni, Co, x = 0.3-0.5) will be synthesized and their degradation mechanism will be investigated. The performance of high-voltage spinel LiNi<sub>0.45</sub>Cr<sub>0.05</sub>Mn<sub>1.5</sub>O<sub>4</sub> will also be further improved. Safety, power rate, and cycling stability of these cathode materials will be improved to satisfy the need for HEV/EVs applications.

**RELEVANT USABC GOALS:** >96 Wh/kg (PHEVs), 5000 deep-discharge cycles, 15-year calendar life, improved abuse tolerance, and less than 20% capacity fade over a 10-year period.

**MILESTONES:**

- (a) Synthesize and electrochemically evaluate Li<sub>2</sub>MnO<sub>3</sub> as a baseline. (Mar. 12) **Complete**
- (b) Utilize rheological phase synthesis of layered composite cathode with 200 mAh/g capacity and stable cycling performance. (Sep. 12) **On schedule**
- (c) Optimize the synthesis approach and inactive components for the high-voltage spinel and composite cathode. (Sep. 12) **On schedule**

## PROGRESS TOWARD MILESTONES

The synthesis and evaluation of  $\text{Li}_2\text{MnO}_3$  were completed this quarter. The structure and cycling ability of  $\text{Li}_2\text{MnO}_3$  prepared at different temperatures were investigated. The optimized calcination temperature for  $\text{Li}_2\text{MnO}_3$  is identified as  $700^\circ\text{C}$ . The long-term cycling stability of a  $700^\circ\text{C}$  treated  $\text{Li}_2\text{MnO}_3$  sample is shown in Fig. 1a. The voltage profiles of  $\text{Li}_2\text{MnO}_3$  at different cycles were also compared (Fig. 1b) in an attempt to understand the voltage decay phenomenon in Mn-based Li-excess layered composites.

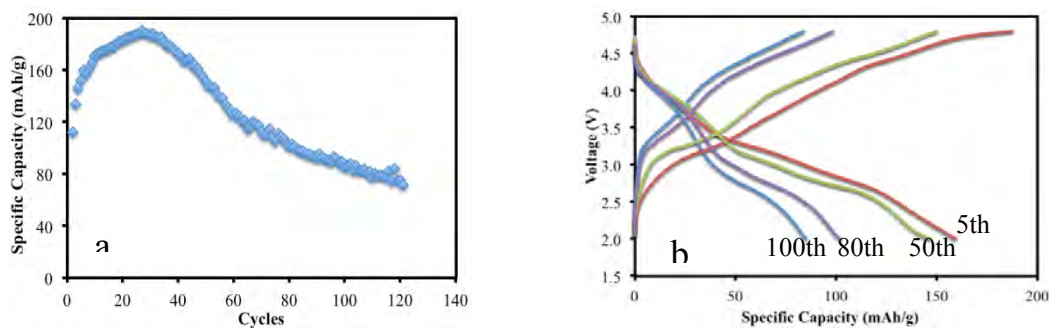


**Figure 1.** Electrochemical performances of  $\text{Li}_2\text{MnO}_3$  baseline synthesized at  $700^\circ\text{C}$ . a) cycling stability and b) voltage profiles at different cycles. The cell was cycled between 2.0 and 4.8 V.

The main purpose for studying the fundamental mechanism of  $\text{Li}_2\text{MnO}_3$  is to understand and/or address the challenges existing in cathodes based on the layered composite, in which  $\text{Li}_2\text{MnO}_3$  is a key component that provides additional capacity to the structure. Figure 1a shows that the discharge capacity of a  $\text{Li}_2\text{MnO}_3$  sample ( $700^\circ\text{C}$  calcinated) increased gradually during the first 40 cycles but decayed eventually after that. It was suspected that the duration of this activation process was related to the non-uniform extraction of  $\text{Li}^+$  during charge, and was dependant on the cut-off charge voltage as well as the current density used in the test. Similar findings were also identified in Li-Mn-rich oxide cathodes, which suggested that these common features may be mainly caused by  $\text{Li}_2\text{MnO}_3$  and is now under investigation. In Fig. 1b, the discharge voltage of  $\text{Li}_2\text{MnO}_3$  exhibited a continuous decline with cycling, exactly as what is observed for Li-rich layered composites. Although the phase transformation from a layered structure to spinel accompanied by  $\text{O}_2$  release has been reported, the fundamental mechanism which is responsible for the continuous voltage decay in these materials is still not clear. More characterizations will be carried out to understand the reaction mechanism.

**Collaborations:** Dr. Xiao-Qing Yang, BNL, for XRD characterizations. Dr. Karim Zaghib, HQ, for material milling. Dr. Kang Xu at Army Research Lab for new electrolyte. Prof. Stan Whittingham, SUNY Binghamton, for characterization.

### Publications:

1. “Reinvestigation on the state-of-the-art nonaqueous carbonate electrolytes for 5 V Li-ion battery applications,” Wu Xu, Xilin Chen, Fei Ding, Jie Xiao, Deyu Wang, Anqiang Pan, Jianming Zheng, Xiaohong S. Li, Asanga B. Padmaperuma, Ji-Guang Zhang, *Journal of Power Sources* **213**, 304-316 (2012).
2. “Effects of cell positive cans and separators on the performance of high-voltage Li-ion batteries,” Xilin Chen, Wu Xu, Jie Xiao, Mark H. Engelhard, Fei Ding, Donghai Mei, Dehong Hu, Jian Zhang, Ji-Guang Zhang, *Journal of Power Sources* **213**, 160-168 (2012).

**Task 4.5- PI, INSTITUTION:** Jordi Cabana, Lawrence Berkeley National Laboratory

**TASK TITLE:** Cathodes – Novel and Optimized Phases for High Energy Density Batteries.

**BASELINE SYSTEM:** Conoco Philips CPG-8 Graphite/1 M LiPF<sub>6</sub>+EC:DEC (1:2)/Toda High-energy layered (NMC)

**BARRIERS:** Low-energy-density, poor cycle life, safety

**OBJECTIVE:** Enable higher density Li-ion batteries through an increase in operation voltage and capacity of the cathode. Design electrode structures that maximize active material utilization and charge density. Understand the structure-composition-properties relationship for bulk and surface in electrodes. Identify new compounds containing non-oxide or polyanions in their crystal structure that are electrochemically active.

**GENERAL APPROACH:** Employ and develop a variety of synthetic methods to produce materials with controlled purity, crystal structure and particle morphology. Use spectroscopic and diffraction techniques and controlled materials to get a complete picture of the different reactions involved in battery electrodes. Explore chemical spaces in search for new phases that may provide performance improvements. Establish the importance of the extended electrode structure on electrochemical performance.

**STATUS OCT. 1, 2011:** Samples of LiNi<sub>1/2</sub>Mn<sub>3/2</sub>O<sub>4</sub> with morphology decoupled from the crystal chemistry (Mn<sup>3+</sup> content, Ni-Mn ordering) were successfully synthesized. Annealing of the samples provided control of these parameters. Analysis of their electrochemical properties as battery electrodes revealed that seemingly small variations among samples produce significant effects on electrochemical performance.

**EXPECTED STATUS SEP. 30, 2012:** The composition and crystal structure of the annealed samples of LiNi<sub>1/2</sub>Mn<sub>3/2</sub>O<sub>4</sub> will have been analyzed by coupling spectroscopic tools with diffraction. The role of oxide additives on the performance of spinel electrodes will have been assessed. The first set of new fluoride-containing phases will have been prepared and their applicability as Li battery cathodes will have been established.

**RELEVANT USABC GOALS:** 40-mile PHEV: Energy/Weight 96 Wh/kg; CD Cycle Life 5000 cycles; Calendar Life @ 40°C 15 years.

**MILESTONES:**

- (a) Complete the crystal-chemical characterization of annealed LiNi<sub>1/2</sub>Mn<sub>3/2</sub>O<sub>4</sub> and identify its role on electrochemical performance. (Mar. 12) **Complete**
- (b) Synthesize and physico-chemically characterize at least two different new phases showing an oxyfluoride network, containing lithium and a light transition metal. (Sep. 12) **On schedule**
- (c) Identify the influence of oxide additives on the extent of electrolyte-electrode side reactions in spinel electrodes. (Sep. 12) **On schedule**

## PROGRESS TOWARD MILESTONES

During the third quarter of FY12, research was directed at **Milestone (c)**. A baseline  $\text{LiNi}_{1/2}\text{Mn}_{3/2}\text{O}_4$  material was selected from the series of annealed samples reported in the previous quarter. This baseline was prepared at  $900^\circ\text{C}$  in air without additional annealings. Post-synthesis coating using MgO was performed by dispersing the powder in a solution of a Mg precursor in a long chain amine solvent. Thermolysis of the precursor led to the formation of  $\text{Mg}(\text{OH})_2$ , which further transformed to MgO above  $400^\circ\text{C}$ . Two post-coating annealing procedures at  $500$  and  $800^\circ\text{C}$  were carried out on two different samples. SEM of the three materials (Fig. 1) revealed that the coating was inhomogeneous after the  $500^\circ\text{C}$  treatment (Fig. 1b). In contrast, the particles obtained following the annealing at  $800^\circ\text{C}$  (Fig. 1c) showed the same smooth surface as the baseline material (Fig. 1a).

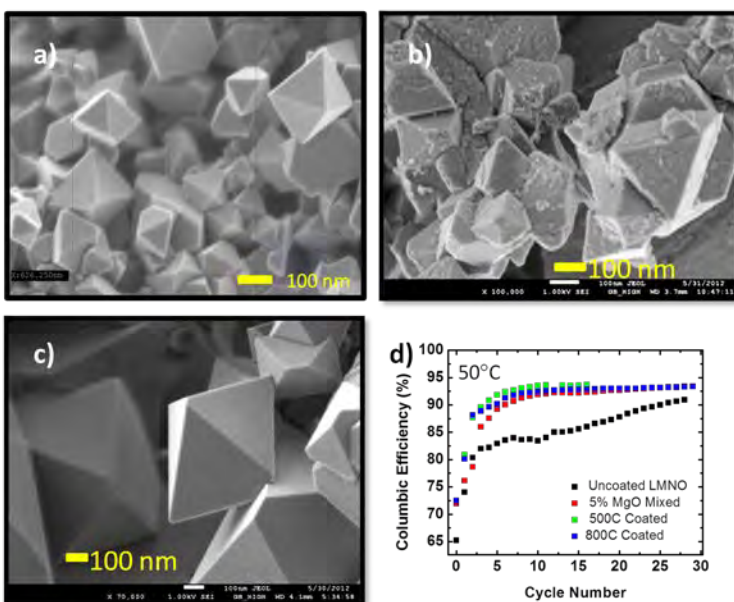


**Figure 1.** SEM of a) baseline  $\text{LiNi}_{1/2}\text{Mn}_{3/2}\text{O}_4$ , and after coating with MgO at b)  $500^\circ\text{C}$ , c)  $800^\circ\text{C}$ . d) Electrochemical performance of the indicated samples at  $50^\circ\text{C}$ .

The modified electrodes was also found (Fig. 1d), although the values were still too low for practical application. This preliminary data is in agreement with previous reports of a beneficial role of the coatings in preventing side reactions. Further cycling is in progress to confirm the reproducibility of these results. Conclusions of this study are expected by the end of FY12, on schedule.

**Collaborations this quarter:** Prof. Grey (SUNY Stony Brook), Prof. Manthiram (UT-Austin), Drs. Persson, Doeff, Richardson, Chen, Guo, Kostecki (LBNL), Dr. Casas-Cabanas (CIC Energigune, Spain), Dr. Chernova, Prof. Whittingham (SUNY Binghamton), Drs. Barenó, Bloom (ANL).

### Publications and Presentations this quarter:

1. T.E. Conry, A. Mehta, J. Cabana, and M.M. Doeff, *J. Electrochem. Soc.*, **2012**, In press.
2. K.A. Aldi, J. Cabana, P.J. Sideris, J. Kim, and C.P. Grey, *Amer. Miner.*, **97**, 883-889, **2012**.
3. "Multiscale reactions in battery electrodes: importance and methods of characterization," *Symposium on Challenges and Opportunities in Energy Storage Materials*, Brown University, Providence, RI (USA), June 1, 2012.

**Task 4.6 - PI, INSTITUTION:** Jason Graetz, Brookhaven National Laboratory

**TASK TITLE:** Cathodes – Novel Materials

**BASELINE SYSTEM:** Conoco Philips CPG-8 Graphite/1 M LiPF<sub>6</sub>+EC:DEC (1:2)/Toda High-energy layered (NMC)

**BARRIERS:** Low energy density and cost

**OBJECTIVE:** Develop low-cost cathode materials that offer high energy density (>660 Wh/kg) and electrochemical properties (cycle life, power density, safety) consistent with USABC goals.

**GENERAL APPROACH:** Our approach is to develop and utilize specialized *in situ* reactors designed to investigate solvothermal synthesis reactions in real-time using synchrotron techniques. This unique capability will allow us to identify intermediate or transient phases and better control phase nucleation, reaction rates and material properties. These new tools and insights will be used to prepare novel high energy density lithium cathode materials ( $\geq 660$  Wh/kg).

**STATUS OCT. 1, 2011:** This project is a new start. All equipment and plans are in place for the initial project tasks.

**EXPECTED STATUS SEP. 30, 2012:** In Year 1 the existing quartz capillary reactor will be modified to accommodate higher pressures and temperatures. A procedure for the synthesis of LiMBO<sub>3</sub> (M = Mn and/or Fe) will be developed and complete preliminary electrochemical measurements.

**RELEVANT USABC GOALS:** 200 Wh/kg (EV requirement); 96 Wh/kg, 3000 cycles (PHEV 40 mile requirement); lower cost batteries.

**MILESTONES:**

- (a) Complete design and order necessary components for second-generation capillary reactor capable of accommodating higher pressures and temperatures. (Apr. 12) **Complete**
- (b) Develop a procedure for the synthesis of LiMBO<sub>3</sub> (M = Mn and/or Fe). (Sep. 12) **On schedule**
- (c) Complete preliminary characterization of synthesis reaction(s) using the *in situ* capillary reactor. (Sep. 12) **On schedule**

## PROGRESS TOWARD MILESTONES

Efforts in the third quarter of FY12 were focused on the preparation of  $\text{Cu}_{0.95}\text{V}_2\text{O}_5$ . The hydrothermal synthesis was performed in deionized water at  $200^\circ\text{C}$  for 10 hours:

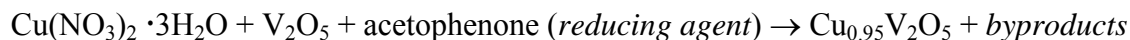
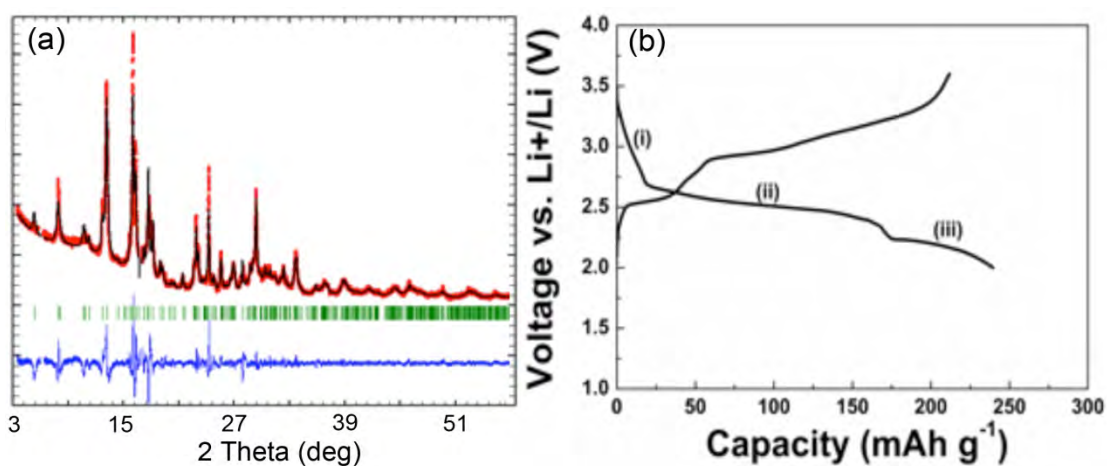


Figure 1(a) shows the synchrotron XRD pattern acquired from the as-synthesized  $\text{Cu}_{0.95}\text{V}_2\text{O}_5$  prepared *via* the hydrothermal reaction. Lattice parameters were determined from a profile fit to data:  $a = 11.765 \text{ \AA}$ ,  $b = 3.694 \text{ \AA}$ ,  $c = 8.971 \text{ \AA}$ ,  $\alpha = \gamma = 90^\circ$ ,  $\beta = 111.5730^\circ$ . The  $a$  parameter, which is the spacing parallel to the  $[\text{V}_2\text{O}_5]_n$  double layer, is slightly lower than the reported value, which suggests that the  $\text{VO}_6$  octahedron in the double-layer stacking may be slightly distorted in this sample. Further optimization of the synthesis recipe may be necessary.



**Figure 1.** (a) Synchrotron XRD pattern and profile fit from  $\text{Cu}_{0.95}\text{V}_2\text{O}_5$  synthesized at  $200^\circ\text{C}$  for 10 h. (b) Initial charge-discharge profile of  $\text{Cu}_{0.95}\text{V}_2\text{O}_5$  showing a 3-step redox reaction.

A small amount of impurity phases,  $\text{Cu}_3(\text{OH})_2\text{V}_2\text{O}_7 \cdot 2\text{H}_2\text{O}$  and  $\text{CuO}$ , were observed in the as-synthesized sample (stuck to the wall of the reactor).  $\text{Cu}_3(\text{OH})_2\text{V}_2\text{O}_7 \cdot 2\text{H}_2\text{O}$  is expected to decompose to form  $\text{Cu}_{0.95}\text{V}_2\text{O}_5$  and  $\text{CuO}$  with the reducing agent and  $\text{CuO}$  should be easily decomposed in the acidic environment. The existence of these intermediate phases on the walls of the reactor suggests that there may be incomplete mixing of the slurry during the reaction.

Figure 1b shows the charge-discharge profiles and the specific capacities of the hydrothermally synthesized  $\text{Cu}_{0.95}\text{V}_2\text{O}_5$  during the first cycle. The first discharge capacity was about  $240 \text{ mAh g}^{-1}$ , which corresponds to a transfer of 2.17 Li, which is less than the previously reported value of  $292 \text{ mAh g}^{-1}$  (2.64 Li). The discharge profile is clearly divided into three regions: (i) steep slope above 2.6 V (*ca.* 0.17 Li), (ii) gentle slope near 2.5 V (*ca.* 1.4 Li), and (iii) gentle slope below 2.2 V (*ca.* 0.6 Li). It is speculated that region (i) is due to Li intercalation into Cu-V-O matrix, region (ii) is due to Cu extrusion, and region (iii) is due to further Li intercalation into the Li-V-O matrix.

**Task 4.7 - PI, INSTITUTION** - Jim Kiggans and Andrew Kercher, Oak Ridge National Laboratory

**TASK TITLE:** Cathodes – Lithium-bearing Mixed Polyanion (LBMP) Glasses as Cathode Materials

**BASELINE SYSTEM:** Conoco Philips CPG-8 Graphite/1 M LiPF<sub>6</sub>+EC:DEC (1:2)/Toda High-energy layered (NMC)

**BARRIERS:** Cathodes for Li-ion batteries require lower cost materials and improved energy density, safety, and cycling stability.

**OBJECTIVE:** Lithium-bearing mixed polyanion (LBMP) glasses are herein proposed as potential cathode materials for lithium ion batteries with superior performance to lithium iron phosphate for use in electric vehicle applications. The composition of LBMP glasses can be tailored to provide higher electrical conductivities, higher redox potentials, and higher specific energies than similar crystalline polyanion framework materials. The disordered covalently bonded structures of LBMP glasses could provide excellent cyclability and safety performance. In addition, LBMP glass compositions may enable cyclable multi-valent changes in the transition metal cations of the cathode material, which has the potential to provide specific energies up to near 1000 mWh/g.

**GENERAL APPROACH:** The experimental approach combines: (1) structure and property modeling, (2) glass processing, (3) glass characterization, (4) conventional cathode production, and (5) electrical and electrochemical testing. Computer modeling will be used to suggest the most promising LBMP glass compositions in terms of electrochemical performance and glass processing capability. Classical heat-quench glass forming and sol gel processing will be used to make the LBMP glasses. Electrochemical performance will be demonstrated on coin cells with LBMP glass cathodes using cycle testing and variable discharge rate testing.

**STATUS May 1, 2012:** Preparations in place for initiation of the project.

**EXPECTED STATUS SEP. 30, 2012:** Initial glass compositions will serve as a baseline for electrochemical properties as well as means to develop our materials synthesis capability and electrode fabrication techniques. Similarly CALPHAD modeling will build from baseline preliminary work on the iron phosphate system. Both efforts will be ready to move to more complex and promising compositions in the following year.

**RELEVANT USABC GOALS:** Reduce the cost of electrochemical energy storage by developing lithium-ion batteries and other advanced energy-storage technologies that afford higher energy densities without sacrificing safety and performance.

**MILESTONES:**

- (a) Synthesize, characterize, and perform electrochemical testing on two of baseline glass cathode compositions. (Sep. 12) **Delayed to Dec. 31, 2012 due to funding delay**
- (b) Create CALPHAD thermodynamic database for the baseline system. (Sep. 12) **Delayed to Dec. 31, 2012 due to funding delay**
- (c) Synthesize and characterize one of baseline glass cathode composition. (Sep. 12) **On schedule**

## **PROGRESS TOWARD MILESTONES**

The program will initially focus on the production, modeling, characterization, and electrochemical testing of simple LBMP glass compositions.

This project was initiated June 22, 2012.

## **BATT TASK 5** **DIAGNOSTICS**

**TASK 5.1 - PI, INSTITUTION:** Robert Kostecki, Lawrence Berkeley National Laboratory

**TASK TITLE - PROJECT:** Diagnostics – Interfacial Processes

**BASELINE SYSTEMS:** Conoco Philips CPG-8 Graphite/1 M LiPF<sub>6</sub>+EC:DEC (1:2)/Toda High-energy layered (NMC)

**BARRIERS:** Low energy (related to cost), poor lithium battery calendar/cycle lifetimes.

**OBJECTIVES:** (i) Establish direct correlations between electrochemical performance of high-energy Li-ion composite cathodes, and surface chemistry, morphology, topology and interfacial phenomena, (ii) improve the capacity and cycle life limitations of Li-alloy anodes

**GENERAL APPROACH:** Our approach is to (i) apply *in situ* and *ex situ* Raman and FTIR far field and near field spectroscopy/microscopy, scanning probe microscopy (SPM), spectroscopic ellipsometry, electron microscopy (SEM, HRTEM), and standard electrochemical techniques to detect and characterize bulk and surface processes in intermetallic anodes, and high-energy cathodes, (ii) design and apply a new model electrochemical experimental setup to study the kinetics of lithium alloying and diffusion in intermetallic anodes, and possible correlations with the formation and long-term stability of the SEI layer.

**STATUS OCT. 1, 2011:** Insight into the mechanism of surface phenomena on thin-film and monocrystal Sn and Si intermetallic anodes is expected to have been gained and their impact on the electrode long-term electrochemical behavior is expected to have been evaluated. Comprehensive fundamental study of the early stages of SEI layer formation on polycrystalline and single crystal face Sn and Si electrodes will be carried out. *In situ* and *ex situ* far- and near-field FTIR and Raman spectroscopy will be employed in conjunction with AFM surface imaging will be applied to detect and monitor surface phenomena at the intermetallic anodes. Similar experimental methodology will be used to detect and characterize surface and bulk processes in high-voltage (>4.3V) model and composite cathodes.

**EXPECTED STATUS SEP. 30, 2012:** The mechanism of electrolyte decomposition at the surface of model anode and cathode materials is expected to be fully understood and its impact on the electrode long-term electrochemical behavior evaluated. The composition and (re)formation dynamics of the surface layer on model monocrystal Sn and Si intermetallic anodes as well as on model single particle and composite high-voltage cathodes will be determined using various complementary spectroscopy techniques. A unique strategy involving the use of *in situ* techniques (AFM, ellipsometry, Raman and fluorescence imaging, FTIR and AP-XPS) in conjunction with *ex situ* techniques (XAS, RBS and NRA) will be applied to monitor and identify surface processes. Preliminary evaluation of near-field optical spectroscopy and imaging techniques for fundamental interfacial studies of Li-ion systems will be carried out.

**RELEVANT USABC GOALS:** *Cycle life:* 5000 (deep) and 300,000 (shallow) cycles. *Available energy:* 96 Wh/kg. *Calendar life:* 15 years.

### **MILESTONES:**

- (a) Resolve SEI layer chemistry of Si and Sn model anodes - collaboration with the BATT Anode Group. (Jul. 12) **Complete**
- (b) Characterize surface phenomena and bulk phenomena in high-voltage composite cathodes - collaboration with the BATT Cathode Group. (Sep. 12) **On schedule**
- (c) Use near-field IR and Raman spectroscopy to characterize battery materials. (Sep. 12). **On schedule**

## PROGRESS TOWARD MILESTONES

In the third quarter the influence of electrolyte additives on the interfacial stability of polycrystalline tin electrodes was studied upon cycling in organic carbonate electrolytes. The selection of additives was consistent with our earlier x-ray spectroscopy investigation of the effect of organic and inorganic electrolyte additives on the SEI layer chemistry at model tin single crystal electrodes (see FY11 3<sup>rd</sup> quarterly report). Figure 1 shows CVs of Sn in two different electrolytes. The upper graph displays the effect of LiF in 1 M LiPF<sub>6</sub>, EC:DEC electrolyte on the cycling behavior of Sn as compared to an electrolyte mixture without additives. The 500 mV shift of the cathodic peak toward lower potentials in the 1<sup>st</sup> CV cycle with LiF additives followed by a significant suppression of electrolyte reduction current in the following cycles indicates that the mechanism of the SEI formation has been altered, resulting in a more protective surface film at the Sn electrode. This is a surprising result because LiF is considered completely insoluble in organic carbonate electrolytes. Interestingly, similar effects were observed in the presence of FEC additive, which is expected to release F<sup>-</sup> in the electrolyte upon decomposition. Replacing LiPF<sub>6</sub> by LiTFSI also suppressed irreversible processes on Sn at 1.3 V, which points out the critical role of the Li salt in achieving interfacial stability of Sn electrodes. This study concludes milestone (a) toward resolution of SEI layer chemistry of Sn anodes.

Our efforts towards milestone (b) focused on fluorescence spectroscopy measurements of surface phenomena at the LiNi<sub>0.5</sub>Mn<sub>1.5</sub>O<sub>4</sub> cathode. Single solvent DEC-based 1 M LiPF<sub>6</sub> electrolytes displayed an increase then decrease of fluorescence upon charge then discharge, as previously observed in 1 M LiPF<sub>6</sub>, EC:DEC electrolytes (see FY11 4<sup>th</sup> quarter report). However, cycling of the LMNO electrode in EC LiPF<sub>6</sub> electrolyte showed no accumulation of insoluble fluorescence compounds upon cycling. This suggests that the insoluble electrolyte decomposition product must predominantly originate from oxidation of DEC. Further detailed investigations of the mechanism of electrolyte oxidation reactions at high-voltage LMNO cathodes and their effect on electrochemical performance are underway.

Preliminary near-field IR imaging measurements toward milestone (c) were carried out to sense the chemical composition of the SEI layer on Sn single crystals. To accomplish this goal, the IR near-filed microscope will be coupled with the IR tunable beam line at the Advanced Light Source of LBNL.

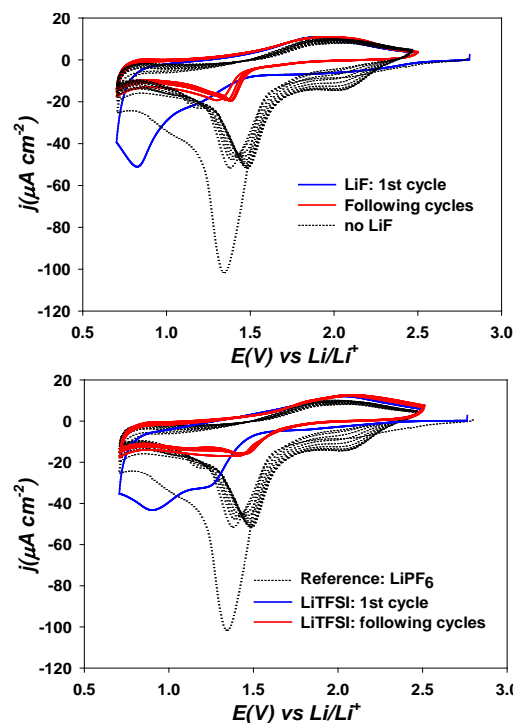


**Figure 1.** CV cycling of tin polycrystalline electrodes in EC:DEC (1:2, w:w) with (top) 1 M LiPF<sub>6</sub> + LiF; (bottom) LiTFSI and their comparison with EC:DEC LiPF<sub>6</sub>.



**Figure 2.** Electrochemical data (top) and corresponding integrated fluorescence intensity (bottom) collected during three CV cycles between 3.5 and 5.0 V for LMNO (blue) in EC 1M LiPF<sub>6</sub>.

**TASK 5.2 - PI, INSTITUTION:** Xiao-Qing Yang and Kyung-Wan Nam, Brookhaven National Laboratory

**TASK TITLE - PROJECT:** Diagnostics – Battery Materials: Structure and Characterization

**BASELINE SYSTEMS:** Conoco Philips CPG-8 Graphite/1 M LiPF<sub>6</sub>+EC:DEC (1:2)/Toda High-energy layered (NMC)

**BARRIERS:** PHEV: Energy density, cycle life; HEV: power density, abuse tolerance

**OBJECTIVES:** To determine the contributions of electrode materials changes, interfacial phenomena, and electrolyte decomposition to cell capacity and power decline in helping the development of high energy density lithium battery with better safety characteristics and longer life.

**GENERAL APPROACH:** To use various synchrotron based X-ray techniques to characterize electrode materials and electrodes taken from baseline BATT Program cells. *Ex situ* soft XAS will be used to distinguish the structural differences between surface and bulk of electrodes. Time resolved X-ray diffraction (TRXRD) technique will be used to understand the reactions that occur in charged cathodes at elevated temperatures.

**STATUS OCT. 1, 2011:** Studies on high energy Li<sub>1.2</sub>Ni<sub>0.2</sub>Mn<sub>0.6</sub>O<sub>2</sub> cathode materials during charge-discharge cycling using combined *in situ* hard XAS and *ex situ* soft XAS will be completed. Important information about the roles of Mn cations will be obtained. The *in situ* XAS and XRD studies on mesoporous LiFe<sub>1-y</sub>Mn<sub>y</sub>PO<sub>4</sub> (0.0≤y≤0.8) cathode materials during charge-discharge cycling will be completed. The effects of particle size and morphology on the phase transition behavior and performance of Li-ion cells will be obtained.

**EXPECTED STATUS SEP. 30, 2012:** Structural studies on the high energy density Li<sub>2</sub>MnO<sub>3</sub>-LiMO<sub>2</sub> (M = Ni, Mn, Co) layered materials (in collaboration with ANL) and *in situ* XRD studies on different types of lithium iron phosphate cathode materials with mesoporous structure will be carried out. The diagnostic studies of high voltage LiMn<sub>2-x</sub>M<sub>x</sub>O<sub>4</sub> (M= Ni, Cu etc.) with spinel structure will be completed. Diagnostic studies on high energy density anode materials, such as Si, Sn and alloys will also be conducted.

**RELEVANT USABC GOALS:** 15 year calendar life, <20% capacity fade over a 10-year period, improved abuse tolerance.

**MILESTONES:**

- (a) Complete *in situ* XRD studies of LiMn<sub>0.4</sub>Fe<sub>0.6</sub>PO<sub>4</sub> cathode material with different particle size and morphology during electrochemical delithiation. (Apr. 12) **Complete**
- (b) Complete *in situ* XRD studies of Li<sub>2</sub>CO<sub>3</sub> during electrochemical decomposition and the potential application of this process. (Apr. 12) **Complete**
- (c) Complete *in situ* XAS studies of high voltage LiMn<sub>2-x</sub>M<sub>x</sub>O<sub>4</sub> (M= Ni, Cu etc.) with spinel structure cathode materials during electrochemical cycling. (Sep. 12) **On schedule**

## PROGRESS TOWARD MILESTONES

In the 3<sup>rd</sup> quarter of FY 2012, milestone (b) was successfully completed and progress toward milestone (c) was made.

In the 3<sup>rd</sup> quarter of FY 2012, research at BNL was focused on the structural changes of  $\text{LiNi}_{0.5}\text{Mn}_{1.5}\text{O}_4$  cathode materials, which may play a critical role in determining the cell's performance. There are two types of structures for  $\text{LiNi}_{0.5}\text{Mn}_{1.5}\text{O}_4$ : ordered  $P4_332$  and disordered  $Fd-3m$ . It is widely accepted that the disordered  $Fd-3m$  structure, which is closely related to the content of  $\text{Mn}^{3+}$  in the material, is the main contributor to good capacity retention and high rate capability. However, too high a  $\text{Mn}^{3+}$  will severely reduce the capacity and cause poor capacity retention. Finding the optimum content of  $\text{Mn}^{3+}$  and synthesis conditions (annealing temperature, time, and atmosphere, as well as cooling rate) are quite important. In this quarter, the local structure changes of the disordered  $\text{LiNi}_{0.5}\text{Mn}_{1.5}\text{O}_4$  ( $Fd-3m$ ) during charge-discharge were studied using *in situ* XAS to monitor the changes of  $\text{Mn}^{3+}$  to  $\text{Mn}^{4+}$  and  $\text{Ni}^{2+}$  to  $\text{Ni}^{4+}$ . XAS results during the first charge are shown in Fig. 1. The Mn and Ni K-edge XANES spectra (Figs. 1b and c), indicate the species most likely to be undergoing oxidation changes as a

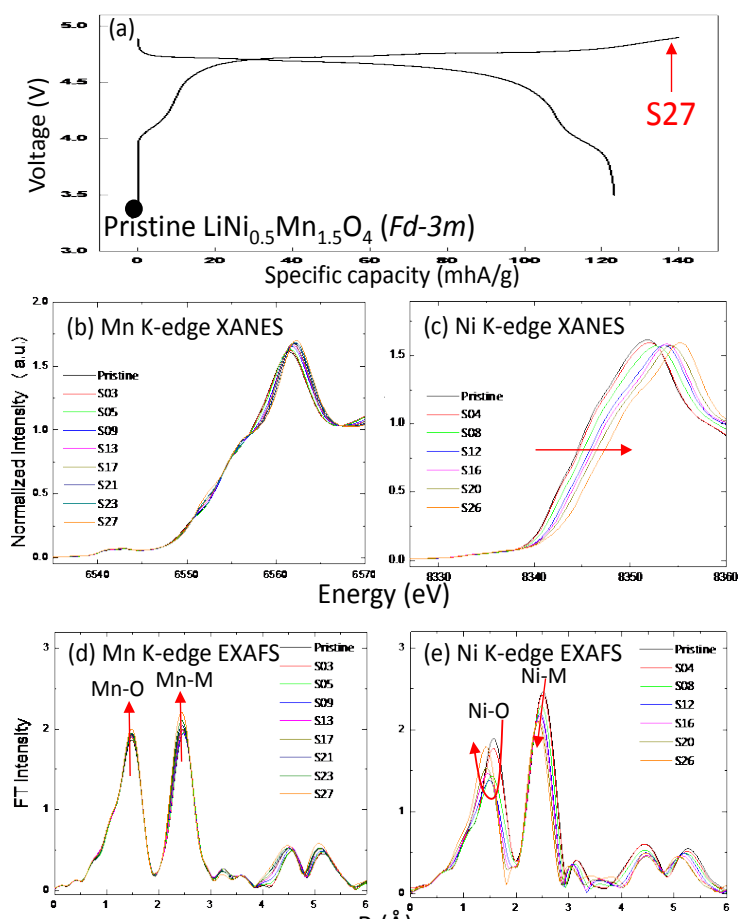


**Figure 1.** (a) charge-discharge profile of the disordered  $\text{LiNi}_{0.5}\text{Mn}_{1.5}\text{O}_4$  cathode material during *in situ* XAS, and corresponding *in situ* XAS spectra at Mn K-edge (b) and (d) and Ni K-edge (c) and (e) during the 1st charge.

result of delithiation. During the early state of charge at *ca.* 4.1V, a slight increase in the Mn-O peak amplitude in the EXAFS spectra, Fig. 1d, is observed. This suggests that a small amount of  $\text{Mn}^{3+}$  ions is oxidized to  $\text{Mn}^{4+}$  ions and is not Jahn-Teller active. In the following high voltage capacity region above 4.6 V, the Ni K-edge EXAFS spectra in Fig. 1e show typical peak feature changes for the first Ni-O bond, confirming the major capacity contribution is coming from the  $\text{Ni}^{2+/4+}$  redox reaction. *In situ* XAS spectra of the disordered  $\text{LiNi}_{0.5}\text{Mn}_{1.5}\text{O}_4$  during discharge showed reversible local structural changes back to the pristine state *via* the redox reaction of  $\text{Ni}^{4+}$  to  $\text{Ni}^{2+}$  at high voltage, and a small amount of redox reaction of  $\text{Mn}^{4+}$  to  $\text{Mn}^{3+}$  at lower voltage. *In situ* XAS of the ordered  $\text{LiNi}_{0.5}\text{Mn}_{1.5}\text{O}_4$  sample during charge-discharge will be completed in the 4<sup>th</sup> quarter of FY 2012 and compared with the local structural changes observed in the disordered material.

**TASK 5.3 - PI, INSTITUTION:** Gerbrand Ceder, Massachusetts Institute of Technology, and Clare Grey, Cambridge University

**TASK TITLE - PROJECT:** Diagnostics - First Principles Calculations and NMR Spectroscopy of Electrode Materials

**BASELINE SYSTEMS:** Conoco Philips CPG-8 Graphite/1 M LiPF<sub>6</sub>+EC:DEC (1:2)/Toda High-energy layered (NMC)

**BARRIERS:** Low rate capabilities; high cost; poor stability; low energy-density

**OBJECTIVES:** Determine the effect of structure on stability and rate capability of cathodes and anodes. Explore relationship between electrochemistry and particle size and shape. Develop new, stable, cathode materials with high energy-density.

**GENERAL APPROACH:** Use solid state NMR and diffraction/TEM to characterize local and long-range structure as a function of particle size, sample preparation method, state of charge and number of charge cycles (cathodes). Use electrochemistry to correlate particle size with rate performance. Continue to develop the use of *in situ* NMR methods to identify structural changes and reactivity in oxides and intermetallics and to examine Li dendrite formation. Use first principles calculations (density functional theory) to identify redox-active metals, relative stability of different structures, the effect of structure and particle size on cell voltages and rate capability. Use high-throughput computing to identify promising cathode materials for BATT applications. Anticipate possible instabilities in materials at high states of charge by using calculations. Use calculations and NMR to identify low activation energy pathways for cation migration and to investigate electronic conductivity. Extend to Na systems.

**STATUS OCT. 1, 2011:** *In situ* NMR of silicon and lithium metal anodes, new phosphocarbonates and high voltage cathodes will be ongoing. Several compounds from computational search under experimental investigation.

**EXPECTED STATUS SEP. 30, 2012:** Completed <sup>29</sup>Si studies of lithium silicides and phosphocarbonates. Insights into viability of several Na cathodes.

**RELEVANT USABC GOALS:** Specific power 300 W/kg, 10 year life, <20% capacity fade

**MILESTONES:**

- (a) Complete <sup>29</sup>Si NMR experiments on crystalline lithium silicides. (Mar. 12) **Complete**
- (b) Complete electrochemical testing of sidorenkites for Li and Na batteries. (Mar. 12) **Complete**
- (c) Complete NMR studies of metal doping of LiMnPO<sub>4</sub>. (Mar. 12) **Delayed. experiments ongoing.**
- (d) Complete work on novel intercalation cathode. (Mar. 12) **Complete**
- (e) Complete <sup>29</sup>Si NMR of amorphous lithium silicide electrodes. (Sep. 12) **On schedule**
- (f) Initiate *in situ* NMR studies of SEI formation on silicon anodes; complete lithium dendrite study. (Sep. 12) **On schedule**
- (g) Suggest at least one new Na intercalation compounds. (Sep. 12) **On schedule**
- (h) Provide computed data on pyrophosphates to Whittingham (Sep. 12) **Complete**

## PROGRESS TOWARD MILESTONES

Lithium and sodium transition-metal carbonophosphates are suggested by our previous reported high-throughput computing and screening to be promising intercalation compounds. The

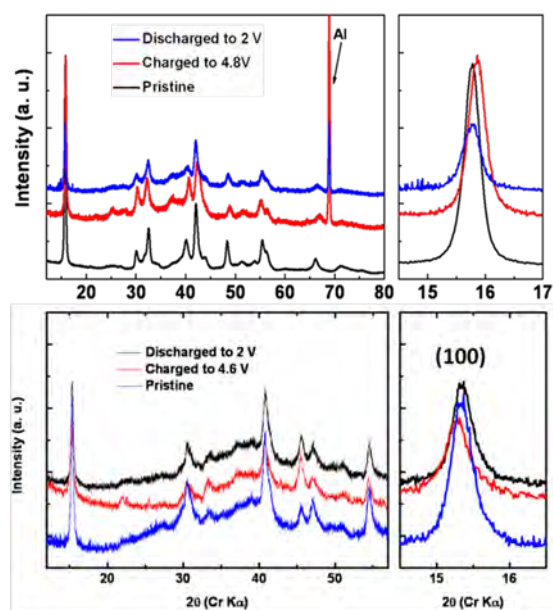


**Figure 1.** XRD patterns of pristine, end of first charge. End of first discharge samples for  $\text{Li}_3\text{FePO}_4\text{CO}_3$  (top) and  $\text{Li}_3\text{MnPO}_4\text{CO}_3$  (bottom)

computation results of their thermodynamic stability indicate that many of the sodium carbonophosphates are stable while all of the Li compounds are either not stable or meta-stable.  $\text{Na}_3\text{FePO}_4\text{CO}_3$  and  $\text{Na}_3\text{MnPO}_4\text{CO}_3$  were successfully synthesized by the hydrothermal method with their Li analogs obtained through Li-Na ion exchange. Stoichiometric  $\text{Li}_3\text{FePO}_4\text{CO}_3$  was obtained through complete ion exchange. However, for  $\text{Na}_3\text{MnPO}_4\text{CO}_3$ , only a fraction of the Na can be replaced by Li, yielding  $\text{Li}_{2.67}\text{Na}_{0.63}\text{Mn}_{0.96}\text{PO}_4\text{CO}_3$ . In collaboration with Dr. Yimei Zhu at BNL, the crystal structure of  $\text{Li}_3\text{FePO}_4\text{CO}_3$  was solved by combining single particle electron diffraction and synchrotron powder diffraction. *In situ* battery cycling XRD experiments were performed for both compounds at NSLS. Both *ex situ* and *in situ* XRD results indicate that Li ion intercalation/deintercalation in both Fe and Mn carbonophosphates are topotactic, with a solid solution pathway.

Both Fe and Mn carbonophosphates show good electrochemical performance.  $\text{Li}_3\text{FePO}_4\text{CO}_3$  shows a capacity of *ca.* 110 mAh/g at C/5 rate after ball-milling with carbon black and the same capacity at 60°C without ball-milling. This capacity is close to 100% of the one-electron theoretical capacity (115 mAh/g). The main plateau at around 3 V agrees well with the computationally predicted intercalation voltage (2.99 V) for the  $\text{Fe}^{2+}/\text{Fe}^{3+}$  redox.  $\text{Li}_{2.67}\text{Na}_{0.63}\text{Mn}_{0.96}\text{PO}_4\text{CO}_3$  shows a capacity of *ca.* 135 mAh/g after ball-milling with carbon, corresponding to 1.2 Li intercalations per formula. This result indicates that not only is the  $\text{Mn}^{2+}/\text{Mn}^{3+}$  redox active, but the  $\text{Mn}^{3+}/\text{Mn}^{4+}$  redox couple is partially active, which is rare in polyanion cathode materials.

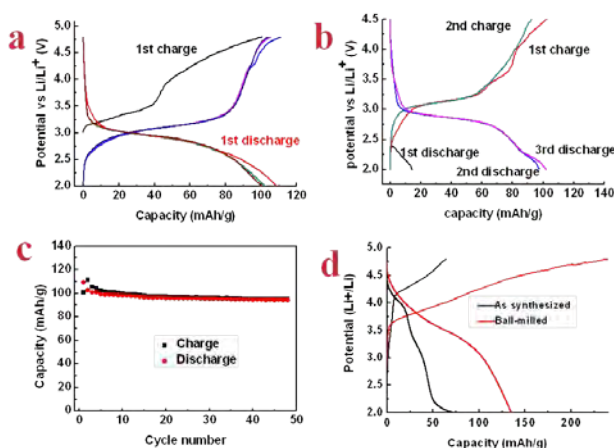


**Figure 2.** (a) The voltage profile of ball-milled  $\text{Li}_3\text{FePO}_4\text{CO}_3$  cycled at C/5 rate from 2 to 4.5 V at room temperature. (b) The voltage profile of non-ball-milled  $\text{Li}_3\text{FePO}_4\text{CO}_3$  cycled from 2 to 4.5 V at 60°C and C/10 rate. (c) The capacity retention of condition (a). (d) The voltage profile of  $\text{Li}_{2.67}\text{Na}_{0.63}\text{Mn}_{0.96}\text{PO}_4\text{CO}_3$ , both ball-milled and non-ball-milled samples, cycled at C/100 rate.

**Task 5.4 - PI, INSTITUTION:** Yang Shao-Horn, Massachusetts Institute of Technology

**TASK TITLE - PROJECT:** Diagnostics - Studies and Design of Chemically and Structurally Stable Surfaces and Structures of Lithium Storage Materials

**BASELINE SYSTEMS:** Conoco Philips CPG-8 Graphite/1 M LiPF<sub>6</sub>+EC:DEC (1:2)/Toda High-energy layered (NMC)

**BARRIERS:** Inadequate energy, and abuse tolerance of Li-ion batteries

**OBJECTIVES:** To develop high-energy and long-cycle-life cathodes.

**GENERAL APPROACH:** Efforts will be focused on exploring the use of lithium peroxides and oxides in the positive electrodes to provide significant enhancement in gravimetric energy relative to conventional lithium interaction compounds. Of particular interest is to examine the influence of catalysts on the charging voltage of such high-energy electrodes. The surface chemistry, microstructure of oxide-electrolyte interface, and oxide crystal structure of high-energy positive electrodes will be examined by a range of techniques such as transmission electron microscopy, synchrotron X-ray diffraction, Raman spectroscopy and X-ray adsorption spectroscopy, and X-ray photoelectron spectroscopy. These surface and structural features and their changes during electrochemical measurements would provide insights into developing strategies in the design of high-energy and long-cycle-life cathodes.

**STATUS OCT. 1, 2011:** Select (Li<sub>2</sub>O<sub>x</sub>)<sub>y</sub>MO<sub>z</sub> electrodes will be prepared and tested in two-electrode and three-electrode cells having lithium as the negative electrode, where the activity of MO<sub>z</sub> such as MnO<sub>2</sub> and Co<sub>3</sub>O<sub>4</sub> for Li<sub>2</sub>O<sub>x</sub> oxidation will be compared with that of the state-of-art precious metal catalysts such as Pt/C.

**EXPECTED STATUS SEP. 30, 2012:** The influence of some metal oxide catalysts on the charging voltage of such high-energy electrodes has been established and compared with Pt/C. Changes in the microstructure and crystal structure of select (Li<sub>2</sub>O<sub>x</sub>)<sub>y</sub>MO<sub>z</sub> electrodes have been identified by scanning or transmission electron microscopy and X-ray diffraction. Application of fundamental insights to design of new and stable surfaces for high-energy cathodes will be ongoing.

**RELEVANT USABC GOALS:** High Energy/Power Ratio Battery, energy density (>100 Wh/kg), power density (>400 W/kg), 15-year calendar life and cycle life (5,000 cycles).

**MILESTONES:**

- (a) Complete XPS analysis of the surface chemistry changes of LiNi<sub>0.5</sub>Mn<sub>1.5</sub>O<sub>4</sub> cycled to two voltages and compare with the surface chemistry changes of Li<sub>x</sub>CoO<sub>2</sub> and LiNi<sub>0.5</sub>Mn<sub>0.5</sub>O<sub>2</sub>. (Jun. 12). **Delayed – due Sep. 12**
- (b) Demonstrate the oxide catalyst influence on the capacities, discharge/charge voltages or cycle life of (Li<sub>2</sub>O<sub>2</sub>)<sub>x</sub>(MO<sub>2</sub>)<sub>y</sub> (where M = Mn, Co, Ni, etc.) in lithium cells. (Jun. 12) **Complete**
- (c) Supply XPS and TEM data demonstrating the surface chemistry and morphological changes of (Li<sub>2</sub>O<sub>2</sub>)<sub>x</sub>(MO<sub>2</sub>)<sub>y</sub> during charge and discharge. (Sep. 12) **On schedule**

## PROGRESS TOWARD MILESTONES

The round-trip efficiency of non-aqueous, rechargeable, Li-air batteries remains limited by the large overpotential during charging, which is attributed to the poor oxidation kinetics of the  $\text{Li}_2\text{O}_2$  formed during discharge. In order to develop strategies to reduce the charging overpotential in Li-air batteries, the reaction using Vulcan XC72 carbon-based electrodes (VC) was studied in which commercially available  $\text{Li}_2\text{O}_2$  particles were introduced into the electrode. In this study, the electrochemical oxidative activity of Li-Li $_2\text{O}_2$  cells with unmodified VC and VC decorated with Ru or Pt nanoparticles was studied. Both Ru and Pt were found to be able to significantly reduce the potential required for  $\text{Li}_2\text{O}_2$  oxidation (Harding *et al.*, *Phys. Chem. Chem. Phys.*, 2012, **14**, 10540-10546).

All electrodes consisted of a VC, 40 wt% Ru on VC (Ru/C), or 40 wt% Pt on VC (Pt/C) with lithiated Nafion® as a binder and mixed with  $\text{Li}_2\text{O}_2$  under argon, then deposited on aluminum foil. For each catalyst, electrodes were prepared with  $\text{Li}_2\text{O}_2$  (denoted by “+ $\text{Li}_2\text{O}_2$ ”, e.g. Ru/C+ $\text{Li}_2\text{O}_2$ ) and without  $\text{Li}_2\text{O}_2$ , which was used to establish the background current. VC electrodes were charged potentiostatically at voltages between 4.0 and 4.4 V vs. Li ( $V_{\text{Li}}$ ) in 0.1 M  $\text{LiClO}_4$  in DME, while Ru/C and Pt/C electrodes were charged between 3.5 and 3.9  $V_{\text{Li}}$ . For both catalysts and at each voltage, electrodes with and without  $\text{Li}_2\text{O}_2$  were charged to allow the estimation of the net current by subtracting the background current due to reactions not involving  $\text{Li}_2\text{O}_2$ . Integrating the net current with respect to time gave the capacity of the electrode associated with  $\text{Li}_2\text{O}_2$  oxidation.

Ru/C was observed to be active several hundred millivolts below that of VC. At 3.9  $V_{\text{Li}}$ , the net oxidative current density of Ru/C and Pt/C approached 1000  $\text{mA/g}_{\text{carbon}}$  (Figure 1), in contrast to VC alone, where no net oxidative current was observed below 4.0  $V_{\text{Li}}$ . Ru/C remained reasonably active to 3.6  $V_{\text{Li}}$ , below which the majority of  $\text{Li}_2\text{O}_2$  could not be oxidized, while Pt/C exhibited very slow charging even at 3.5  $V_{\text{Li}}$ . XRD (Figure 2) and SEM analyses indicate reduced  $\text{Li}_2\text{O}_2$  content in partially-charged electrodes, and indicate the absence of  $\text{Li}_2\text{O}_2$  after complete charging.

The mechanism of this activity enhancement remains unknown. We are developing solid-state Li-air cells to be studied *in situ* in collaboration with Zhi Liu of the ALS at LBNL in order to resolve the chemical state of the discharge products over the course of this reaction.

**Collaborations:** Collaborations with Dr. A. Mansour at the NSWC for XPS and X-ray absorption spectroscopy measurements through a subcontract of MIT would preferred to be continued. Collaborations will continue with M.M. Thackeray in using TEM and XPS to study the atomic structure and surface chemistry, respectively, of layered  $\text{Li}_x\text{Ni}_x\text{Mn}_y\text{O}_z$  materials.

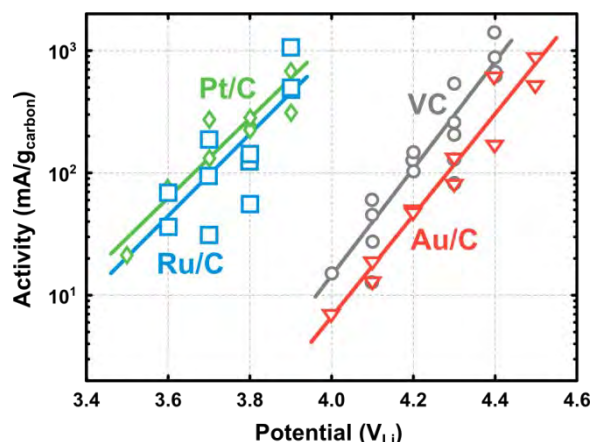


Figure 2 Oxidative activity of Pt/C+, Ru/C+, Au/C+, and VC+ $\text{Li}_2\text{O}_2$  cells. Pt/C+ and Ru/C+  $\text{Li}_2\text{O}_2$  are more than two orders of magnitude more active than VC+ and Au/C+ $\text{Li}_2\text{O}_2$ .

to allow the estimation of the net current by

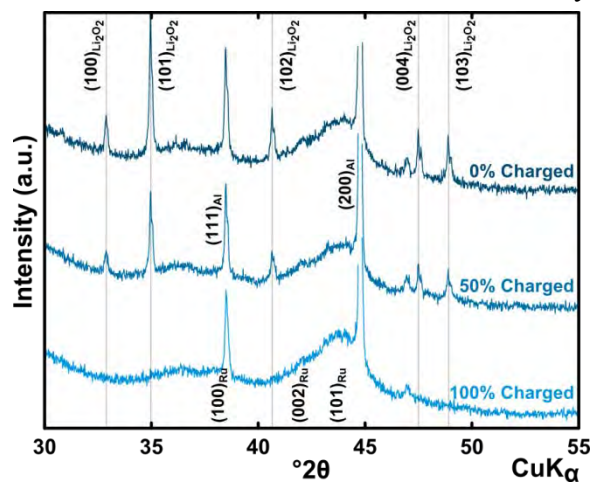


Figure 3 XRD of Ru/C+ $\text{Li}_2\text{O}_2$  electrodes after various amounts of charging. Peaks attributed to  $\text{Li}_2\text{O}_2$  become smaller with some charging and are not visible after complete charging.

**BATT TASK 6**  
**MODELING**

**TASK 6.1 - PI, INSTITUTION:** John Newman, Lawrence Berkeley National Laboratory

**TASK TITLE – PROJECT:** Modeling - Improved Electrochemical Models

**BASELINE SYSTEMS:** Conoco Philips CPG-8 Graphite/1 M LiPF<sub>6</sub>+EC:DEC (1:2)/Toda High-energy layered (NMC)

**BARRIERS:** Poor transport properties, capacity and power fade

**OBJECTIVES:** Develop experimental methods for measuring transport, kinetic, and thermodynamic properties. Model electrochemical systems to optimize performance, identify limiting factors, and mitigate failure mechanisms.

**GENERAL APPROACH:** Use simulations to improve understanding of limitations in cell performance. Develop improved experimental methods for measuring transport and kinetic properties.

**STATUS OCT. 1, 2011:** Experiments measuring the kinetics of ferrocene reduction through a passivating film on glassy carbon will be complete. Characterization of the SEI on highly-oriented-pyrolytic graphite (HOPG) will be ongoing. Comparison of ferrocene kinetics in the presence and absence of additives will be ongoing.

**EXPECTED STATUS SEP. 30, 2012:** Characterization of the SEI on HOPG will be complete. Comparison of ferrocene kinetics in the presence and absence of additives will be complete. A model for the formation of the SEI will be complete.

**RELEVANT USABC GOALS:**  
300,000 shallow discharge cycles  
15 year calendar life

**MILESTONES:**

- (a) Obtain AFM and ferrocene kinetic measurements of SEI on HOPG. (Dec. 11).  
**Complete/canceled**
- (b) Compare through-film ferrocene kinetics for SEI formed in presence of VC and FEC.  
(Apr. 12) **Canceled due to change in research direction**
- (c) Develop model to explain current-time curves for film formation. (Aug. 12) **On schedule**

## PROGRESS TOWARD MILESTONES

In the previous quarterly, a ferrocene characterization method was used to find that the SEI products formed at lower potential are inherently more passivating than those formed at higher potential. Both the through-film limiting current ( $i_{lim,f}$ ) and effective rate constant ( $k_{eff}$ ) are smaller for the same amount of formation charge as the formation potential is decreased. Previous work in our group has suggested that a decrease in the film porosity is responsible for a similar trend of transport and kinetics. In this quarter, the study continued and a manuscript submitted to the Journal of the Electrochemical Society. It is currently under review. A BATT seminar on the subject was also given on June 11.

Figure 1 shows the porosity of the SEI calculated using either the value of  $i_{lim,f}$  or  $k_{eff}$ . Only data at 0.45 V formation are shown. The two methods both yield reasonable values, but do not agree exactly. Although adjusting the assumed thickness can improve the agreement slightly, the difference between the calculated values increases at greater amounts of formation charge. The same trends apply for data at different formation potentials (not pictured). While this disagreement may seem to contradict the explanation of decreasing porosity, the disagreement could also point to the existence of a porosity gradient through the SEI. If the porosity is smaller at the compact/porous layer interface than it is at the porous layer/electrolyte interface, the accessible area for charge-transfer reaction will be smaller than the area limiting transport through the SEI.

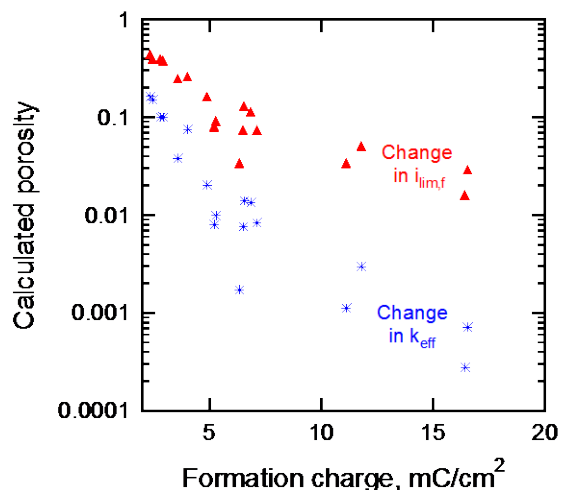


Figure 1. Calculated porosity of 0.45 V formation

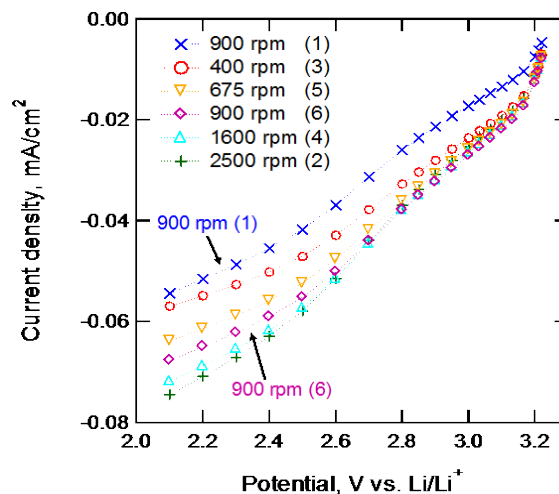


Figure 2. Instability of SEI formed at 0.1 V

Figure 2 shows another result that suggests that porosity is indeed the limiting phenomenon for through-film ferrocenium reduction. The data shown are for through-film reduction after 10 seconds of formation at 0.1 V. The order of measurement is shown in parentheses. The Fig. shows that current increases with order of measurement (parentheses) and rotation speed; thus, the film is unstable. However, the open circuit potential does not change, and from fitting the curves (not pictured), both  $i_{lim,f}$  and  $i_0$  increase with time. Thus, either the thickness and the rate constant decrease simultaneously at open-circuit conditions, or the porosity increases, possibly because intermediates diffuse away and open up void space in the film.

More details on this work can be found in the submitted manuscript, which **completes Milestone c)**. We initially planned to experiment with additives instead of varying the formation potential; therefore, **Milestone b) is cancelled** due to the change in research direction.

**TASK 6.2 - PI, INSTITUTION:** Venkat Srinivasan, Lawrence Berkeley National Laboratory

**TASK TITLE – PROJECT:** Modeling – Model Experimental Studies on Next-generation Li-ion Battery Materials

**BASELINE SYSTEMS:** Conoco Philips CPG-8 Graphite/1 M LiPF<sub>6</sub>+EC:DEC (1:2)/Toda High-energy layered (NMC)

**BARRIERS:** Low calendar/cycle life; Low energy, High cost

**OBJECTIVES:**

1. Quantify power limitations in porous cathodes and its relationship to design.
2. Develop a model to account for porosity in electrode secondary particles and quantify effect on performance
3. Develop a model for mechanical degradation of electrodes with consideration of particles and binder.

**GENERAL APPROACH:** Develop mathematical models for candidate Li-ion chemistries. Design experiments to test theoretical predictions and to estimate properties needed for the models. Use models to connect fundamental material properties to performance and degradation modes and provide guidance to material-synthesis and cell-development PIs. Use models to quantify the ability of the candidate chemistry to meet DOE performance goals.

**STATUS OCT. 1, 2011:** A preliminary model that quantifies the importance of incorporating binder effects in predicting failure of particles will be complete. The impact on low volume change systems like graphite and high volume change systems like silicon will be examined. The rate capability of NCM cathodes on a particle scale will be quantified and the relevant transport properties measured.

**EXPECTED STATUS SEP. 30, 2012:** The performance models for Si anode with the NMC cathode will be complete and comparison made with the baseline. The degradation of graphite and candidate alloy anodes that takes into account the interaction of the active material and the binder will be complete. A model that accounts for the reaction distribution across the electrode will be developed and compared to experimental data.

**MILESTONES:**

- (a) Construct a silicon anode particle model that incorporates a coupling between kinetics and stress during lithiation and delithiation. (Feb. 12) **Complete**
- (b) Compare the porous electrode model with experimental data of NCM cathode and quantify effect of porosity and conductive aids on performance. (Mar. 12) **Complete**
- (c) Develop a model for porous particles applying to Ni/Mn spinel oxides and report on the effects of secondary particle porosity on battery performance. (Sep. 12) **On schedule**
- (d) Couple the particle model with a model of the surrounding binder material to quantify the effect of binder properties on damage to the binder and binder-particle interface. (Sep. 12) **On schedule**

## PROGRESS TOWARD MILESTONES

**Modeling NMC Cathode:** The rate performance of a lithium-ion battery was previously shown to be limited by transport in the solution phase of the porous electrode. In the last quarter, the diffusion limitations in the solution phase were studied by examining the electrode porosity and tortuosity using a mathematical model. It was found that the ratio of porosity to tortuosity plays an important role in the battery performance, and as long as the ratio is fixed, the calculated discharge potentials were the same.

In this quarter, efforts continue to focus on the porous-particle scale. Figure 1 shows the model-experiment comparisons at different discharge rates on a NMC electrode with an average porosity of 0.37. As seen in the figure, a small change in electrode porosity results in a significant change in performance at 5C and 10C rates. Although the model is still unable to fit the experiment, the comparisons show that the rate performance is highly sensitive to the electrode porosity. To further elucidate this effect, in the next quarter, more experiments will be performed on NMC electrodes to investigate experimentally the influence of electrode porosity and thickness on the electrode performance.

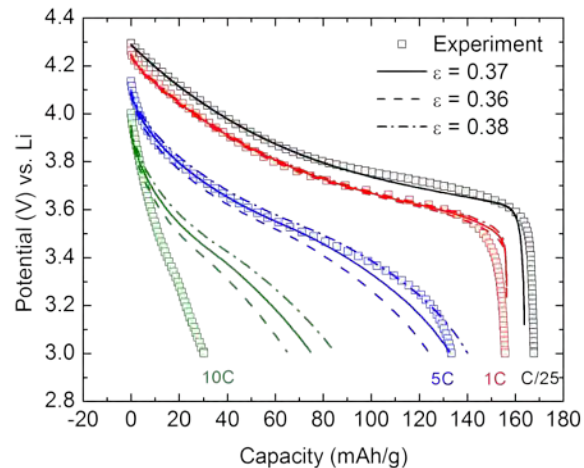


**Figure 1.** Model-experiment comparisons at different discharge rates. The experimental data was obtained on a NMC cathode with a thickness of 70  $\mu\text{m}$  and an average porosity of 0.37. The calculated potentials were obtained using Bruggeman coefficient of 4.2 and different values of average porosity.

**Understanding Mechanical Degradation in Silicon Anodes:** Mechanical degradation resulting in electrical isolation of active material is an important source of capacity fade in silicon anodes. Mathematical models are being developed to investigate particle-level damage in these electrodes.

For the present, electrode particles are assumed to consist of amorphous silicon. The model of Christensen and Newman (2006), which describes a spherical, isotropic electrode particle undergoing large deformation due to lithium insertion and removal, has been adapted for this purpose. Our implementation also recognizes the influence of composition on the Young's modulus and Poisson's ratio of the lithiated silicon, as obtained by Shenoy, Johari, and Qi (2010). Further, this model has been extended to include a binder layer of user-specified thickness on the surface of the electrode particle, with continuity of displacement and stress enforced at the interface between particle and binder. Additionally, a methodology has been developed to include the influence of stress on reaction kinetics at the particle surface.

This satisfies the relevant September milestone; the model now allows monitoring of the evolution of stress throughout the particle-binder system and comparison against the local material yield-stress as a threshold for damage. The investigation into stress-influenced kinetics has suggested an alternative approach to modeling particles undergoing lithiation and delithiation, specifically for materials that alloy with lithium, such as silicon. Development of this model is ongoing. Once completed, this model is expected to offer a more detailed description of diffusion and stress development in alloying materials.

**TASK 6.3 - PI, INSTITUTION:** Jonghyun Park, University of Michigan

**TASK TITLE - PROJECT:** Modeling – Thermo-electrochemistry, Capacity Degradation, and Mechanics with SEI Layer

**BASELINE SYSTEMS:** Conoco Philips CPG-8 Graphite/1 M LiPF<sub>6</sub>+EC:DEC (1:2)/Toda High-energy layered (NMC)

**BARRIER:** Prediction of capacity and power degradation, and excessive additive materials which penalize energy and power density and increase cost.

**OBJECTIVES:** (i) multiscale FE modeling considering phase transition and the mismatch between active material and SEI layer, (ii) simulation in Li-ion batteries including microscale features, (iii) measurement of mechanical properties (*i.e.*, Young's modulus and thickness) of the SEI layer

**GENERAL APPROACH:** Parallel numerical and experimental approaches to study the interrelationships of the solid electrolyte interphase and lithium manganese oxide will be used. The numerical approach will rely upon voxelation of real particle geometries and the finite element technique to solve the complex multiphysics problem of the electrochemical, mechanical and thermal aspects of the SEI layer. Experimentally, the composition, morphology, and physical and electrochemical properties of the SEI using ATR-FTIR, TEM, and AFM, as well as electrochemical techniques to measure the diffusivity and conductivity of the SEI layer will be measured.

**STATUS OCT. 1, 2011:** A multiscale FE model considering particle aggregation, its effect on cathode structure, and the effect in turn on cathode dissolution has been established. An SEI layer formation model and parametric studies for different electrochemical systems have also been established. Finally, experimental techniques (*ex-situ* and/or *in-situ*) will be applied to validate the SEI layer formation model. With these three objectives completed, capacity degradation of Li-ion batteries can be correlated to the properties of SEI layers and particle microstructures.

**EXPECTED STATUS SEP. 30, 2012:** To have (1) applied finite element methods to the phase change/intercalation interrelationship to graphitic anodes, (2) applied numerical techniques to the modeling of the SEI layer on complex electrode geometries, and (3) verified the model using experimental data collected on the physical properties of the SEI layer.

**RELEVANT USABC GOALS:** *Available energy for CD mode:* 3.4 kWh (10 miles) and 11.6 kWh (40 miles); *Cycle life:* 5000 cycles (10 miles) and 300,000 cycles (40 miles); *10- s discharge power:* 45 kW (10 miles) and 38 kW (40 miles); *Calendar life:* 15 years (40°C).

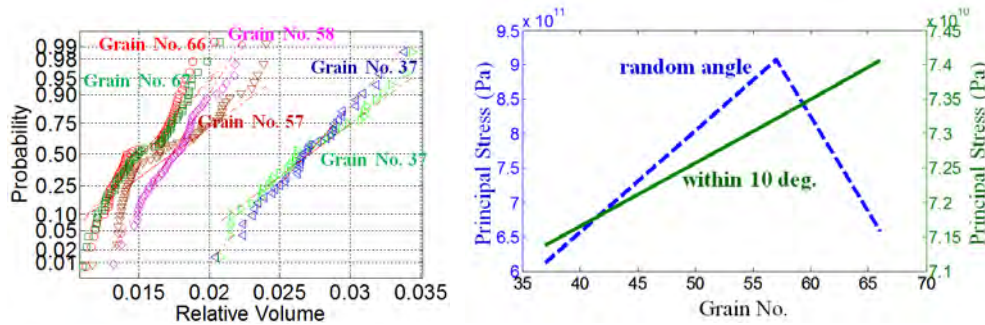
**MILESTONES:**

- (a) Implement multiscale modeling for stresses in active material considering SEI layer. (Mar. 12) **Complete**
- (b) Couple the 1D electrochemical model with a previously developed micro scale model. (May 12) **Complete**
- (c) Quantify variation in the mechanical properties of the SEI layer as a function of cycle number. (Aug. 12) **On schedule**

## PROGRESS TOWARD MILESTONES

### 1) Intercalation- and Misfit-Induced Stress in the Graphite Electrodes

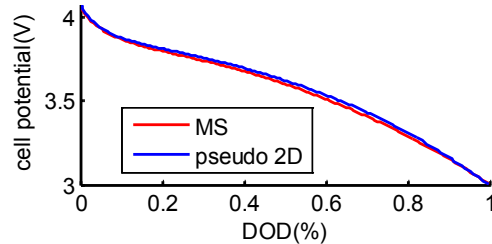
The effect of anisotropic grain size on the maximum principal stress in a graphite particle was examined *via* electrochemical-mechanical modeling during a galvanostatic condition. The particle size was controlled by changing the number of grains in a fixed volume. The left figure shows the normal probability of each case. The right figure shows the maximum principal stress, where the dotted blue line indicates the case of random angle distribution and the solid green indicates the case of controlled angle distribution ( $<10^\circ$ ). The maximum stress increased as the angle was more irregular due either to random selection or increase of the grain number. This tendency coincided with the previous result that maximum principal stress was increased as the misorientation angle increased.



### 2) Multiscale modeling with self-assembly and dissolution

In order to verify the developed variational multiscale model (VMM), calculations of a discharge curve were compared to those of a pseudo 2D model, based on the effective properties (table) determined from a randomly generated microstructure. The discharge curves (right figure) from both approaches showed similar patterns, since the VMM result included the aggregated network effect in the electrode.

parameter	unit	value
solid phase volume fraction	-	0.4104
specific surface area	1/m	$1.26 \times 10^5$
solid phase tortuosity	-	1.2803
electrolyte phase tortuosity	-	1.2307
ionic diffusivity	$\text{m}^2/\text{s}$	$1.64 \times 10^{-11}$
electronic conductivity	S/m	0.9514



### 3) Characterization of SEI layers

To investigate the capacity loss due to an additive-derived surface layer, a constant current cycling experiment was carried out using Li/LMO half cells. There were three cases for each set including 1) no additive and 2) FEC additive. FEC additive was selected in this experiment due to its resiliency to Mn dissolution as compared to VEC, according to ICP tests conducted during Q2. As shown in the table, the case of 5% FEC additive resulted in a larger capacity fade compared to the case of the no-additive cell after 10 cycles (C/4) at room temperature. These serial experimental results in Q2 and Q3 suggested that FEC could aggravate the capacity due to increased Mn dissolution.

	No additive included cells	FEC additive included cells
Discharge capacity reduction	avg. 31.02 %	avg. 52.74 %

**TASK 6.4 - PI, INSTITUTION:** Kristin Persson, Lawrence Berkeley National Laboratory

**TASK TITLE – PROJECT:** Modeling – Predicting and Understanding New Li-ion Materials Using *Ab Initio* Atomistic Computational Methods

**BASELINE SYSTEMS:** Conoco Philips CPG-8 Graphite/1 M LiPF<sub>6</sub>+EC:DEC (1:2)/Toda High-energy layered (NMC)

**BARRIERS:** High cost, low energy, low rate, poor cyclability.

**OBJECTIVES:** 1) Predict new chemistries and crystal structures for improved electrodes as defined by the goals of USABC. 2) Understand diffusion-limiting behavior in current and novel electrode materials in order to suggest chemical or morphological improvements. 3) Understand surface interactions in electrode materials to optimize stability and kinetics.

**GENERAL APPROACH:** Use computational *ab initio* atomistic modeling methods to understand current Li-ion battery electrode materials and use this knowledge to suggest improvements as well as new electrode materials. Use statistical mechanics models to understand Li diffusion in bulk and on surfaces. Combine and make efficient access to all relevant calculated knowledge in a searchable database, facilitating computational materials design.

**STATUS OCT. 1, 2011:** Evaluation of Al substitution effect on LiNi<sub>1/3</sub>Mn<sub>1/3</sub>Co<sub>1/3-x</sub>Al<sub>x</sub>O<sub>2</sub> in terms of Li mobility and electronic conductivity has been concluded. The study of Li absorption on graphene and multi-layer graphene surfaces will be underway. The Li and cation interactions in LiNi<sub>1/2</sub>Mn<sub>3/2</sub>O<sub>2</sub> will be understood as a function of Li content. The materials genome web site is launched from LBNL.

**EXPECTED STATUS SEP. 30, 2012:** Li kinetics on graphene and multi-layer graphite is concluded. Electronic structure studies of surface facet stability of electrode materials (LiMnO<sub>2</sub> and LiFePO<sub>4</sub>) will be underway. Phase diagram of LiNi<sub>1/2</sub>Mn<sub>3/2</sub>O<sub>2</sub> will be concluded. The study of Li kinetics and electronic structure of Li<sub>x</sub>Ni<sub>1/2</sub>Mn<sub>3/2</sub>O<sub>2</sub> as a function of Li content will be underway.

**RELEVANT USABC GOALS:** PHEV: 96 Wh/kg, 5000 cycles; Operating charging temperature: -30 to 52 °C

**MILESTONES:**

- (a) Go online with the Materials Genome database from LBNL. (Oct. 11) **Complete**
- (b) Map the electronic structure of Li<sub>x</sub>Ni<sub>1/2</sub>Mn<sub>3/2</sub>O<sub>2</sub> as a function of Li content. (Oct. 11) **Complete**
- (c) Calculate the band structures of LiMnO<sub>2</sub> surfaces. (Dec. 11) **Complete**
- (d) Predict the stable phases of the Li-graphene and Li-multi-graphene. (Feb. 12) **Complete**
- (e) Complete the phase diagram of Li<sub>x</sub>Ni<sub>1/2</sub>Mn<sub>3/2</sub>O<sub>2</sub>. (Mar. 12) **Complete**
- (f) Calculate the surface DOS of LiFePO<sub>4</sub> with different absorbents. (May 12) **Delayed – due Sep. 12**
- (g) Complete the kinetics of Li-graphene. (Sep. 12) **On schedule**

## PROGRESS TOWARD MILESTONES

This concludes the investigation of the  $\text{LiMn}_2\text{O}_4$  spinel as part of our effort to model electrode surface effects from first-principles. Bulk properties were used primarily to bench mark the calculational methods. The  $\text{LiMn}_2\text{O}_4$  spinel system exhibits charge-ordering and magnetic ordering among the  $\text{Mn}^{3+}$  and  $\text{Mn}^{4+}$  as well as Jahn-Teller distortion on the  $\text{Mn}^{3+}$  sites. Once a satisfactory bulk description was obtained, subsequent surface calculations were approached using the ground state bulk magnetic and electronic state as a starting point. Many different terminations - exploring O, Mn, Li, and combinations thereof - of the low-index surfaces and their electronic structure were calculated and evaluated for stability using both GGA and GGA+U. With the use of the most stable surface configurations, this provided the ability to predict the thermodynamically stable morphology of  $\text{LiMn}_2\text{O}_4$ , see Fig. 1. As can be seen from the figure, the favorable shape is a cuboctahedra with predominant [111] surface facets, in agreement with numerous reports for compounds with the spinel phase. Surface voltage profiles and the electronic structure of the surfaces were also obtained.

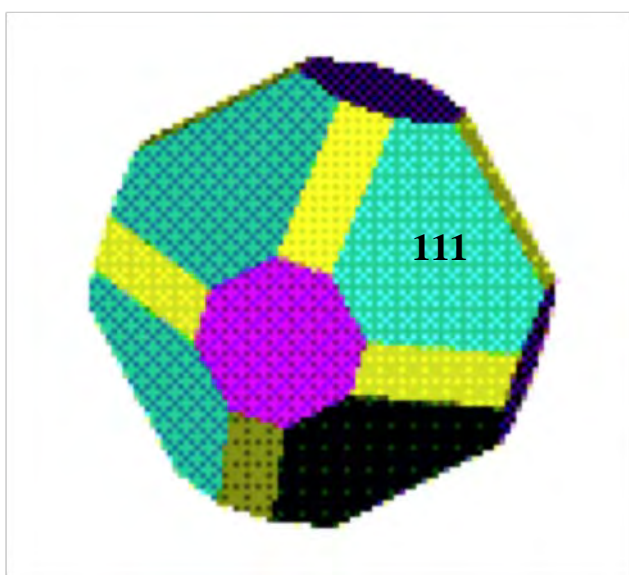


**Figure 1.** Thermodynamically stable morphology of  $\text{LiMn}_2\text{O}_4$  calculated by GGA+U.

We have concluded the work on the phase diagram and voltage profile of  $\text{Li}_x\text{Ni}_{0.5}\text{Mn}_{1.5}\text{O}_4$  calculated by a grand canonical Monte Carlo simulation based on the *ab initio* cluster expansion model, which was developed in our previous work on the high-voltage spinel. Grand canonical Monte Carlo simulations were performed by changing the chemical potential and temperature. At each case of chemical potential and temperature, two simulations are performed for two different initial conditions of Li content: the fully lithiated and delithiated states, to simulate the charge and discharge process, respectively. From this, information about order-disordered transition temperatures as

a function of Li content and temperature were obtained. From the analysis on the chemical potential vs. the Li content, the voltage profile at finite temperature is predicted.

**Collaborations:** Prof Gerbrand Ceder (MIT), Dr. Jordi Cabana (LBNL), Dr. Robert Kostecki (LBNL), Dr. Phil Ross (LBNL).